Microphone Array Processing for Robust Speech Recognition

Michael L. Seltzer

Thesis Committee:
Richard M. Stern, Chair
Tsuhan Chen
Gary W. Elko
B. V. K. Vijaya Kumar

Submitted to the Department of Electrical and Computer Engineering in partial fulfillment of the requirements for the degree of Doctor of Philosophy at

Carnegie Mellon University
Pittsburgh, PA 15213
July 2003

To my parents.

Abstract

Speech recognition performance degrades significantly in distant-talking environments, where the speech signals can be severely distorted by additive noise and reverberation. In such environments, the use of microphone arrays has been proposed as a means of improving the quality of captured speech signals. Currently, microphone-array-based speech recognition is performed in two independent stages: array processing and then recognition. Array processing algorithms designed for signal enhancement are applied in order to reduce the distortion in the speech waveform prior to feature extraction and recognition.

This approach assumes that improving the quality of the speech waveform will necessarily result in improved recognition performance. However, speech recognition systems are statistical pattern classifiers that process features derived from the speech waveform, not the waveform itself. An array processing algorithm can therefore only be expected to improve recognition if it maximizes or at least increases the likelihood of the correct hypothesis, relative to other competing hypotheses.

In this thesis a new approach to microphone-array processing is proposed in which the goal of the array processing is not to generate an enhanced output waveform but rather to generate a sequence of features which maximizes the likelihood of the correct hypothesis. In this approach, called *Likelihood Maximizing Beamforming* (LIMABEAM), information from the speech recognition system itself is used to optimize a filter-and-sum beamformer. Using LIMABEAM, significant improvements in recognition accuracy over conventional array processing approaches are obtained in moderately reverberant environments over a wide range of signal-to-noise ratios. However, only limited improvements are obtained in environments with more severe reverberation.

To address this issue, a subband filtering approach to LIMABEAM is proposed, called *Subband-Likelihood Maximizing Beamforming* (S-LIMABEAM). S-LIMABEAM employs a new subband filter-and-sum architecture which explicitly considers how the features used for recognition are computed. This enables S-LIMABEAM to achieve dramatically improved performance over the original LIMABEAM algorithm in highly reverberant environments.

Because the algorithms in this thesis are data-driven, they do not require *a priori* knowledge of the room impulse response, nor any particular number of microphones or array geometry. To demonstrate this, LIMABEAM and S-LIMABEAM are evaluated using multiple array configurations and environments including an array-equipped personal digital assistant (PDA) and a meeting room with a few tabletop microphones. In all cases, the proposed algorithms significantly outperform conventional array processing approaches.

Acknowledgments

This thesis would not have been possible without the support and encouragement of many people. To the following people, I owe an enormous debt of gratitude.

My advisor, Professor Richard Stern, who welcomed me into his group when I arrived at CMU knowing absolutely nothing about speech recognition. Rich gave me the guidance I needed to become a capable researcher and the freedom to pursue my own ideas. He has been a role model of professionalism and integrity, as well as a good friend.

Dr. Gary Elko, whose expertise in microphone arrays and acoustics was invaluable. He was very generous with his time and always quick to respond to my questions.

Professor B. V. K. Vijaya Kumar and Professor Tsuhan Chen, who made many valuable suggestions that really improved the quality of this dissertation.

The members of the CMU Robust Speech Group, past and present, from whom I learned a great deal and with whom I shared many laughs. Rita Singh, Juan Huerta, and Sam-Joo Doh never grew tired of answering my endless stream of questions during my first two years here. Jon Nedel, Evandro Gouvêa, Xiang Li, and Pablo Hennings were always around for discussions and their camaraderie created a great work environment.

Bhiksha Raj, who has been a mentor, a collaborator, and a good friend. He taught me not to shy away from tough research problems and his positive attitude in the face of some difficult circumstances amazes and inspires me.

Tom Sullivan and Yasunari Obuchi, who recorded the microphone array data used in this thesis, and the ICSI speech group, who graciously gave me their meeting room data.

Kevin Dixon, Jay Wylie, Dan Gaugel, Stefanie Tomko, Mike Stout, George Lopez, and Rich Malak, whose friendship was a constant reminder that there is more to graduate school than research and work. They were a limitless source of support, fun, and laughs, and I feel extremely lucky to be able to call them my friends.

Julie, who has given me more love and encouragement during this process than anyone can possibly ask for. Her boundless support kept me going when things were difficult, and I can't wait to start the next chapter of my life with her.

My sister Gabrielle, who has been my biggest cheerleader throughout my life and to whom I have grown closer over the past five years, despite the distance between us.

Finally, there is no way I would be where I am today without the immeasurable love, support, and encouragement of my parents. I cannot thank them enough for all the opportunities they have given me in my life and for always believing in me. They are an incredible inspiration to me.

Table of Contents

List of Figures

List of Tables

Chapter 1

Introduction

State-of-the-art automatic speech recognition (ASR) systems are known to perform reasonably well when the speech signals are captured in a noise-free environment using a close-talking microphone worn near the mouth of the speaker. Such technology has progressed to the point where commercial systems have been deployed for some small tasks. However, the benefits of speech-driven interfaces have yet to be fully realized, due in large part to the significant degradation in performance these systems exhibit in real-world environments. In such environments, the signal may be corrupted by a wide variety of sources including additive noise, linear and non-linear distortion, transmission and coding effects, and other phenomena.

This thesis is particularly interested in those environments in which either safety or convenience preclude the use of a close-talking microphone. For example, while operating a vehicle, the very act of wearing a microphone is distracting and dangerous. In a meeting room, microphones restrict the movement of the participants by tethering them to their seats by wires. And it is unlikely that users of an information kiosk will want to put on a headset before asking for help. In all of these situations, wires can break and tangle, creating a frustrating experience for the user.

In such settings, a better alternative to head-mounted microphones is to place a fixed microphone some distance from the user. Unfortunately, as the distance between the user and the microphone grows, the speech signal becomes increasingly degraded by the effects of additive noise and reverberation, which in turn degrade speech recognition accuracy. In such distant-talking environments, the use of an array of microphones, rather than a single microphone, can compensate for this distortion by providing spatial filtering to the sound field, effectively focusing attention in a desired direction.

Many signal processing techniques using arrays of sensors have been proposed in speech

and other application domains which improve the quality of the output signal and achieve a substantial improvement in the signal-to-noise ratio (SNR). The most well-known general class of array processing methods are *beamforming* methods. Beamforming refers to any method that algorithmically, rather than physically, steers the sensors in the array toward a target signal. The direction the array is steered is commonly called the *look direction*. The simplest and most common method of beamforming is called *delay-and-sum* (Johnson & Dudgeon, 1993). In delay-and-sum beamforming, the signals received by the microphones in the array are time-aligned with respect to each other in order to adjust for the path-length differences between the speech source and each of the microphones. The now time-aligned signals are then weighted and added together. Any interfering signals from noise sources that are not coincident with the speech source remain misaligned and are thus attenuated when the signals are combined. A natural extension to delay-and-sum beamforming is *filter-and-sum* beamforming, in which each microphone has an associated filter, and the received signals are first filtered and then combined.

If the weights or filter parameters are adjusted online during processing, the methods are referred to as *adaptive* beamforming techniques. These methods, such as (Frost, 1972; Griffiths & Jim, 1982), update the array parameters on a sample-by-sample or frame-by-frame basis according to a specified criterion. Typical criteria used in adaptive beamforming include a distortionless response in the look direction and/or the minimization of the energy from all directions not considered the look direction.

Conventionally, speech recognition using microphone arrays is generally performed in two independent stages: array processing and then recognition. The array processing is considered a pre-processing step to enhance the waveform prior to conventional feature extraction and recognition. In this approach, the array processing is used to produce an enhanced output waveform, as measured quantitatively by SNR or other distortion metric, or by improved scores on perceptual tests by human listeners. A sequence of speech recognition feature vectors are derived from this enhanced waveform and passed to the recognition engine for decoding. This configuration is depicted in Figure 1.1.

This approach to microphone array processing for speech recognition suffers from several drawbacks. Most notably, it implicitly makes the assumption that generating a higher quality output waveform will necessarily result in improved recognition performance. However, a speech recognition system does not interpret waveform-level information directly. It is a statistical pattern classifier whose goal is to hypothesize the correct transcription. This is usually accomplished by finding the word string that has the maximum likelihood of generating the sequence of features derived from the observed waveform. As a result, an array processing scheme can only be expected to improve recognition accuracy if it generates a

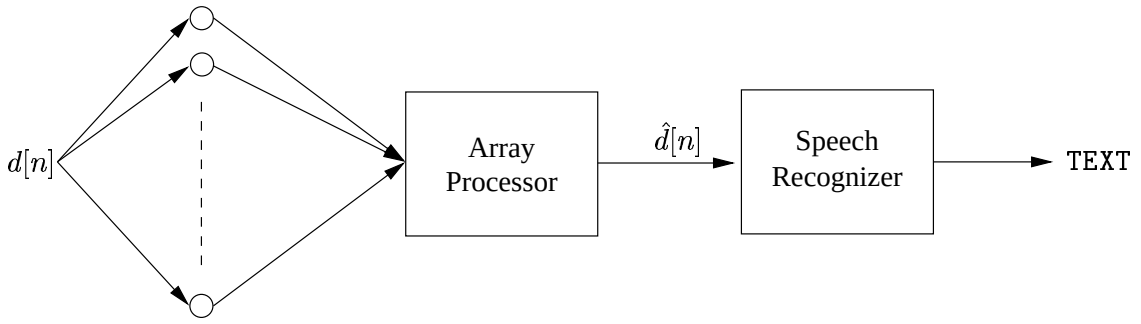

Figure 1.1: Conventional architecture of speech recognition systems with microphone array front-ends. The objective of the array processing is to estimate the clean *waveform*.

sequence of features which maximizes, or at least increases, the likelihood of the correct transcription, relative to other hypotheses. It is believed that this is the underlying reason why many array processing methods proposed in the literature which produce high quality output waveforms do not result in significant improvements in speech recognition accuracy compared to simpler methods such as delay-and-sum beamforming.

1.1 What this thesis is about

In this thesis, we propose an alternative approach to this problem by considering the array processor and the speech recognizer not as two independent entities cascaded together, but rather as two interconnected components of a single system, sharing the common goal of improved speech recognition accuracy. This will enable important information from the recognition engine to be integrated into the design of the array processing scheme. Specifically, the proposed microphone-array-based speech recognition system will be considered a single closed-loop system, with information from the statistical models of the recognition system used as feedback to tune the parameters of the array processing scheme. By using this architecture, shown in Figure 1.2, we can overcome the drawbacks of previously proposed array processing methods and achieve better recognition accuracy in environments in which the speech is corrupted by additive noise and reverberation.

This approach has several advantages over current array processing methods. First, by incorporating the statistical models of the recognizer into the array processing stage, we ensure that the processing enhances those signal components important for recognition accuracy without undue emphasis on less important components. Second, no assumptions about the interfering signals are made. In contrast, methods which assume that the noise

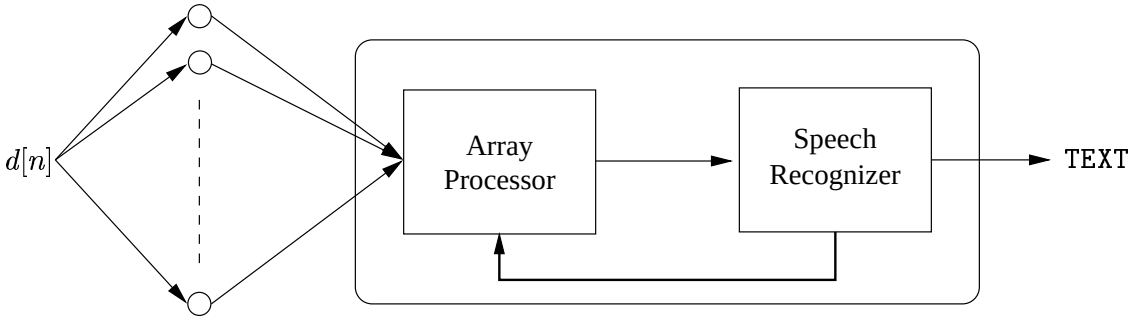

Figure 1.2: An architecture for array processing optimized for speech recognition performance. The array processor and the speech recognizer are fully connected, allowing information from the recognizer to be used in the array processing. Note that the system no longer attempts to estimate the clean waveform.

and the speech are uncorrelated suffer from signal cancellation effects in reverberant environments. Third, the proposed approach requires no *a priori* knowledge of the room configuration, array geometry, or source-to-sensor room impulse responses.

The approach described is used to develop two array processing algorithms for speech recognition applications. In the first algorithm, the parameters of a conventional filter-and-sum beamformer are optimized for recognition performance. In the second algorithm, subband processing is performed in the spectral domain, also in a filter-and-sum manner. This second approach has several characteristics which enable significant improvements to be achieved in highly reverberant environments. In addition, we present two different implementations of these algorithms, one for use in situations where the environmental conditions are stationary or slow-varying, and the other for use in time-varying environments.

1.2 Dissertation Outline

This thesis is organized as follows:

Chapter 2 provides an overview of automatic speech recognition. We discuss in detail some aspects of HMM-based recognition systems relevant to the work presented in this thesis, and describe the performance of such systems when speech is corrupted by additive noise and reverberation.

In Chapter 3 we review the basic concepts of microphone array processing. We describe some current microphone array processing algorithms and their performance in speech recognition applications. We also describe some relevant single-channel speech recognition compensation algorithms. Lastly, we present the speech corpora that will be used to evaluate

the techniques proposed in this thesis.

In Chapter 4 we introduce the framework used to develop the algorithms in this thesis. We show how the objectives of the array processor and the speech recognizer can be unified, and then develop and evaluate a filter-and-sum beamforming algorithm that does so.

In Chapter 5 we look more closely at the difficulties of recognizing speech in highly reverberant environments. We present an algorithm which incorporates subband filtering into the framework established in Chapter 4 and show that this approach is able to overcome many of the difficulties encountered by previous dereverberation methods.

In Chapter 6 we apply the proposed algorithms to two alternative multi-channel speech recognition applications. We show that the methods presented are capable of good performance even in highly sub-optimal microphone configurations.

Finally, Chapter 7 summarizes the major results and contributions of this thesis and highlights some directions for further research.

Chapter 2

A Review of Automatic Speech Recognition

2.1 Introduction

This thesis deals with the processing of signals received by an array of microphones for input into a speech recognition system. In this work, we wish to develop methods of performing such processing specifically aimed at improving speech recognition accuracy. In order to do so, we must understand the manner in which speech recognition systems operate. In this chapter, we review this process, describing how a speech waveform is converted into a sequence of feature vectors, and how these feature vectors are then processed by the recognition system in order to generate a hypothesis of the words that were spoken. We begin with a description of mel-frequency cepstral coefficients (MFCC) (Davis & Mermelstein, 1980), the features used in this thesis. We then describe the operation of speech recognition systems, limiting our discussion to those systems that are based on Hidden Markov Models (HMM). We then discuss speech recognition in distant-talking environments, and specifically the effects that additive noise and reverberation have on recognition accuracy in such environments.

2.2 HMM-based Automatic Speech Recognition

Speech recognition systems are pattern classification systems (Rabiner & Juang, 1993). In these systems, sounds or sequences of sounds, such as phonemes, groups of phonemes, or words are modeled by distinct classes. The goal of the speech recognition system is to estimate the correct sequence of classes, *i.e.* sounds, that make up the incoming utterance,

and hence, the words that were spoken.

In state-of-the-art recognition systems, speech recognition is not performed directly on the speech signal. Rather, the speech waveform is divided into short segments or *frames* and a vector of *features* is extracted from the samples of each frame. If we let $\mathcal{Z}$ represent a sequence of feature vectors extracted from a speech waveform, speech recognition systems operate according to the optimal classification equation

$$\hat{\boldsymbol{w}} = \underset{\boldsymbol{w} \in \mathcal{W}}{\operatorname{argmax}} \, P(\boldsymbol{w}|\mathcal{Z}) \tag{2.1}$$

where $\hat{\boldsymbol{w}}$ is the sequence of words hypothesized by the recognition system and $\mathcal{W}$ is the set of all possible word sequences that can be hypothesized by the recognition system. However, this expression is not actually computed by recognition systems. Instead, Bayes rule is used to rewrite Equation (2.1) as

$$\hat{\boldsymbol{w}} = \underset{\boldsymbol{w} \in \mathcal{W}}{\operatorname{argmax}} \, \frac{P(\mathcal{Z}|\boldsymbol{w})P(\boldsymbol{w})}{P(\mathcal{Z})} \tag{2.2}$$

where $P(\mathcal{Z}|\boldsymbol{w})$ is the *acoustic likelihood* or *acoustic score*, representing the probability that feature sequence $\mathcal{Z}$ is observed given that word sequence $\boldsymbol{w}$ was spoken, and $P(\boldsymbol{w})$ is the *language score*, the *a priori* probability of a particular word sequence $\boldsymbol{w}$. This latter term is computed using a *language model*. Because we are maximizing Equation (2.3) with respect to the word sequence $\boldsymbol{w}$ for a given (and therefore fixed) sequence of observations $\mathcal{Z}$, the denominator term $P(\mathcal{Z})$ can be ignored in the maximization, resulting in

$$\hat{\boldsymbol{w}} = \underset{\boldsymbol{w} \in \mathcal{W}}{\operatorname{argmax}} \, P(\mathcal{Z}|\boldsymbol{w})P(\boldsymbol{w}) \tag{2.3}$$

Thus, the process of recognizing an utterance of speech can be dividing into two main stages, *feature extraction*, where a speech signal is parameterized into a sequence of feature vectors, and *decoding*, in which the most likely word sequence is hypothesized based on the observed features, according to Equation (2.3). In the following sections, we describe how a speech signal is converted into sequence of MFCC feature vectors, and how these vectors are then processed by an HMM-based recognition system to estimate the spoken word sequence.

2.2.1 Feature Extraction

Speech recognition systems do not interpret the speech signal directly, but rather a set of feature vectors derived from the speech signal. In this thesis, as in most current speech

recognition systems, the speech signal is parameterized into a sequence of vectors called mel-frequency cepstral coefficients (MFCC) (Davis & Mermelstein, 1980), or simply *cepstral coefficients*. Because much of the work in this thesis is concerned with the feature generation process, we will now examine the derivation of cepstral coefficients in detail.

Cepstral coefficients attempt to approximate the spectral processing of the auditory system in a computationally efficient manner. The incoming speech signal is divided into a sequence of short overlapping segments, called *frames*. Each frame is processed as follows. The frame is windowed and then transformed to the frequency domain using a Short-Time Fourier Transform (STFT) (Nawab & Quatieri, 1988). The magnitude squared of the STFT is computed and then multiplied by a series of overlapping triangular weighting functions called *mel filters*. These triangular filters are equally distributed along the mel frequency scale with a 50% overlap between consecutive triangles. These filters are spaced in frequency approximately linearly at low frequencies and logarithmically at higher frequencies. The *mel spectrum* of the frame is computed as a vector whose components represent the energy in each of the mel filters. To approximate human auditory processing more closely, the natural logarithm of each of the elements in the mel spectral vector is then computed, producing the *log mel spectrum* of the frame. Finally, this vector is converted to mel-frequency cepstra via a Discrete-Cosine Transform (DCT) and then truncated. The feature extraction process is shown in Figure 2.1.

The input to a speech recognition system is typically a sequence of vectors composed of the mel-frequency cepstral coefficients as well as their first and second temporal derivatives, approximated by using first and second differences of neighboring frames, respectively.

2.2.2 HMM-based Modeling of the Distributions of Sequences of Feature Vectors

In frame-based statistical speech recognition systems, the speech production mechanism is characterized as a random process which generates a sequence of feature vectors. In Hidden Markov Model (HMM) speech recognition systems, the random process which corresponds to a particular word is modeled as an HMM (Rabiner & Juang, 1993). An HMM can be characterized by the following:

- a finite number of states
- a state-transition probability distribution which describes the probability associated with moving to another state (or possibly back to the same state) at the next time instant, given the current state
- a output probability distribution function associated with each state

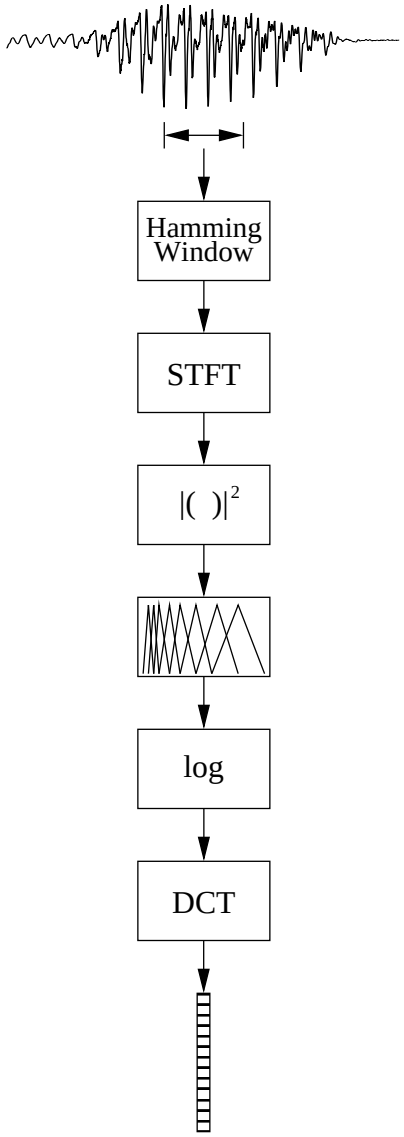

Figure 2.1: Flow chart depicting generation of mel-frequency cepstral coefficients from a frame of speech. Typically, a frame size of 25 ms is used, with a frame shift of 10 ms.

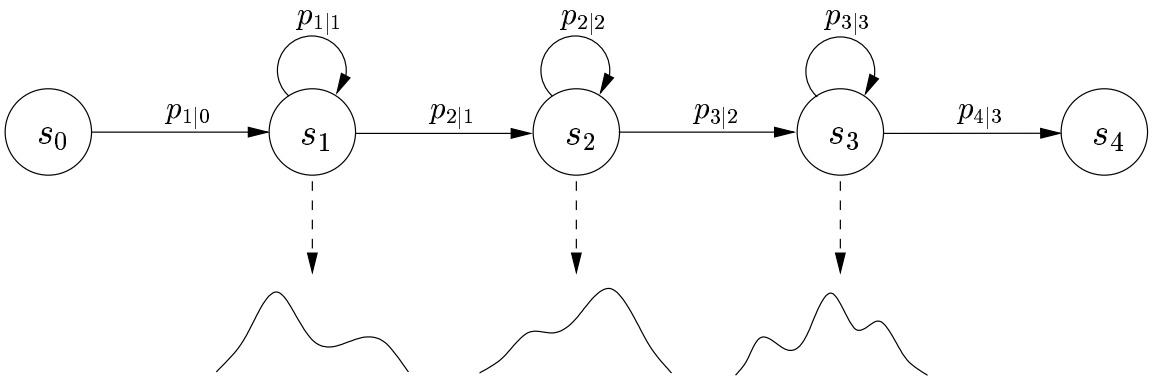

Figure 2.2: An example of a 5-state left-to-right HMM. The solid arrows represent the allowable transitions from each state, and the probability of going from state i to state j is labeled on each arrow as $p_{i|j}$. The dotted arrows point to the probability distributions associated with each state. Note that the initial and final states are non-emitting. No observations are associated with these states.

An example HMM is shown in Figure 2.2. This HMM has five states. As shown by the solid arrows, the only allowable transitions in this HMM are back to the current state or to the state immediately to the right. All other state transitions have probability zero. The initial and final states are non-emitting states. In these states, no observations (feature vectors) are generated as there are no probability distributions associated with these states. The final state is also an *absorbing* state, in that when this state is reached, no further transitions are permitted.

The statistical behavior of an HMM representing a given word is governed by its state transition probabilities and the output distributions of its constituent states. For an HMM modeling word w, the transition probabilities are represented by a *transition matrix*, A_w. The elements of this matrix, $a_w(i,j)$ represent the probability of transiting to state j at time $t+1$ given that state i is occupied time t. Thus, if the HMM for word w has N states,

$$\sum_{j=1}^{N} a_w(i,j) = 1 \tag{2.4}$$

In speech recognition the state output probability distribution functions are usually modeled as Gaussians or mixtures of Gaussians. Typically, in order to improve computational efficiency, the Gaussians are assumed to have diagonal covariance matrices. Thus, the output probability of a feature vector $\boldsymbol{z}$ belonging to the state i of an HMM for word

w, is represented as

$$b_w(\boldsymbol{z}, i) = \sum_k \alpha_{ik}^w \mathcal{N}(\boldsymbol{z}; \boldsymbol{\mu}_{ik}^w, \boldsymbol{\Sigma}_{ik}^w) \tag{2.5}$$

where α_{ik}^w, $\boldsymbol{\mu}_{ik}^w$, and $\boldsymbol{\Sigma}_{ik}^w$ are the mixture weight, mean vector and covariance matrix associated with the kth Gaussian in the mixture density of state i of the HMM of word w. We define B_w as the set of parameters $\{\alpha_{ik}^w, \boldsymbol{\mu}_{ik}^w, \boldsymbol{\Sigma}_{ik}^w\}$ for all mixture components for all states in the HMM for word w. We can then define $\lambda_w = (A_w, B_w)$ as the complete set of statistical parameters that define the HMM for word w.

To generate a sequence of feature vectors for the word modeled by this HMM, we enter the model at the initial non-emitting state and then transit through the states of the HMM until the final absorbing state is reached. At each time instant, a feature vector is drawn from the probability distribution of the state currently occupied. We then either remain in the current state or move to a different state, based on a draw from the current state's transition probability distribution.

We now wish to compute the probability that a given sequence of feature vectors $\mathcal{Z} = \{\boldsymbol{z}_1, \boldsymbol{z}_2, \ldots, \boldsymbol{z}_N\}$, was generated by the HMM for word w. For convenience, we refer to the HMM that models word w as HMM_w. If we let $\mathcal{S}$ denote the set of all possible state sequences of length N through HMM_w, the total probability that HMM_w generated $\mathcal{Z}$ can be expressed as

$$P(\mathcal{Z}|w) = \sum_{\boldsymbol{s} \in \mathcal{S}} P(\mathcal{Z}, \boldsymbol{s}|w) = \sum_{\boldsymbol{s} \in \mathcal{S}} P(\mathcal{Z}|\boldsymbol{s}) P(\boldsymbol{s}|w) \tag{2.6}$$

where $\boldsymbol{s} = \{s_1, s_2, \ldots, s_N\}$ represents a particular state sequence through HMM_w. The expression $P(\boldsymbol{s}|w)$ represents the probability of a particular state sequence and is computed from the state transition matrix A_w. The expression $P(\mathcal{Z}|\boldsymbol{s})$ represents the probability of a particular sequence of feature vectors given a state sequence, and is computed from the state output probability distributions using Equation (2.5). Thus, we can rewrite Equation (2.6) as

$$P(\mathcal{Z}|w) = \sum_{\boldsymbol{s} \in \mathcal{S}} \left(\prod_{t=1}^{N} a_w(s_t, s_{t+1}) \right) \left(\prod_{t=1}^{N} b_w(\boldsymbol{z}_t, s_t) \right) \tag{2.7}$$

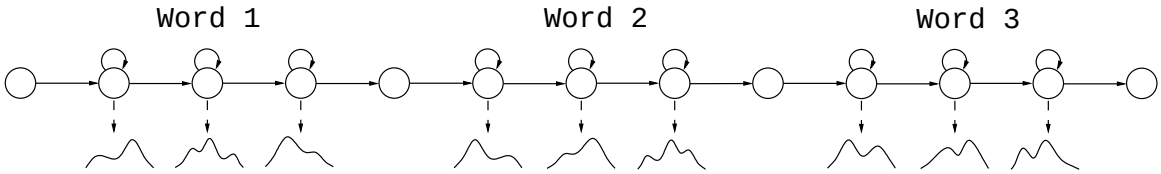

Figure 2.3: An HMM for a sequence of words can be built from the individual HMMs of its constituent words.

Substituting Equation (2.7) into Equation (2.3) leads us to the expression used to perform speech recognition

$$\hat{w} = \underset{w}{\operatorname{argmax}} \left\{ P(w) \sum_{\boldsymbol{s} \in \mathcal{S}} \left(\prod_{t=1}^{N} a_w(s_t, s_{t+1}) \right) \left(\prod_{t=1}^{N} b_w(\boldsymbol{z}_t, s_t) \right) \right\} \tag{2.8}$$

However, for computational efficiency, most HMM speech recognition systems estimate the best state sequence, *i.e.* the state sequence with the highest likelihood, associated with the estimated hypothesis. Thus, recognition is actually performed as

$$\hat{w} = \underset{w, \boldsymbol{s} \in \mathcal{S}}{\operatorname{argmax}} \left\{ P(w) \left(\prod_{t=1}^{N} a_w(s_t, s_{t+1}) \right) \left(\prod_{t=1}^{N} b_w(\boldsymbol{z}_t, s_t) \right) \right\} \tag{2.9}$$

While this discussion has involved the recognition of single words, the HMM framework can easily be expanded to model strings of words, $\boldsymbol{w} = [w_1, w_2, \ldots, w_T]$. If individual words are modeled by unique HMMs in the manner described, then HMMs corresponding to sequences of words can easily be made by concatenating the HMMs of the constituent words. An example of this is shown in Figure 2.3 for an utterance composed of three words.

In this case, however, recognition becomes significantly more computationally demanding and in fact impractical, because Equation (2.9) would have to evaluated for every possible word sequence in the language. As a result, the Viterbi algorithm (Viterbi, 1967), an efficient dynamic programming method, is used in practice to obtain a locally optimal estimate of the word sequence $\hat{\boldsymbol{w}}$.

The CMU Sphinx-3 HMM speech recognition system (Placeway et al., 1997) has been used for all experiments in this thesis. Like most large vocabulary continuous speech recognition (LVCSR) systems, it is a phoneme-based system. Words are broken down into their constituent phonemes and each unique phoneme is modeled by an HMM. The HMMs for words are built by concatenating these phoneme HMMs, in the same manner that word sequence HMMs were constructed from individual word HMMs. To reduce the total number

of parameters needed by the HMMs for all phonemes modeled by the recognition system, the parameters of the Gaussian distributions are shared across states of various phonemes. States which share parameters in this manner are called *tied states* or *senones*. More information on procedures for this parameter sharing can be found in (Hwang & Huang, 1993; Hwang, 1993).

2.3 ASR Performance in Distant-talking Environments

Speech recognition systems operate on the premise that the distributions which model the various sound classes are representative of the speech being recognized. That is, there is an underlying assumption that the test and training data were generated from the same or very similar distributions. More specifically, a speech recognition system that has been trained on clean speech can only be expected to perform accurately when the test data is clean as well. When the test data has been corrupted in some manner, it is no longer well represented by the statistical models of the recognizer, and as a result, performance degrades, *e.g.* (Moreno, 1996). This problem can be alleviated somewhat by subjecting the training data to the exact same distortion as the test speech, and retraining the speech recognition system. However, this situation is impractical, as it is difficult, if not impossible to generate training data in this manner. There is simply too much variability in the sources and levels of distortion possible in the test speech. In distant-talking environments, there are two primary sources of distortion which degrade speech recognition performance: additive noise and reverberation.

2.3.1 The Effect of Additive Noise on Recognition Accuracy

There are several types of noise that can corrupt the speech signal in a distant-talking environment. *Point sources* or *coherent sources* are noise sources with a distinct point of origin, such as a radio or another talker. Such sources propagate to the microphone in much the same manner as the speech signal. On the other hand, when noise of approximately equal energy propagates in all directions at once, a *diffuse noise field* is created. Offices and vehicles are examples of environments where diffuse noise fields commonly exist. Finally, the speech signal can be corrupted by electrical noise in the microphone itself. However, this type of noise generally produces minimal distortion and has a negligible effect on speech recognition performance. In distant-talking environments, the microphone is located at some distance from the user. Because the signal amplitude decays as a function of the distance traveled (Beranek, 1954), the energy of the direct speech signal at the microphone

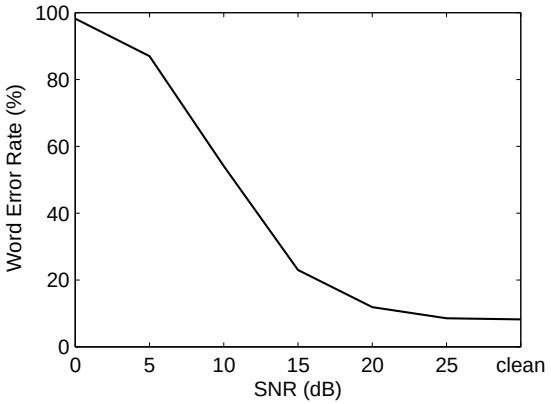

Figure 2.4: WER vs. SNR for speech corrupted by additive white noise when the recognition system is trained on clean speech.

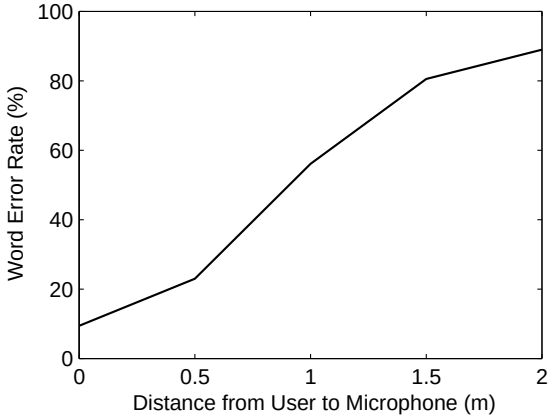

Figure 2.5: WER vs. distance from the user to the microphone in an anechoic room. A fixed white noise source was placed 1 m from the microphone, while the user's distance to the microphone was varied.

decreases as the distance between the user and the microphone increases. As a result, the SNR of the signal captured by the microphone decreases. The decrease in SNR causes an increase in the Word Error Rate (WER) of the speech recognition system.

Figure 2.4 shows the effect of additive noise on speech recognition performance on the Wall Street Journal (WSJ) corpus (Paul & Baker, 1992). The recognition system was trained on clean speech. To generate the test data, white noise was added to clean speech at various SNRs. As the plot shows, the WER increases significantly at SNRs less than 20 dB.

Figure 2.5 shows the effect that the distance from the user to the microphone has on recognition accuracy in an anechoic environment given a noise source at a fixed location. In this experiment, a noise source was placed one meter from the microphone and the user's distance to the microphone was varied between zero and two meters. When the user was one meter from the microphone, the SNR was 10 dB. As the user's distance to the microphone increases and the location of the noise source remains fixed, the SNR of the signal received by the microphone decreases, resulting in an increase in WER.

2.3.2 The Effect of Reverberation on Recognition Accuracy

Reverberation can be loosely defined as the effect an environment, *e.g.* a room, has on the propagation of an acoustic signal produced within it. An acoustic signal will travel in a straight line directly to a receiver located in the room. This is called the *direct path*.

The signal also propagates in all directions, hitting the various surfaces in the room (walls, furniture, other sources, etc.). These surfaces absorb some of the signal's energy and reflect the rest. The reflected signals arrive at the receiver essentially as delayed and attenuated copies of the direct-path signal. Although reverberation is a function of many factors, including the materials covering the surfaces of the room, frequency, temperature, and other acoustical phenomena, it can be modeled quite effectively as a linear Finite-Impulse-Response (FIR) filter. We refer to the impulse response of such a filter as the *room impulse response*. An acoustic signal propagating in a reverberant environment is therefore well modeled by convolving the signal with the room impulse response.

The room impulse response can be obtained either by direct measurement or simulation. The basic method of measuring a room impulse response is to play an impulsive sound from a loudspeaker, record the signal, and then deconvolve the original and recorded signals to obtain the impulse response. A commonly used signal for this task is called the *time-stretched pulse* (TSP). More information about the TSP and the details of the impulse response measurement technique can be found in (Suzuki et al., 1995).

Room impulse responses can also be simulated using a technique called the *image method* (Allen & Berkley, 1979). This method relies on some strong acoustic assumptions in order to create a mathematical model of sound reflections in a rectangular enclosure. Specifically, it assumes that all room surfaces are nearly rigid and the absorption coefficients of the surface materials are frequency independent. In spite of its shortcomings, the image method remains a popular and convenient method for simulating a room impulse response because it requires no actual acoustical measurements and is relatively simple to implement.

Figure 2.6 shows a room impulse response recorded by the TSP method. The notable characteristics of an impulse response are the large initial impulse corresponding the the direct path signal, the impulses corresponding to the first several reflections or *early echos*, and the long tail which is composed of myriads of late reflections decaying in amplitude exponentially.

The reverberation of an enclosure is characterized by its reverberation time, denoted by T_{60} and defined as the time it takes for the energy of a sound source to decay 60 dB immediately after it is turned off.* The impulse response shown in Figure 2.6 was measured in a room with $T_{60} = 0.47$ s. Conference rooms and offices have reverberation times typically on the order of $0.2 - 0.6$ s. In contrast, the reverberation times in large concert halls and auditoriums can be upwards of 2 s.

The effect of reverberation on a speech signal is to smear the signal across time. This

*Reverberation time varies with frequency, and in the acoustics community, is measured and reported as such. However, for our purposes, a single broadband measurement is sufficient.

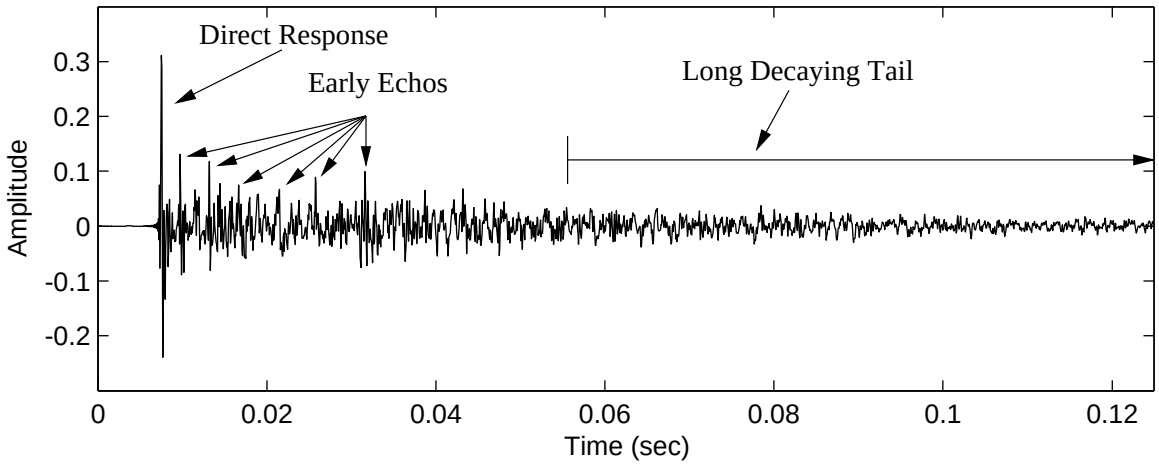

Figure 2.6: The room impulse response from a room with a reverberation time of 0.47 s measured using the TSP method. Only the first 0.125 s of the impulse response is shown here in order to highlight the prominent features.

is quite intuitive if one considers that the room impulse response is simply a collection of delayed and attenuated impulses. The amount of smearing is a function of both the reverberation time, which generally dictates the length of the room impulse response, and the signal-to-reverberation ratio (SRR), the ratio of energy in the direct path impulse to the energy in the remainder of the impulse response. Because of the manner in which the amplitude of speech decays as a function of distance traveled, the SRR is inversely proportional to the distance between the source and the receiver.

Figure 2.7 shows four different spectrograms of the utterance "`AND EXPECTS THE NUMBER`". Figure 2.7a shows the spectrogram of the original close-talking recording. The speech was then convolved with three room impulse responses, with values of T_{60} equal to 0.2 s, 0.5 s, and 0.75 s. The spectrograms of these signals, shown in Figures 2.7b–d, respectively, show the smearing across time caused by reverberation.

The distortion caused by the temporal smearing in a reverberant speech signal results in a degradation in speech recognition performance. The speech energy at a particular time instant or frame, is no longer local to that precise frame, but now is spread over the following frames as well. Because this distortion is spread over multiple frames, conventional frame-based speech recognition compensation techniques fail to improve recognition accuracy in reverberant environments. Figure 2.8 shows the speech recognition performance as a function of reverberation time for the WSJ corpus. In this experiment, the image method

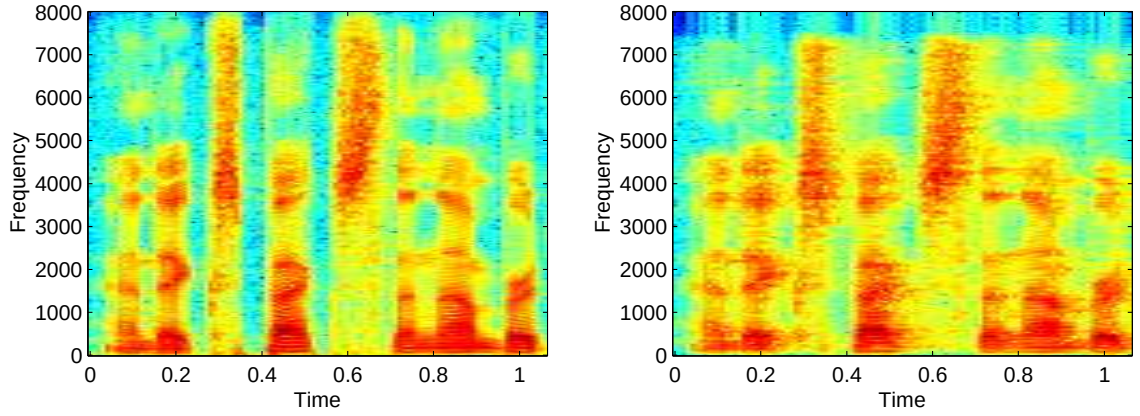

(a) close-talking

(b) T_{60}= 0.2 s

(c) T_{60}= 0.5 s

(d) T_{60}= 0.75 s

Figure 2.7: Wideband spectrograms of the utterance "AND EXPECTS THE NUMBER" for (a) close-talking recording (b) $T_{60} = 0.2$ s (c) $T_{60} = 0.5$ s (d) $T_{60} = 0.75$ s. As the reverberation time increases, the smearing effect increases.

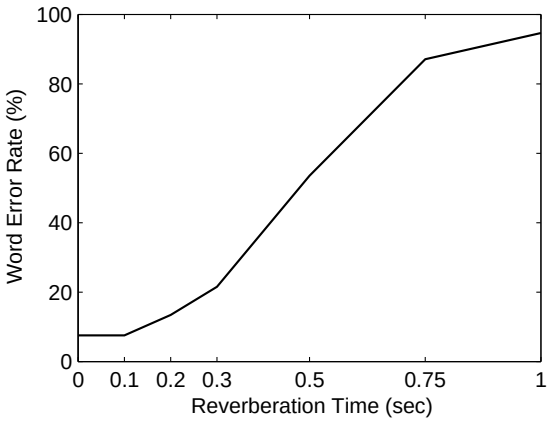

Figure 2.8: WER vs. reverberation time when the recognition system is trained on clean speech recorded from a close-talking microphone.

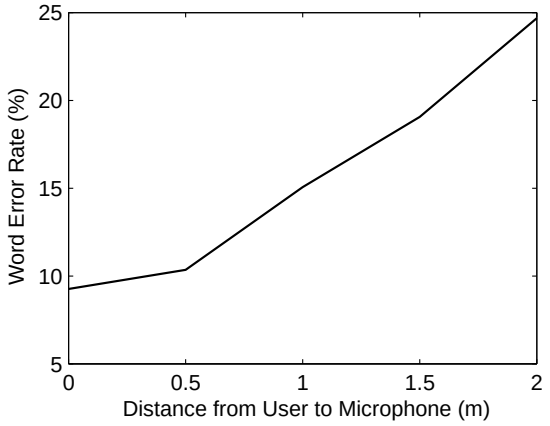

Figure 2.9: WER vs. distance from the user to the microphone in an room with a reverberation time of 0.2 s.

was used to create impulse responses for a room 6 m × 4 m × 3.5 m. The microphone was located in the center of one of the 4 m walls, 1.5 m off the ground. The user was 1.75 m tall and directly in front of the microphone at a distance of 1 m. The room dimensions and source/receiver configuration were kept constant and the absorption coefficients of the room's surfaces were varied, resulting in different reverberation times. The WSJ test utterances were convolved with the impulse responses of rooms of varying reverberation times from 0 s (anechoic) up to 1 s. The recognition was performed using HMMs trained from clean speech. In this experiments, Cepstral Mean Normalization (CMN) (Liu et al., 1992) was applied to the test speech. However, like most feature-domain compensation algorithms, CMN is a frame-based algorithm. Because reverberation smears the energy of each frame of speech across several of the following frames, frame-based approaches such as CMN fail to significantly improve recognition accuracy.

Another experiment was performed in which the room dimensions, microphone location, and reverberation time were all kept constant and the distance between the speaker and the microphone was varied. Figure 2.9 shows the effect that the distance between the user and the microphone has on speech recognition accuracy in an environment with a reverberation time of 0.2 s. Varying the speaker's position in this manner alters the SRR. As the distance between the microphone and the speaker increases, the SRR decreases and as a result, the recognition accuracy decreases as well.

2.4 Summary

In this chapter, the basic operations of an HMM-based speech recognition system have been described. The feature extraction process, by which an incoming speech waveform is converted into a series of MFCC vectors, was described in detail. We then saw how Hidden Markov Models are used to model the distributions of sequences of feature vectors, and how such models can be used to obtain an estimate of the words spoken based on an observed sequence of feature vectors. We then considered the performance of speech recognition systems in distant-talking environments, and showed how recognition accuracy degrades significantly when the speech is distorted by additive noise and reverberation.

In the next chapter, we will discuss how the use of an array of microphones can improve the quality of the received speech signal in distant-talking environments.

Chapter 3

An Introduction to Microphone Array Processing for Speech Recognition

3.1 Introduction

As discussed in the previous chapter, speech signals captured by a microphone located away from the user can be significantly corrupted by additive noise and reverberation. One method of reducing the signal distortion and improving the quality of the signal is to use multiple microphones rather than a single microphone. Array processing refers to the joint processing of signals captured by multiple spatially-separated sensors. Array processing is a relatively mature field, developed initially to process narrowband signals for radar and sonar applications, and then later applied to broadband signals such as speech. More recently, the demand for hands-free speech communication and recognition has increased and as a result, newer techniques have been developed to address the specific issues involved in the enhancement of speech signals captured by a microphone array.

In this chapter, we present a brief overview of microphone array processing and show how it can help reduce the distortion of signals captured in distant-talking scenarios. The major families of array processing methods are described, with specific emphasis on their benefits and drawbacks when used for speech recognition applications. In addition, we discuss some single-channel speech recognition compensation algorithms that have been applied to the output of a microphone array in order to improve the recognition accuracy.

We also use this chapter to introduce the experimental framework used to evaluate the algorithms presented in this thesis. The speech databases and the speech recognition system

used in this thesis are described in detail. Finally, some of the array processing methods described in this chapter are evaluted through a series of speech recognition experiments.

3.2 Fundamentals of Array Processing

The basic premise behind array processing is best illustrated with a simple example. Let us consider two acoustic sources s_1 and s_2 located a distance r_1 and r_2, respectively, from a pair of microphones, $\{m_1, m_2\}$. Source s_1 is equidistant from both microphones ("on-axis"), while source 2 is closer to microphone m_2 than microphone m_1 ("off-axis"). This configuration is shown in Figure 3.1a. We consider the output to be the sum of the signals received by the two microphones. Because the path lengths between source s_1 and the two microphones are equal, signals generated by s_1 will arrive in phase and their combination will amplify the signal by a factor of two. However, the path lengths between source s_2 and the two microphones are different. This difference is dependent on the angle of incidence of the source and the distance between the two microphones, as shown in Figure 3.1b. Because of the difference in path lengths, signals generated by source s_2 will arrive at the two microphones somewhat out of phase and thus combining them will cause signal s_2 to be attenuated.

We now expand this example to consider an arbitrary source $x[n]$ at some location (r, θ) from the center of an array of M microphones spaced linearly with an inter-element spacing d. If the source is assumed to be located in the far-field*, the combined output of M microphones $y[n]$ can be expressed as

$$y[n] = \sum_{m=0}^{M-1} x[n - m\tau] \tag{3.1}$$

where the delay τ can be computed using the speed of sound ν as

$$\tau = \frac{d \cos(\theta)}{\nu} \tag{3.2}$$

If we let $x[n] = \delta[n]$ then $y[n] = h[n]$, the impulse response of the system. We can determine the frequency response of $h[n]$ by taking its discrete Fourier transform using

*A *far-field* source propagates as a plane wave. In contrast, a *near-field* source propagates with a *spherical* wavefront. A source is considered to be in the far-field if $r > 2L^2/\lambda$, where r is the distance to the array, L is the length of the array and λ is the wavelength of the arriving wave.

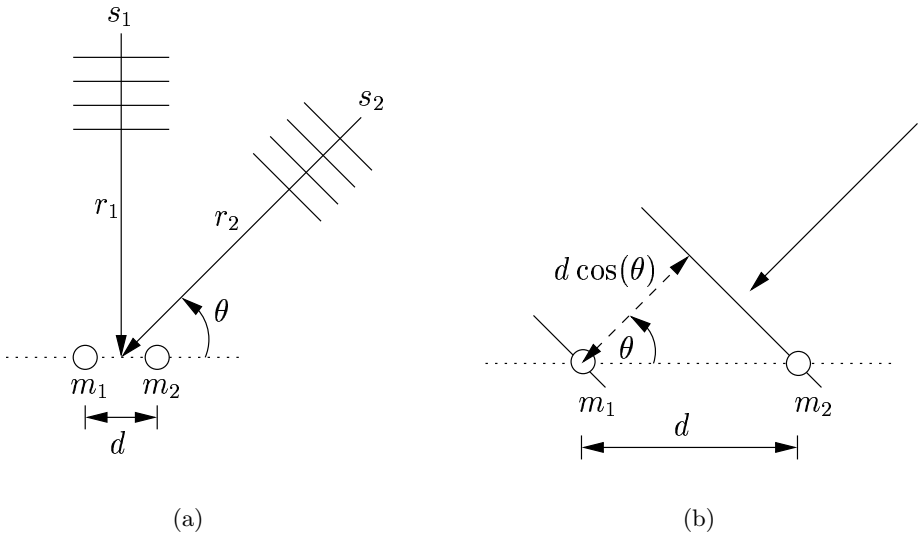

(a) (b)

Figure 3.1: (a) Two acoustic sources propagating toward two microphones. The wavefront of source s_1 arrives at the two microphones simultaneously while the wavefront of source s_2 arrives at microphone m_2 prior to m_1. (b) The additional distance the source travels to m_1 can be determined from the angle of arrival θ and the distance between the microphones d.

Equation (3.1). This gives

$$\begin{aligned} H(\omega,\theta) &= \sum_{m=0}^{M-1} e^{-j2\pi\omega(m\tau)} \\ &= \sum_{m=0}^{M-1} e^{-j2\pi\omega(m(\frac{d\cos(\theta)}{\nu})} \end{aligned} \tag{3.3}$$

As Equation (3.3) indicates, the frequency response is dependent on the number of elements M, the microphone spacing d, the spectral frequency ω and the angle of incidence θ. The spatial response can be visualized by plotting the magnitude of $H(\omega,\theta)$ as a function of θ while d, M, and ω are held fixed . Such a representation, plotted in polar coordinates, is called a *directivity pattern* or *beampattern*. For a given array configuration, the directivity pattern is usually shown for several frequencies. Figure 3.2 shows the directivity patterns over a four-octave frequency range for a linear array of microphones 7 cm apart. The microphone array is located along the $0-180^\circ$ axis. The outer solid line shows the directivity pattern for an array of 4 microphones and the inner dashed line shows the pattern for an array of 8 microphones. These figures demonstrate the key idea of array processing:

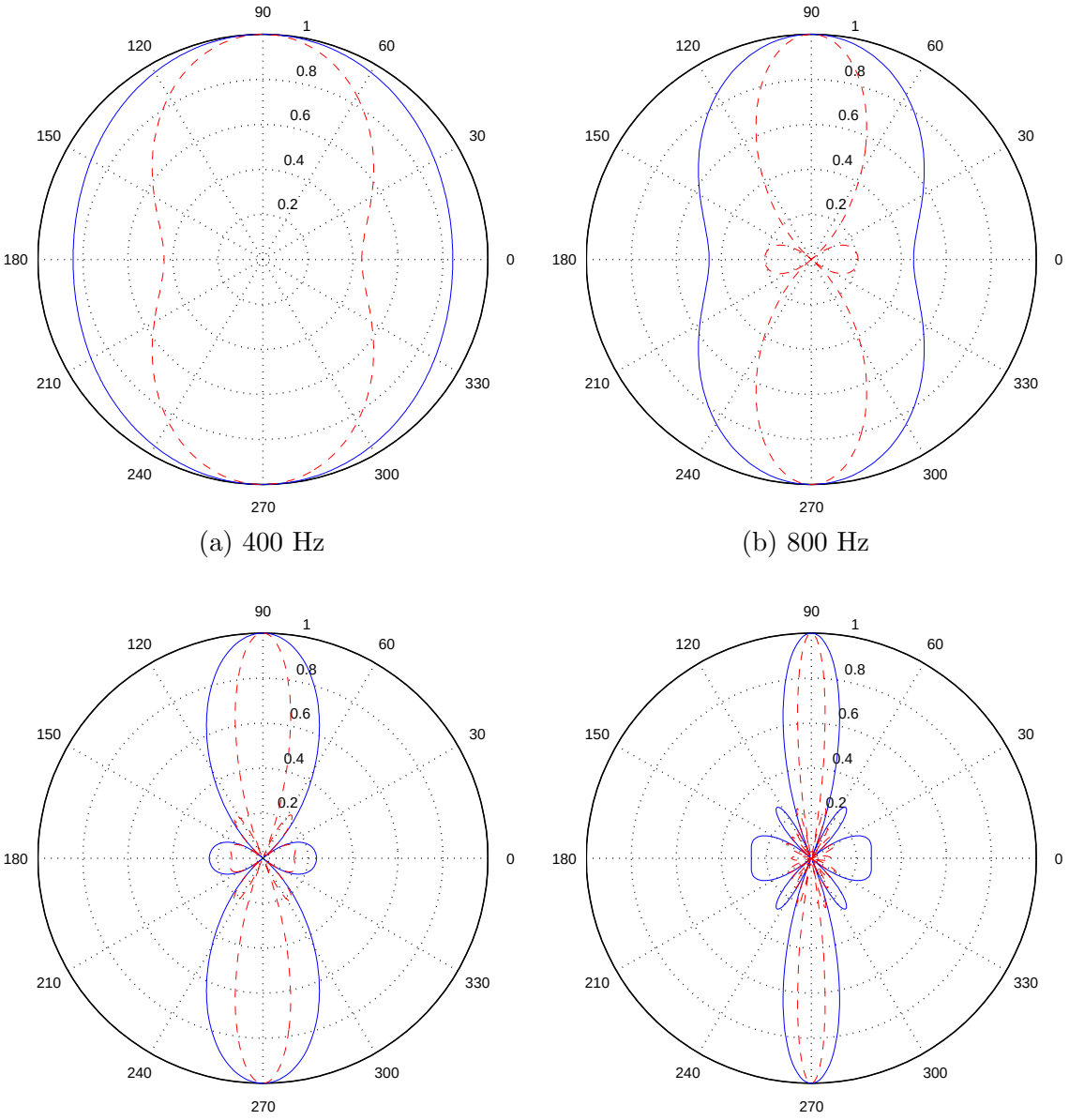

(a) 400 Hz (b) 800 Hz

(c) 1600 Hz (d) 3200 Hz

Figure 3.2: The directivity patterns of a linear microphone array over a four octave frequency range. The solid outer plots show the directivity patterns of a 4-element array while the dashed inner plots correspond to an 8-element array. In both cases, the inter-element spacing is 7 cm.

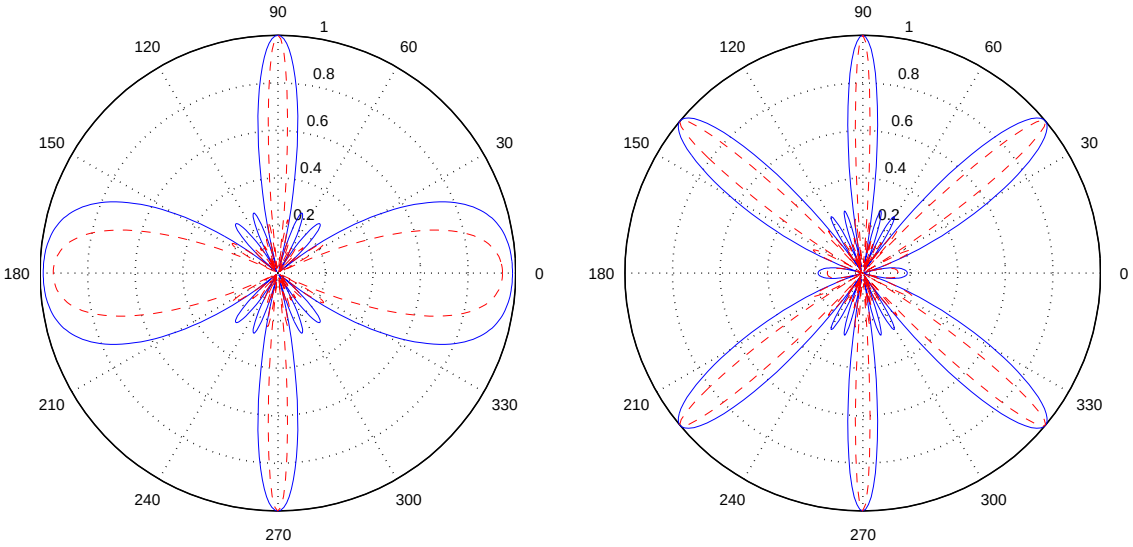

(a) 4800 Hz (b) 6400 Hz

Figure 3.3: The beampatterns for the same microphone array configurations used in Figure 3.2 at frequencies which violate the spatial sampling theorem. The large unwanted sidelobes are the result of spatial aliasing.

By using an array of microphones rather than a single microphone, we are able to achieve spatial selectivity, reinforcing sources propagating from a particular direction, while attenuating sources propagating from other directions.

It is apparent from examining the beampatterns that this "spatial selectivity" varies as a function of frequency. A linear array generally has a wide beamwidth at low frequencies, which narrows as the frequency increases. An array of microphones essentially samples the sound field at different points in space. As a result, array processing is subject to a spatial analog of temporal aliasing that occurs when signals are sampled too slowly. When *spatial aliasing* occurs, the array is unable to distinguish between multiple arrival angles for a given frequency and large sidelobes appear in unwanted directions, as shown in Figure 3.3. To prevent spatial aliasing in linear arrays, the *spatial sampling theorem* must be followed, which states that if λ_{min} is the minimum wavelength of interest and d is the microphone spacing, then $d < \lambda_{min}/2$ (Johnson & Dudgeon, 1993). Spatial aliasing can also be avoided by using a nested harmonic array (Flanagan et al., 1985) or a "randomly distributed" array.

3.3 Microphone Array Processing Approaches

3.3.1 Classical Beamforming

The concept of algorithmically steering the main lobe or *beam* of a directivity pattern in a desired direction is called *beamforming*. The direction the array is steered is called the *look direction*. In order to steer an array of arbitrary configuration and number of sensors, the signals received by the array are first delayed to compensate for the path length differences from the source to the various microphones and then the signals are combined together. This technique, appropriately known as *delay-and-sum beamforming*, can be mathematically expressed simply as

$$y[n] = \sum_{m=0}^{M-1} \alpha_m x_m[n - \tau_m] \tag{3.4}$$

where α_m is a weight applied to the signal received by microphone m. There are several methods for choosing the weights $\alpha_0 \ldots \alpha_{M-1}$. The simplest and most common method is to set them all equal to $1/M$. This technique simply averages the time-aligned signals and is referred to as *unweighted* delay-and-sum beamforming. The process of finding the delays is known as *time-delay estimation* (TDE) and is closely related to the problem of source localization. Many TDE methods exist in the literature, and most are based on cross-correlation. More information about TDE and source localization for speech signals can be found in (Brandstein & Ward, 2001). It can be shown that if the noise signals corrupting each microphone channel are uncorrelated to each other and the target signal, delay-and-sum processing results in a 3 dB increase in the SNR of the output signal for every doubling of the number of microphones in the array (Johnson & Dudgeon, 1993). Many microphone-array-based speech recognition systems have successfully used delay-and-sum processing to improve recognition performance, and because of its simplicity, it remains the method of choice for many array-based speech recognition systems, *e.g.* (Omologo et al., 1997; Hughes et al., 1999). The delay-and-sum beamformer can be generalized to a *filter-and-sum* beamformer where rather than a single weight, each microphone signal has an associated filter and the captured signals are filtered before they are combined. Filter-and-sum beamforming can be expressed as

$$y[n] = \sum_{m=0}^{M-1} \sum_{p=0}^{P-1} h_m[p] x_m[n - p - \tau_m] \tag{3.5}$$

where $h_m[p]$ is the pth tap of the filter associated with microphone m. Clearly, delay-and-sum processing is simply filter-and-sum with a 1-tap filter for each microphone.

Both the delay-and-sum and filter-and-sum methods are examples of fixed beamforming algorithms, as the array processing parameters do not change dynamically over time. If the source moves then the delay values will of course change, but these algorithms are still considered fixed parameter algorithms. In the next section, we give a brief overview of adaptive array processing methods, where parameters are time-varying and adjusted to track changes in the target signal and environment.

3.3.2 Adaptive Array Processing

In adaptive beamforming, the array-processing parameters are dynamically adjusted according to some optimization criterion, either on a sample-by-sample or on a frame-by-frame basis. The Frost algorithm (1972) is arguably the most well-known adaptive beamforming technique. This algorithm is a constrained LMS algorithm in which filter taps (weights) applied to each signal in the array are adaptively adjusted to minimize the output power of the array while maintaining a desired frequency response in the look direction.

Griffiths and Jim (1982) proposed the *Generalized Sidelobe Canceller* (GSC) as an alternative architecture for the Frost beamformer. The GSC consists of two structures, a fixed beamformer which produces a non-adaptive output and an adaptive structure for sidelobe cancellation. The adaptive structure of the GSC is preceded by a *blocking matrix* which blocks signals coming from the look direction. The weights of the adaptive structure are then adjusted to cancel any signal common to both structures. The architecture of the Griffiths-Jim GSC is shown in Figure 3.4.

In some cases, the filter parameters can be calibrated to a particular environment or user. For example, Nordholm et al. (1999) proposed a calibration scheme designed for a hands-free telephone environment in an automobile. A series of typical target signals from the speaker, as well as jammer signals from the hands-free loudspeaker, are captured in the car and used for initial calibration of the parameters of a filter-and-sum beamforming system. These parameters are then adapted during use based on the stored calibration signals and updated noise estimates.

Adaptive-filter methods generally assume that the target and jammer signals are uncorrelated. When this assumption is violated, as is the case for speech in a reverberant environment, the methods suffer from signal cancellation because reflected copies of the target signal appear as unwanted jammer signals. This seriously degrades the quality of the output signal and results in poor speech recognition performance. Van Compernolle (1990)

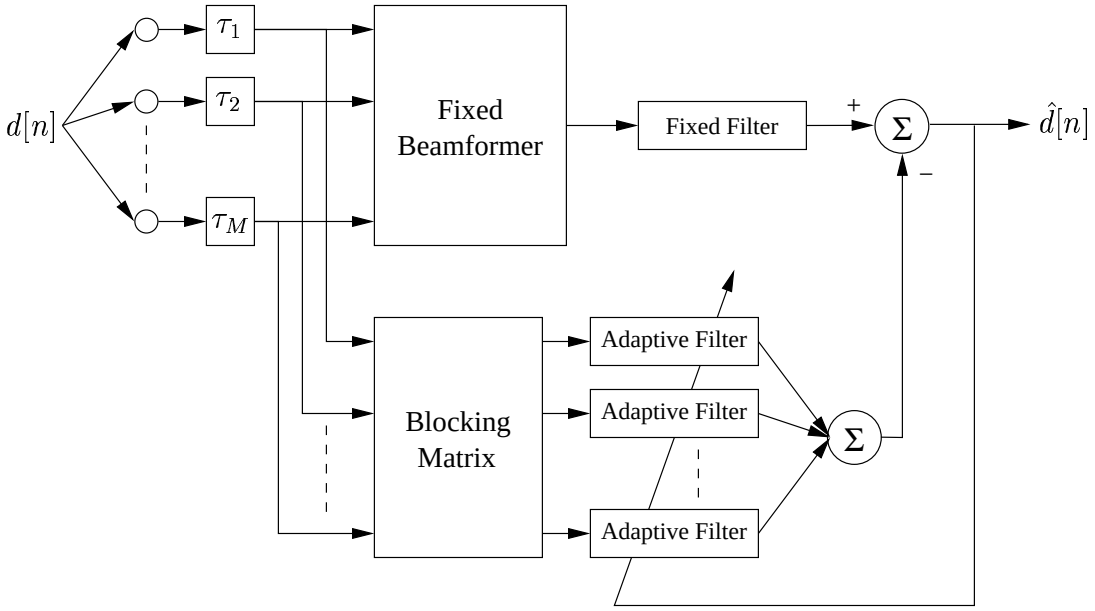

Figure 3.4: The Griffiths-Jim Generalized Sidelobe Canceller

showed that signal cancellation in adaptive filtering methods can be reduced somewhat by adapting the parameters only during silence regions when no speech is present in the signals. Hoshuyama et al. (1999) improved the robustness of the GSC by reducing the signal cancellation that results from tracking errors. However, significant signal cancellation still arises from the target signal reflections in reverberant environments. As a result, conventional adaptive filtering approaches have not gained widespread acceptance for speech recognition applications.

3.3.3 Additional Microphone Array Processing Methods

Dereverberation Techniques

As discussed in Chapter 2, reverberation is a significant cause of poor speech recognition performance in microphone-array-based speech recognition systems. Because traditional beamforming methods do not successfully compensate for the negative effects of reverberation on the speech signal, much recent research has focused on this area. One obvious approach to dereverberation is to estimate and then invert the room impulse response. However, room impulse responses are generally non-minimum phase (Neely & Allen, 1979) which causes inverse dereverberation filters to be unstable. As a result, approximations to the true inverse of the transfer functions have to be used. Miyoshi and Kaneda (1988)

show that if multiple channels are used and the room transfer functions of all channels are known *a priori*, the exact inverse is possible to obtain if the transfer functions have no common zeros. However, concerns about the numerical stability and hence, practicality, of this method have been raised because of the extremely large matrix inversions required (Putnam et al., 1995; Silverman et al., 1996).

Another class of algorithms attempts to exploit characteristics of the speech signal or room transfer functions to perform dereverberation. For example, Gillespie et al. (2001) maximized the kurtosis of the linear prediction residual of the speech signal to perform dereverberation. While they reported significant dereverberation as measured by informal listening tests, little improvement in speech recognition performance was achieved (Malvar, 2002). Liu et al. (1996) break up room transfer functions into minimum phase and all-pass components and process these components separately to remove the effects of reverberation. However, even in simulated environments, they report implementation difficulties in applying this method to continuous speech signals.

Flanagan et al. (1993) approach dereverberation as a matched filter problem. They measure the transfer function of the source-to-sensor room response for each microphone and then use a truncated, time-reversed version of this estimate as a matched-filter for that source-sensor pair. The matched filters are used in a filter-and-sum manner to process the array signals. While the authors are able to demonstrated that the matched filter approach has theoretical benefits over conventional delay-and-sum beamforming in terms of SNR, the matched filter approach provides minimal improvements in recognition accuracy over conventional delay-and-sum processing (Gillespie & Atlas, 2002).

Most of these dereverberation methods require that the room transfer functions from the source to each microphone in the array be static and known *a priori*. While the transfer functions can be measured, this is both inconvenient and unrealistic, as it requires the use of additional hardware to estimate the impulse responses. Furthermore, the transfer functions are assumed to be fixed, which implies that the location of the talker and the environmental conditions in the room will not change over time. Even with such knowledge, these methods have not proven to be substantially more effective than classical array processing approaches at improving speech recognition performance.

Blind Source Separation

Blind source separation (BSS) can also be interpreted as a microphone array processing problem, *e.g.* (Kurita et al., 2000). In the general BSS framework, observed signals from multiple sensors are assumed to be the result of a combination of source signals and some

unknown mixing matrix. In one family of BSS techniques, called *independent component analysis* (ICA), the inverse of this unknown mixing matrix is estimated in the frequency domain for each DFT bin independently using iterative optimization methods (Bell & Sejnowski, 1995). Using this estimated inverse matrix, the microphone signals are "separated" on a frequency-component basis and then recombined to form the output signals. Informal listenings of the separation produced by this method applied to a recording of two sources captured by two microphones were quite compelling. However, in practice, frequency-domain BSS algorithms often suffer from a permutation problem, *i.e.* there is no guarantee that the separated frequency components at a particular output will always correspond to the same speaker. Furthermore, these methods assume that the number of competing sound sources is both known *a priori* and less than or equal to the number of microphones present. Acero et al. (2000) attempt to relieve some of these problems by removing some of "blindness" in the source separation. They consider the source mixtures to contain only one signal, the target speech signal of interest, and treat the other signal as unwanted noise. A probabilistic model of speech (a vector quantized codebook of linear prediction coefficient vectors trained from clean speech) is then used to guide the source separation process to obtain the desired signal. However, no measurable results of the performance of this method were given, and the authors reported that performance of this method varied widely (Acero, 2002). Araki et al. (2003) performed an analysis of frequency-domain BSS for the separation of convolutive mixtures of speech. They found that BSS is in fact equivalent to conventional adaptive beamforming, and therefore cannot produce significant dereverberation.

Auditory Model-based Array Processing

The auditory system is an excellent array processor, capable to isolating target signals in extremely difficult acoustic conditions with only two sensors. In auditory model-based methods, no output waveform is produced, but rather some representation of the processing believed to occur in the auditory system. Features can be extracted from this auditory representation and used directly in speech recognition. Sullivan and Stern (1993) devised such a scheme in which the speech from each microphone was bandpass filtered and then the cross-correlations among all the microphones in each subband were computed. The peak values of the cross-correlation outputs were used to derive a set of speech recognition features. Processing the speech in this manner produced only marginal improvements in speech recognition accuracy over delay-and-sum processing and was realized only at great computational cost.

3.4 Speech Recognition Compensation Methods

Once the multiple array signals have been processed into a single output signal, there are several classical single-channel speech recognition compensation techniques that can be used to try to improve the recognition performance further. In this section we review some of those that have been applied to microphone-array-based speech recognition.

3.4.1 CDCN and VTS

Codeword Dependent Cepstral Normalization (CDCN) (Acero, 1993) and Vector Taylor Series (VTS) (Moreno, 1996) are compensation methods that assume an analytical model of the environmental effects on speech. Noisy speech is assumed to be clean speech that has been passed through a linear filter and then corrupted by additive noise. This model is represented in the cepstral domain by the following non-linear equation

$$\mathbf{z} = \mathbf{x} + \mathbf{h} + IDFT\left\{\log\left(1 + e^{DFT(\mathbf{n}-\mathbf{h}-\mathbf{x})}\right)\right\} \tag{3.6}$$

which relates the cepstrum of the noisy speech $\mathbf{z}$ to the cepstrum of the clean speech $\mathbf{x}$, the cepstrum of the unknown noise $\mathbf{n}$, and the cepstrum of the impulse response of the unknown filter, $\mathbf{h}$.

Both CDCN and VTS are algorithms that assume no *a priori* knowledge of the filter or the noise. These methods estimate the parameters by maximizing the likelihood of the observed cepstra of noisy speech, given a Gaussian mixture distribution for the cepstra of clean speech. Since the transformation that relates the noisy cepstra to the clean cepstra is nonlinear, both CDCN and VTS approximate it as a truncated Taylor series in order to estimate it. While CDCN uses a zeroth-order Taylor series approximation, VTS uses a first-order approximation. The estimated filter and noise parameters are then used to estimate the clean cepstra from the noisy cepstra or to adapt the HMMs to reflect the noisy conditions of the speech to be recognized. Both CDCN and VTS are highly efficient at medium levels of noise, *i.e.* at SNRs of 10 dB and above, but VTS performs slightly better. However, both algorithms assume that the noise is stationary, and thus, both perform poorly when this assumption is violated. Sullivan (1996) applied CDCN to features derived from both delay-and-sum beamforming and cross-correlation-based auditory processing with improvements in recognition performance seen in both cases. However, both CDCN and VTS are frame-based compensation schemes, so the improvement obtained in highly reverberant environments is expected to be limited.

3.4.2 Maximum Likelihood Linear Regression

Maximum Likelihood Linear Regression (MLLR) assumes that the Gaussian means of the state distributions of the Hidden Markov Models (HMM) representing noisy speech are related to the corresponding clean speech Gaussian means by a linear regression (Leggetter & Woodland, 1994). The regression has the form

$$\boldsymbol{\mu}_n = \mathbf{A}\boldsymbol{\mu}_c + \mathbf{b} \tag{3.7}$$

where $\boldsymbol{\mu}_n$ is the Gaussian mean vector of the noisy speech, $\boldsymbol{\mu}_c$ is the Gaussian mean vector of the clean speech and $\mathbf{A}$ and $\mathbf{b}$ are regression factors that transform $\boldsymbol{\mu}_c$ to $\boldsymbol{\mu}_n$. These parameters are estimated from noisy adaptation data to maximize the likelihood of the data. MLLR adaptation can be either supervised or unsupervised. In the supervised adaptation scheme, MLLR requires a set of adaptation data to learn the noisy means. For the unsupervised adaptation scheme, the adaptation is performed on the data to be recognized itself. MLLR has been observed to work very well in many situations, including microphone array environments (Giuliani et al., 1998). However, since the adapted models are assumed to be truly representative of the speech to be recognized, all of the adaptation data and the test data need to be acoustically similar. This amounts to requiring that the corrupting noise be quasi-stationary. Furthermore, the performance of MLLR is dependent on the amount of adaptation data available. In microphone array environments, it is unrealistic in many cases to have such data in abundance, as environmental conditions simply change too fast, and the adaptation data are no longer representative of the current acoustical environment.

3.5 Speech Recognition with Microphone Arrays

This thesis is concerned with improving speech recognition performance in noisy and reverberant environments using microphone arrays. As such, recognition accuracy is the only measure suitable for judging the performance of array processing algorithms. As described in this chapter, microphone array processing methods are designed according to various waveform-level criteria, *e.g.* maximum SNR, maximum array gain, or minimum mean squared error. However, generating an improved output waveform does not necessarily result in improved recognition accuracy. As a result, throughout this thesis, array processing methods will be judged primarily on the basis of recognition accuracy.

3.5.1 Experimental Setup and Corpora

Throughout this thesis, Sphinx-3, an HMM-based large-vocabulary speech recognition system (Placeway et al., 1997), was used for all speech recognition experiments. The system was trained using the speaker-independent WSJ training set, which consists of 7000 utterances. The system was trained using 39-dimensional feature vectors consisting of 13-dimensional MFCC parameters, along with their delta and delta-delta parameters, computed as described in Section 2.2.1. A 25-ms window duration and a frame rate of 100 frames per second, corresponding to a 10-ms frame shift, were used. Context-dependent 3-state left-to-right HMMs with no skips were trained and each state distribution was modeled by a mixture of 8 Gaussians. The system had a total of 4000 senones. Cepstral mean normalization (CMN) was performed on the training utterances.

In order to test recognition performance under a variety of noise and reverberation conditions, a variety of microphone array corpora were used for the experiments in this thesis.

CMU 8-Microphone Linear Array Corpus

This corpus, hereafter referred to as "CMU-8", was recorded by Sullivan (1996) in the CMU Robust Speech Recognition Laboratory. The utterances were recorded by a linear microphone array with 8 elements spaced 7 cm apart. The array was placed on a desk and the user was seated directly in front of the array at a distance of 1 m. Each user wore a close-talking microphone during the recording, so each array recording has a corresponding clean control recording. The sampling rate for the recording was 16 kHz. The laboratory had multiple noise sources, including several computer fans and overhead air blowers. The reverberation time of the room was measure to be 240 ms. The average SNR of the recordings is 6.5 dB. The corpus consists of 140 utterances (10 speakers $\times$ 14 utterances). The utterances consist of strings of keywords as well as alphanumeric strings, where the user spelled out answers to various census questions, *e.g.* name, address, etc. Speech recognition was performed using a flat unigram language model. While the vocabulary size of this corpus is small (138 words), it is nevertheless a challenging recognition task for two reasons. First, recognition is performed without the use of any linguistic or syntactic information. Second, the vocabulary consists of many acoustically confusable words.

ATR Reverberant 7-Microphone Linear Array Corpus

Researchers from ATR in Japan created a microphone array database consisting of room impulse responses recorded in several different rooms of varying size and reverberation times

using a 14-channel linear array and a 16-channel circular array (Nakamura et al., 2000). The recordings were made using the TSP method described in Section 2.3.2.

These impulse responses were used to create reverberant WSJ corpora by convolving the utterances from the WSJ test set with the impulse responses from 7 channels of the linear array. Five test sets, with T_{60} from 0.3 to 1.3 s were created. In all cases, the spacing between the microphones was 5.66 cm and the speaker was directly in front of the array at a distance of 2 m. The sampling rate was 16 kHz. The WSJ test set has a 5000 word vocabulary. Recognition was performed using a trigram language model. These corpora will be referred to as $\text{WSJ}_{T_{60}}$ with a subscript indicating the reverberation time, *e.g.* the corpus from a room with $T_{60} = 0.3$ s will be referred to as $\text{WSJ}_{0.3}$.

3.5.2 Evaluating Performance and Determining Statistical Significance

The merit of the various array processing algorithms presented in this thesis will be judged primarily by comparing the speech recognition accuracy obtained using these methods to that obtained using a conventional array processing algorithm. Recognition accuracy is determined by comparing the word string generated by the recognizer, *i.e.* the *hypothesis*, to the word string actually spoken by the user, *i.e.* the *reference*, using a non-linear string matching program. The *Word Error Rate* (WER) is computed as ratio of the total number of errors, including insertions, deletions, and substitutions, to the total number of tokens in the reference transcription.

When speech recognition accuracy is used as the means of comparing two algorithms, it is important to verify that any apparent difference in the performance of the two algorithms is statistically significant. Several methods of evaluating statistical significance for speech recognition applications have been proposed. One widely accepted method for doing so is the Matched-Pairs test proposed by Gillick and Cox (1989), which assumes that recognition errors are independent across speech segments, but not within each segment. This method has been adopted by the National Institute of Standards and Technology (NIST) for use in standard speech recognition evaluations, and is the method we use in this thesis as well.

The statistical significance of a particular outcome is dependent on many factors including the difference in the error rates of the competing algorithms, the number of segments or *utterances* in the test set, the size of the vocabulary, the grammar, and the overall range of accuracy. Except where noted, the results in this thesis are statistically significant with $p \leq 0.01$.

3.5.3 Recognition Results

The first series of experiments was performed on the CMU-8 corpus to determine the recognition accuracy obtained using conventional delay-and-sum beamforming. For each utterance, the array signals were upsampled by a factor of 3 to increase temporal resolution and the delays in each channel were estimated using the Phase Transform (PHAT) method (Knapp & Carter, 1976). The channels were then aligned based on the estimated delays and downsampled to their original sampling rate. The aligned channels were then averaged to generate the unweighted delay-and-sum output signal. MFCC feature vectors were then extracted from the output signal and passed to the recognition system for decoding. CMN was applied to the feature vectors prior to decoding. Experiments were performed using 2, 4, and 8 channels of the array.

Additionally, experiments were performed using the Griffiths-Jim GSC. As expected, when the adaptation was performed continuously, the algorithm produced a severely distorted output signal due to signal cancellation and the recognition performance was significantly worse than even single-channel recognition. When the adaptation was only performed during the silence segments, as suggested by Van Compernolle (1990), performance improved, but even with a large number of filter parameters, the performance was only marginally better than delay-and-sum processing.

Figure 3.5 shows the word error rate (WER) for the CMU-8 corpus with only a single channel and with delay-and-sum beamforming using 2, 4, and 8 array channels. The figure also shows the performance of using the GSC method with all 8 channels when 50 and 200 taps are used in the adaptive filters. The performance did not improve when more taps were used. The performance using the close-talking microphone, indicating the upper bound on performance, is shown as well.

As the figure indicates, microphone array processing provides a significant improvement in recognition accuracy over a single channel alone. However, while performing delay-and-sum beamforming on 8 channels is able to reduce the relative WER by more than 40% compared to a single channel, the performance is still more than 100% worse than that obtained with a close-talking microphone. Furthermore, it is apparent that adaptive array processing algorithms, such as the GSC, which depend on the assumption that the signals coming from directions other than the look direction are uncorrelated with the target signal do not improve speech recognition over classical delay-and-sum beamforming, and in fact often perform worse.

These experiments were repeated for the reverberant WSJ corpora. Based on the previous results, only delay-and-sum beamforming was performed. The results for these ex-

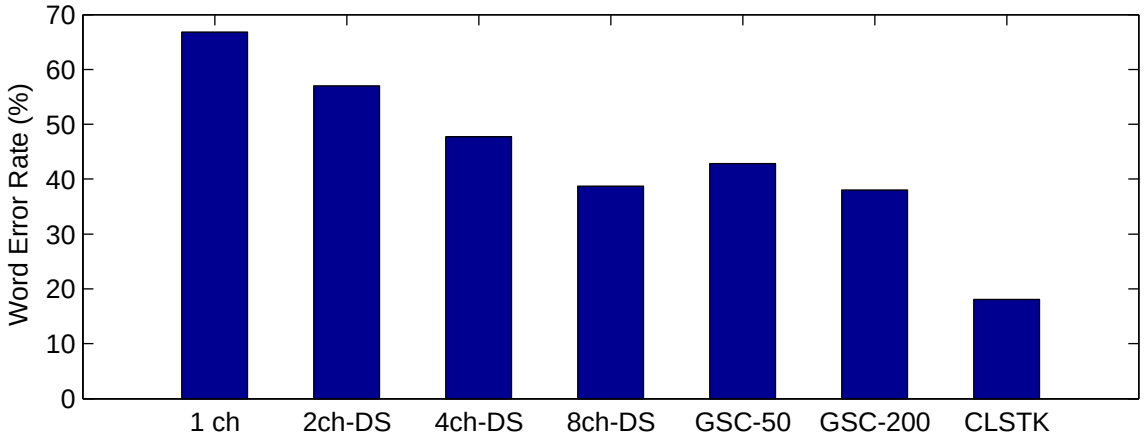

Figure 3.5: Speech recognition performance on the CMU-8 corpus using a single channel, delay-and-sum beamforming, and the GSC adapting only during silence regions. The performance of delay-and-sum is shown for 2, 4, and 8 channels, and the performance of the GSC is shown using 8 channels and adaptive filters with 50 and 200 taps. The performance obtained using a close-talking microphone is also shown.

periments are shown in Figure 3.6. While delay-and-sum processing is able to improve speech recognition over a single channel alone, the improvement is smaller in an environment dominated by reverberation rather than noise. Additionally, as the figure indicates, the relative improvement obtained using delay-and-sum beamforming rather than a single channel decreases substantially as the reverberation time increases.

Finally, the level of performance indicated by Figures 3.5 and 3.6 raises the question of how much improvement in WER must be made in order for a speech recognizer deployed in such distant-talking environments to be considered *usable*. However, this question is difficult to answer because in most ASR-based applications, the recognition engine is only one of many components of a complex dialog system, *e.g.* (Rudnicky et al., 1999). These dialog systems are typically evaluated not on the basis of WER, but according to higher-level measures such as user satisfaction and task completion rate, which are dependent on many factors in addition to WER (Walker et al., 2002). Furthermore, many of these systems employ error-handling techniques, *e.g.* (Hazen et al., 2002), aimed at improving the robustness of the system to recognition errors. As a result, it is possible for a well-crafted dialog system to achieve high user satisfaction and a high task completion rate even in the presence of a significant number of recognition errors (Sanders et al., 2002).

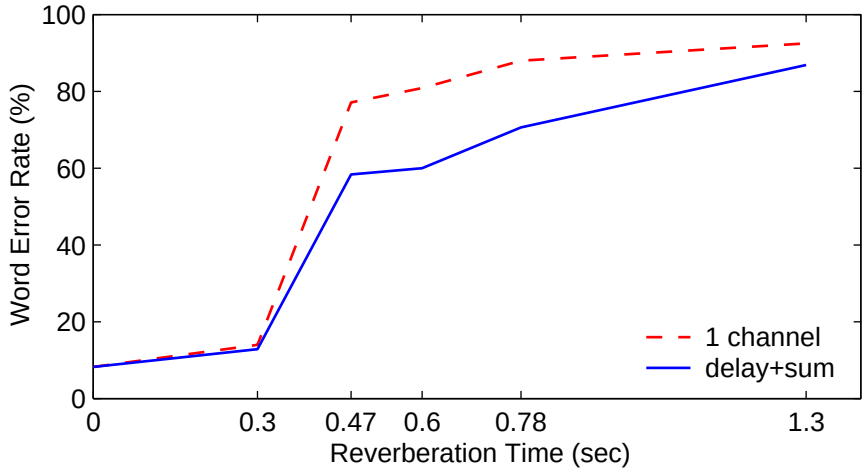

Figure 3.6: WER obtained on the reverberant WSJ corpora using a single microphone and delay-and-sum beamforming, shown as a function of reverberation time. The performance using clean speech is shown as a reverberation time of 0 s.

3.6 Summary

In this chapter, we have presented an overview of array processing techniques that have been developed for multi-channel speech processing and examined their suitability for use in speech recognition applications. We also described some compensation algorithms originally developed for single-channel speech recognition that have been successfully applied to microphone-array-based speech recognition.

Conventionally, microphone array processing has been viewed as a means of improving the quality of a speech *waveform* captured in a distant-talking environment. As shown in Section 3.5, speech recognition with microphone arrays is performed by using one of these methods to generate the best output waveform possible which then gets treated as a single-channel input to the recognizer.

This approach to microphone-array-based speech recognition ignores a fundamental difference in the objectives of the two systems. In array processing, the goal is to produce a distortion-free waveform. On the other hand, the goal of speech recognition is to hypothesize the correct transcription of the utterance that was spoken. As described in Chapter 2, this is performed by maximizing the likelihood of the speech recognition features derived from the waveform.

Maintaining this dichotomy between the objective criteria of two systems limits the performance of the system as a whole. Simply put, generating an enhanced waveform does

not necessarily improve recognition. The array processing scheme can only be expected to improve recognition if it results in a sequence of features which maximizes, or at least increases, the likelihood of the correct transcription.

We believe that this is why many array processing algorithms that are capable of generating significantly better output waveforms than simpler methods do not also produce comparable gains in speech recognition accuracy. In the next chapter, we present a framework for a new array processing methodology specifically designed for improved speech recognition performance.

Chapter 4

Likelihood Maximizing Beamforming

4.1 Introduction

Microphone array processing methods have historically been designed according to principles pertinent to signal enhancement applications. These algorithms are usually concerned with generating the optimal output waveform and as such, they process the array signals according to various signal-level criteria, *e.g.* minimizing signal error or maximizing SNR. However, such criteria do not necessarily result in an improvement in the features subsequently derived for input to a speech recognition system. As a result, complicated array processing schemes which are capable of producing high quality output signals may not result in significant improvements in speech recognition accuracy over much simpler methods, such as delay-and-sum beamforming.

These methods approach the problem of microphone array processing for speech recognition as a signal processing problem. However, as described in Chapter 2, speech recognition is not a signal processing problem but rather a pattern classification problem. Sound classes are modeled by probability distribution functions. The speech waveform is converted into a sequence of features vectors and the recognizer then compares these vectors to the statistical class models. The output is a label corresponding to the sound class or sequence of sound classes that has the maximum likelihood of generating the observed vectors. Therefore, in order to improve speech recognition performance, the likelihood of the correct class must be maximized, or at least increased relative to the other (incorrect) classes for a given input. In order to do so, the following must be considered:

1. the manner in which information is input to the recognition system, *i.e.* the feature extraction process

2. the manner in which these features are processed by the recognizer in order to generate a hypothesis

Thus, we recast the microphone array processing problem as one of finding the set of array parameters which maximizes the likelihood of the correct hypothesis. In this chapter, we present a solution to this problem in which these considerations are incorporated into the framework of a filter-and-sum beamformer. We refer to this approach as *LIkelihood MAximizing BEAMforming* (LIMABEAM). In this approach, information from the speech recognition system itself will be used to find the array parameters that improve speech recognition performance.

4.2 Filter-and-Sum Array Processing

In this work, we assume that filter-and-sum array processing can effectively compensate for the distortion induced by additive noise and reverberation. In the filter-and-sum architecture, each microphone in the array has a corresponding filter. The signal captured by each microphone is convolved with its corresponding filter and the filter outputs are then summed together. Time-delay compensation may be applied prior to filtering, or may be incorporated into the filters themselves, simply as a time-shift of the coefficients.

Assuming the filters have a finite impulse response (FIR), filter-and-sum processing is expressed mathematically as

$$y[n] = \sum_{m=0}^{M-1} \sum_{p=0}^{P-1} h_m[p] x_m[n - p - \tau_m] \tag{4.1}$$

where M is the number of microphones in the array, P is the length of the FIR filters, and τ_m is the delay induced in the signal received by microphone m to align it to the other array channels.

We define $\boldsymbol{\xi}$ to be the vector of all filter coefficients for all microphones, as

$$\boldsymbol{\xi} = [h_0[0], h_0[1], \ldots, h_{M-1}[P-2], h_{M-1}[P-1]]^T \tag{4.2}$$

Conventionally, filter parameters are chosen to optimize the beampattern, minimize signal distortion, or suppress interfering signals, *i.e.* criteria that focus on the notion of a *desired signal*. In contrast, because our goal is improved speech recognition performance, we

consider the output waveform $y[n]$ to be incidental and desire to find the filter parameters that optimize recognition accuracy. Therefore, we forgo the notion of a desired signal, and instead focus on a *desired hypothesis*.

4.3 Likelihood Maximizing Beamforming (LIMABEAM)

Speech recognition systems operate by finding the word string most likely to generate the observed sequence of feature vectors, as measured by the statistical models of the recognition system. In Chapter 2, we described how this can be performed according to Bayes optimal classification as

$$\hat{\boldsymbol{w}} = \underset{\boldsymbol{w}}{\operatorname{argmax}}\ P(\mathcal{Z}|\boldsymbol{w})P(\boldsymbol{w}) \tag{4.3}$$

where $\mathcal{Z} = \{\boldsymbol{z}_1, \boldsymbol{z}_2, \ldots, \boldsymbol{z}_T\}$ is the sequence of observed feature vectors, $\boldsymbol{w} = \{w_1, w_2, \ldots, w_N\}$ represents a possible word string and $P(\mathcal{Z}|\boldsymbol{w})$ and $P(\boldsymbol{w})$ are the corresponding acoustic and language scores, respectively.

When speech is captured by a microphone array, the feature vectors $\mathcal{Z}$ are a function of both the incoming speech and the array processing parameters, $\boldsymbol{\xi}$. By rewriting Equation (4.3) to reflect the influence the array parameters have on recognition, we can see that in microphone array scenarios, speech recognition is performed as

$$\hat{\boldsymbol{w}} = \underset{\boldsymbol{w}}{\operatorname{argmax}}\ P(\mathcal{Z}(\boldsymbol{\xi})|\boldsymbol{w})P(\boldsymbol{w}) \tag{4.4}$$

Our goal is to find the parameter vector $\boldsymbol{\xi}$ that will optimize recognition performance. One logical approach to doing so is to choose the array parameters that maximize the likelihood of the correct transcription of the utterance that was spoken. This will increase the difference between the likelihood score of the correct transcription and the scores of competing incorrect hypotheses, and thus, increase the probability that the correct transcription will be hypothesized.

For the time being, let us assume that the correct transcription of the utterance, which we notate as $\boldsymbol{w}_C$, is known. We can then maximize Equation (4.4) for the array parameters $\boldsymbol{\xi}$, as

$$\hat{\boldsymbol{\xi}} = \underset{\boldsymbol{\xi}}{\operatorname{argmax}}\ P(\mathcal{Z}(\boldsymbol{\xi})|\boldsymbol{w}_C)P(\boldsymbol{w}_C) \tag{4.5}$$

Because the transcription is assumed to be known *a priori*, $P(\boldsymbol{w}_C)$ will not change

regardless of the value of $\boldsymbol{\xi}$ and can be neglected. The maximum likelihood (ML) estimate of the array parameters can now be defined as the vector that maximizes the acoustic likelihood of the given sequence of words. This can be expressed as

$$\hat{\boldsymbol{\xi}} = \underset{\boldsymbol{\xi}}{\operatorname{argmax}}\, P(\mathcal{Z}(\boldsymbol{\xi})|\boldsymbol{w}_C) \tag{4.6}$$

In an HMM-based speech recognition system, the acoustic likelihood $P(\mathcal{Z}(\boldsymbol{\xi})|\boldsymbol{w}_C)$ is computed as the total likelihood of all possible paths, *i.e.* state sequences, through $\text{HMM}_{\boldsymbol{w}_C}$, the HMM for the sequence of words in the transcription $\boldsymbol{w}_C$. If $\mathcal{S}_C$ represents the set of all possible state sequences through $\text{HMM}_{\boldsymbol{w}_C}$, and $\boldsymbol{s}$ represents one such state sequence, then the maximum likelihood estimate of $\boldsymbol{\xi}$ can be written as

$$\hat{\boldsymbol{\xi}} = \underset{\boldsymbol{\xi}}{\operatorname{argmax}} \sum_{\boldsymbol{s}\in\mathcal{S}_C} \left(\prod_i P(\boldsymbol{z}_i(\boldsymbol{\xi})|s_i) P(s_i|s_{i-1}, \boldsymbol{w}_C) \right) \tag{4.7}$$

While the maximum likelihood formulation is computed over all possible state sequences for a given transcription, many of these sequences are highly unlikely. For computational efficiency, we assume that the likelihood of a given transcription is largely represented by the single most likely state sequence through $\text{HMM}_{\boldsymbol{w}_C}$. Under this assumption, the ML estimate of $\boldsymbol{\xi}$ becomes

$$\hat{\boldsymbol{\xi}} = \underset{\boldsymbol{\xi},\boldsymbol{s}\in\mathcal{S}_C}{\operatorname{argmax}} \prod_i P(\boldsymbol{z}_i(\boldsymbol{\xi})|s_i) P(s_i|s_{i-1}, \boldsymbol{w}_C) \tag{4.8}$$

It will be more convenient and entirely equivalent to maximize the log likelihood rather than the likelihood itself. Thus, Equation (4.8), becomes

$$\hat{\boldsymbol{\xi}} = \underset{\boldsymbol{\xi},\boldsymbol{s}\in\mathcal{S}_C}{\operatorname{argmax}} \left\{ \sum_i \log(P(\boldsymbol{z}_i(\boldsymbol{\xi})|s_i) + \sum_i \log(P(s_i|s_{i-1}, \boldsymbol{w}_C) \right\} \tag{4.9}$$

According to Equation (4.9), in order to find $\hat{\boldsymbol{\xi}}$, the likelihood of the correct transcription must be *jointly optimized* with respect to both the array parameters and the state sequence. This joint optimization can be performed by alternately optimizing the state sequence and the array processing parameters in an iterative manner, *i.e.* fixing the array parameters and finding the optimal state sequence, then fixing the state sequence and finding the optimal array parameters, and so on. This approach corresponds to alternately optimizing the left and right summation terms in Equation (4.9).

In the following sections, we describe how to optimize the state sequence and the array

parameters.

4.4 Optimizing the State Sequence

Given set of array parameters $\boldsymbol{\xi}$, the speech can be processed by the array and a sequence of feature vectors $\mathcal{Z}(\boldsymbol{\xi})$ produced. Using the features vectors and the transcription $\boldsymbol{w}_C$, we want to find the state sequence $\hat{\boldsymbol{s}} = \{\hat{s}_1, \hat{s}_2, \ldots, \hat{s}_T\}$ such that

$$\hat{\boldsymbol{s}} = \underset{\boldsymbol{s} \in \mathcal{S}_C}{\operatorname{argmax}} \sum_i \log(P(s_i | s_{i-1}, \boldsymbol{w}_C, \mathcal{Z}(\boldsymbol{\xi})) \tag{4.10}$$

This state sequence $\hat{\boldsymbol{s}}$ can be determined using the Viterbi algorithm (Viterbi, 1967). This procedure is known as *forced alignment* or *Viterbi alignment*. In forced alignment, the sentence HMM corresponding to the given transcription is assembled and then the alignment between the states of the HMM and the given sequence of feature vectors that results in the maximum overall likelihood is found using dynamic programming. This is done in an efficient, recursive manner by exploiting the fact that the underlying random process modeled by the HMM (in this case, speech), is assumed to be Markov. More details about forced alignment can be found in (Rabiner & Juang, 1993; Jelinek, 1997).

4.5 Optimizing the Array Parameters

We now turn to the question of how to find the array parameters which maximize the likelihood of a given state sequence, $\hat{\boldsymbol{s}}$. That is, we are interested in finding $\hat{\boldsymbol{\xi}}$ such that

$$\hat{\boldsymbol{\xi}} = \underset{\boldsymbol{\xi}}{\operatorname{argmax}} \sum_i \log(P(\boldsymbol{z}_i(\boldsymbol{\xi}) | \hat{s}_i) \tag{4.11}$$

This acoustic likelihood expression cannot be directly maximized with respect to the array parameters $\boldsymbol{\xi}$ for two reasons. First, the state distributions used in most HMM-based speech recognition systems are complicated density functions, *i.e* mixtures of Gaussians. Second, the acoustic likelihood of an utterance and the parameter vector $\boldsymbol{\xi}$ are related through a series of linear and non-linear mathematical operations performed to convert a waveform into a sequence of feature vectors, as discussed in Section 2.2.1. Therefore, for a given HMM state sequence, no closed-form solution for the optimal value of $\boldsymbol{\xi}$ exists. As a result, non-linear optimization methods must be used.

We will employ a gradient-based approach to finding the optimal value of $\boldsymbol{\xi}$. For convenience, we define $\mathcal{L}(\boldsymbol{\xi})$ to be the total log likelihood of the observation vectors given an

HMM state sequence. Thus,

$$\mathcal{L}(\boldsymbol{\xi}) = \sum_i \log(P(\boldsymbol{z}_i(\boldsymbol{\xi})|s_i) \tag{4.12}$$

Thus, we need to compute the gradient of $\mathcal{L}(\boldsymbol{\xi})$ with respect to the array parameters $\boldsymbol{\xi}$. Using the definition of $\boldsymbol{\xi}$ given by Equation (4.2), we define the gradient vector $\nabla_{\boldsymbol{\xi}}\mathcal{L}(\boldsymbol{\xi})$ as

$$\nabla_{\boldsymbol{\xi}}\mathcal{L}(\boldsymbol{\xi}) = \left[\frac{\partial\mathcal{L}(\boldsymbol{\xi})}{\partial h_0[0]}, \frac{\partial\mathcal{L}(\boldsymbol{\xi})}{\partial h_0[1]}, \ldots, \frac{\partial\mathcal{L}(\boldsymbol{\xi})}{\partial h_{M-1}[P-1]}\right]^T \tag{4.13}$$

Clearly, the computation of gradient vector is dependent on the form of the state distributions used by the recognition system and the features used for recognition. In the following sections, we derive the gradient expressions when the state distributions are modeled as Gaussian distributions or mixtures of Gaussians. In both cases, the features are assumed to be mel frequency cepstral coefficients or log mel spectra.

4.5.1 Gaussian State Output Distributions

We now derive the expression for $\nabla_{\boldsymbol{\xi}}\mathcal{L}(\boldsymbol{\xi})$ for the case where the HMM state distributions are multivariate Gaussian distributions with diagonal covariance matrices. This is the simplest density function commonly used by HMM-based recognition systems. If we define $\boldsymbol{\mu}_i$ and $\boldsymbol{\Sigma}_i$ to be the mean vector and covariance matrix, respectively, of the pdf of the most likely HMM state at frame i, the total log likelihood for an utterance can be expressed as

$$\mathcal{L}(\boldsymbol{\xi}) = \sum_i -\frac{1}{2}\left(\boldsymbol{z}_i(\boldsymbol{\xi}) - \boldsymbol{\mu}_i\right)^T \boldsymbol{\Sigma}_i^{-1}\left(\boldsymbol{z}_i(\boldsymbol{\xi}) - \boldsymbol{\mu}_i\right) + \kappa_i \tag{4.14}$$

where κ_i is a normalizing constant. We are interested in computed the gradient of $\mathcal{L}(\boldsymbol{\xi})$ with respect to $\boldsymbol{\xi}$. Using the chain rule, this is expressed as

$$\nabla_{\boldsymbol{\xi}}\mathcal{L}(\boldsymbol{\xi}) = -\sum_i \frac{\partial\boldsymbol{z}_i(\boldsymbol{\xi})}{\partial\boldsymbol{\xi}}\boldsymbol{\Sigma}_i^{-1}\left(\boldsymbol{z}_i(\boldsymbol{\xi}) - \boldsymbol{\mu}_i\right) \tag{4.15}$$

where $\partial\boldsymbol{z}_i(\boldsymbol{\xi})/\partial\boldsymbol{\xi}$ is the *Jacobian matrix*, composed of the partial derivatives of each element of the feature vector with respect to each of array parameters. The Jacobian is of dimension $MP \times L$ where M is the number of microphones, P is the number of parameters per microphone, and L is the dimension of the feature vector. The full derivation of the Jacobian matrix when the array parameters are FIR filter coefficients and the feature vectors are mel frequency cepstra or log mel spectra is given in Appendix A.

4.5.2 Mixture of Gaussians State Output Distributions

Most state-of-the-art recognizers do not model the state output distributions as single Gaussians but rather as mixtures of Gaussians. We now develop the gradient expression for this case. The log likelihood that a feature vector at frame i was generated by HMM state s_i, modeled as a mixture of K Gaussians, can be expressed as

$$\log(P(\boldsymbol{z}_i(\boldsymbol{\xi})|s_i)) = \log\left\{\sum_{k=1}^{K}\alpha_{ik}\kappa_{ik}\exp\left(-\frac{1}{2}\left(\boldsymbol{z}_i(\boldsymbol{\xi})-\boldsymbol{\mu}_{ik}\right)^T\boldsymbol{\Sigma}_{ik}^{-1}\left(\boldsymbol{z}_i(\boldsymbol{\xi})-\boldsymbol{\mu}_{ik}\right)\right)\right\} \tag{4.16}$$

$$= \log\left\{\sum_{k=1}^{K}\exp\left(-\frac{1}{2}\left(\boldsymbol{z}_i(\boldsymbol{\xi})-\boldsymbol{\mu}_{ik}\right)^T\boldsymbol{\Sigma}_{ik}^{-1}\left(\boldsymbol{z}_i(\boldsymbol{\xi})-\boldsymbol{\mu}_{ik}\right)+\log(\alpha_{ik}\kappa_{ik})\right)\right\} \tag{4.17}$$

where α_{ik} is the mixture weight of the kth Gaussian in state s_i and κ_{ik} is a normalizing constant as before.

For convenience, we represent the term inside the exp() operator in Equation (4.17) as $G_{ik}(\boldsymbol{\xi})$. The total log likelihood of a given state sequence whose output distributions are modeled as mixtures of Gaussians can then be expressed compactly as

$$\mathcal{L}(\boldsymbol{\xi}) = \sum_i \log\left(\sum_{k=1}^{K}\exp\left(G_{ik}(\boldsymbol{\xi})\right)\right) \tag{4.18}$$

As before, the gradient of Equation (4.18) is computed using the chain rule, giving

$$\nabla_{\boldsymbol{\xi}}\mathcal{L}(\boldsymbol{\xi}) = \sum_i\left\{\frac{1}{\sum_{j=1}^{K}\exp\left(G_{ij}(\boldsymbol{\xi})\right)}\sum_{k=1}^{K}\exp\left(G_{ik}(\boldsymbol{\xi})\right)\frac{\partial G_{ik}(\boldsymbol{\xi})}{\partial\boldsymbol{\xi}}\right\} \tag{4.19}$$

where we have introduced the summation index j for clarity. This can be rewritten as

$$\nabla_{\boldsymbol{\xi}}\mathcal{L}(\boldsymbol{\xi}) = \sum_i\sum_{k=1}^{K}\left(\frac{\exp\left(G_{ik}(\boldsymbol{\xi})\right)}{\sum_{j=1}^{K}\exp\left(G_{ij}(\boldsymbol{\xi})\right)}\right)\frac{\partial G_{ik}(\boldsymbol{\xi})}{\partial\boldsymbol{\xi}} \tag{4.20}$$

The term in the parenthesis represents the *a posteriori* probability of the kth mixture component, which we represent as $\gamma_{ik}(\boldsymbol{\xi})$ to reflect its dependence on the array parameters $\boldsymbol{\xi}$. We can therefore compactly rewrite Equation (4.20) as

$$\nabla_{\boldsymbol{\xi}}\mathcal{L}(\boldsymbol{\xi}) = \sum_i\sum_{k=1}^{K}\gamma_{ik}(\boldsymbol{\xi})\frac{\partial G_{ik}(\boldsymbol{\xi})}{\partial\boldsymbol{\xi}} \tag{4.21}$$

Using Equation (4.15), the expression for the gradient of $G_{ik}(\boldsymbol{\xi})$ can be expressed as

$$\frac{\partial G_{ik}(\boldsymbol{\xi})}{\partial \boldsymbol{\xi}} = -\frac{\partial \boldsymbol{z}_i(\boldsymbol{\xi})}{\partial \boldsymbol{\xi}} \boldsymbol{\Sigma}_{ik}^{-1} \left(\boldsymbol{z}_i(\boldsymbol{\xi}) - \boldsymbol{\mu}_{ik}\right) \tag{4.22}$$

where $\partial \boldsymbol{z}_i(\boldsymbol{\xi})/\partial \boldsymbol{\xi}$ is the Jacobian matrix, as before.

Thus, the complete gradient expression when the HMM state distributions are modeled as mixtures of Gaussians is

$$\nabla_{\boldsymbol{\xi}} \mathcal{L}(\boldsymbol{\xi}) = -\sum_i \sum_{k=1}^{K} \gamma_{ik}(\boldsymbol{\xi}) \frac{\partial \boldsymbol{z}_i(\boldsymbol{\xi})}{\partial \boldsymbol{\xi}} \boldsymbol{\Sigma}_{ik}^{-1} \left(\boldsymbol{z}_i(\boldsymbol{\xi}) - \boldsymbol{\mu}_{ik}\right) \tag{4.23}$$

Comparing Equations (4.15) and (4.23), the gradient expresssion in the Gaussian mixture case is simply a weighted sum of the gradients of each of the Gaussian components in the mixture, where the weight on each mixture component represents its *a posteriori* probability of generating the observed feature vector.

4.5.3 Gradient-based Array Parameter Optimization

Using the gradient vector defined in either Equation (4.15) or Equation (4.23), the array parameters can be optimized using hill-climbing techniques, such as conventional gradient descent (Haykin, 2002). However, improved convergence performance can be achieved by methods which utilize second-order derivative information, *i.e.* the Hessian, estimated from first-order gradients. In this work, we perform optimization using the method of conjugate gradients. More information about conjugate gradient optimization can be found in (Nocedal & Wright, 1999).

4.6 Evaluating LIMABEAM Using Oracle State Sequences

To test the proposed gradient-based array parameter optimization scheme, experiments were performed in which the filter parameters were optimized using state sequences generated from *a priori* knowledge of the utterance transcriptions and features derived from close-talking microphone recordings. Because these state sequences were derived from information normally not available, we refer to them as *oracle state sequences*. By using oracle state sequences, the upper bound on the performance of the proposed LIMABEAM algorithm can be studied.

Array parameter optimization was performed in the log mel spectral domain. This was done for two reasons. First, because the log mel spectra are derived from the energy in a

series of triangular weighting functions of unity area, all components of the vectors have approximately the same magnitude. In contrast, the magnitude of cepstral coefficients decreases significantly with increasing cepstral order. Having vector components of similar magnitude is advantageous for gradient-descent-based optimization schemes. When there is a large disparity in the magnitudes of the components of a vector, the larger components dominate the objective function and tend to be optimized at the expense of smaller components. Using log mel spectra avoids this potential problem. Second, because there is a 50% overlap between adjacent mel triangles, the resulting log mel spectral components are highly correlated to each other. Again, this correlation is advantageous in a gradient-descent algorithm because the optimization of a particular log mel spectral component tends to optimize neighboring components as well.

In order to do perform the array parameter optimization in the log mel spectral domain (but still decode on cepstral coefficients), we employ a parallel set of HMMs trained on log mel spectra, rather than cepstra. To obtain parallel models, we perform a single pass of Baum-Welch training where the E-step (computing the *a posteriori* probabilities of mixture component occupancies) is performed using the cepstral features and models, and using this alignment, the M-step (computing the Gaussian parameters) is computed using the log mel spectral features. This method, called *Single Pass Retraining* (SPR) (Woodland et al., 1996) or *Statistical Re-estimation* (STAR) (Moreno et al., 1995), ensures that the two sets of models have identical frame-to-state alignments.

These parallel log mel spectral models were trained without feature mean normalization, since mean normalization is not incorporated into the optimization framework (we will revisit this issue in Section 4.10.1).

4.6.1 Experiments Using Gaussian Distributions

In the first series, of experiments, it was assumed that for the purposes of filter optimization, the HMM state output distributions are well modeled by Gaussian distributions. Experiments were performed using the CMU-8 corpus described in Section 3.5.1. Experiments were performed as follows.

Time-delay compensation (TDC) was first performed in the array signals using the PHAT algorithm (Knapp & Carter, 1976). The aligned array signals were then aligned to the close-talking microphone signal in order to ensure that the oracle state sequence derived from the close-talking microphone signal would map to the array signals. Following TDC, the

filter parameters were initialized to the following unweighted delay-and-sum configuration:

$$h_m[p] = \begin{cases} 1/M & p = 0, \forall\ m \\ 0 & p \neq 0, \forall\ m \end{cases} \tag{4.24}$$

Using the oracle state sequence and the corresponding HMM Gaussian parameters, the filter parameters were optimized using conjugate gradient descent with Equations (4.14) and (4.15).

After the filter parameters were optimized, the array signals were convolved with the optimized filters and combined in the conventional filter-and-sum manner. The output signal was then converted into a sequence of cepstral feature vectors and input to the recognizer. Cepstral mean normalization was applied and decoding was performed using HMMs with mixtures of 8 Gaussians per state. This optimization procedure was repeated for every utterance in the test set.

In the first experiment, the described optimization procedure was repeated for filters of various lengths. The results are shown in Figure 4.1. As the figure indicates, optimizing 20-tap filters results in an 18.3% relative improvement over delay-and-sum beamforming, and this improvement increases to 25.0% when 200-tap filters are optimized. While these results were of course obtained using oracle state sequences, the experiment nonetheless demonstrates the potential improvements on recognition accuracy that can be achieved using the proposed maximum likelihood array processing approach.

In these experiments, the conjugate gradient algorithm was allowed to iterate until the likelihood of the most likely state sequence converged. However, the ideal stopping criterion would be the point at which the word error rate converges. While we cannot know this *a priori*, it would be interesting to see how well these two criteria relate. Figure 4.2 shows the WER plotted versus the number of iterations of filter optimization performed when 20, 50, 100, and 200 taps are used per filter. A maximum of 500 iterations was performed for every utterance. If the filter optimization for a particular utterance converged prior to 500 iterations (and the vast majority did), then the error rate at the last iteration performed was carried over to the higher iterations for plotting purposes. In all plots, the average number of iterations to convergence is shown with a '$\circ$'. Based on these plots, it appears that the word error rate produced by these optimal filters converges faster than the likelihood during the filter optimization process itself. This suggests that we can use a more aggressive criterion for convergence.

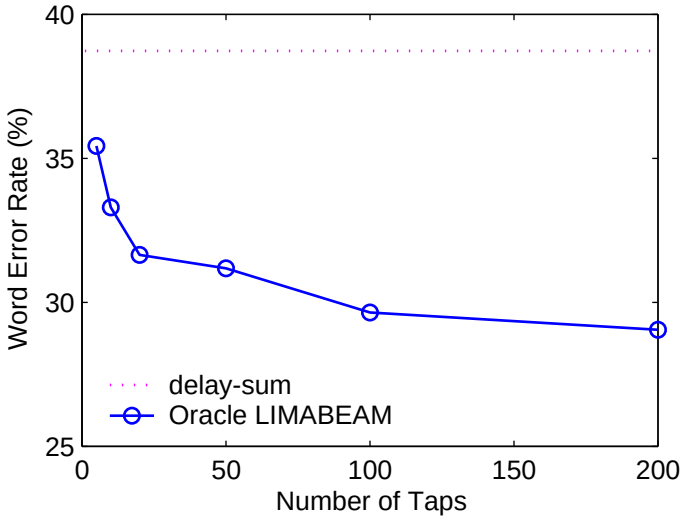

Figure 4.1: WER vs. filter length for the proposed array processing approach. The filter parameters were optimized using a state sequence derived from the close-talking signal and the transcript.

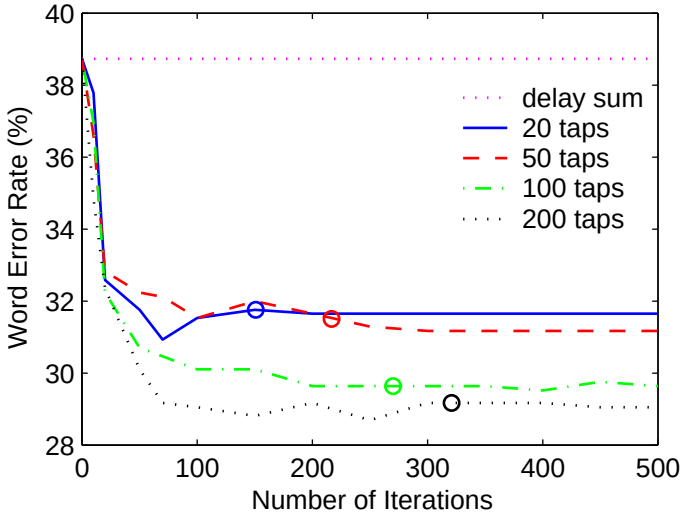

Figure 4.2: WER vs. the number of iterations of filter optimization for the proposed array processing approach. The filter parameters were optimized using a state sequence derived from the close-talking signal and the transcript. The circles show the average number of iterations to convergence in each case.

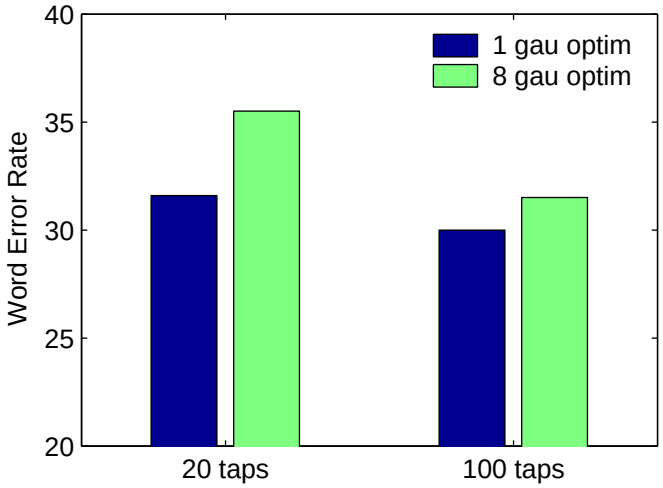

Figure 4.3: The WER obtained using oracle state sequences in the LIMABEAM algorithm. For optimization, state output distributions were modeled by a single Gaussian per state or 8 Gaussians per state. All decoding was performed using 8 Gaussians per state.

4.6.2 Experiments Using Mixtures of Gaussians

Although the gradient expression in Equation (4.23) is more cumbersome than that in Equation (4.15), the gradient expression for the single Gaussian case, it more accurately reflects the HMMs used by the recognizer for decoding. To evaluate the benefit of maximizing the likelihood of mixtures of Gaussians rather than single Gaussians for filter parameter optimization, the experiment from the previous section was repeated using HMMs whose state output distributions are modeled by mixtures of 8 Gaussians. As before, the most likely state sequence was determined using by Viterbi alignment of the features derived from the close-talking microphone signal to the correct transcription for the utterance, both assumed to be known *a priori*. In these experiments, filters composed of 20 taps and 100 taps were optimized. The results are shown in Figure 4.3. The figure shows the word error rates achieved by maximizing the likelihood expression composed of single Gaussian densities or mixtures of Gaussians.

As the figure indicates, the performance when mixture densities are used for optimization is worse than using only single Gaussians. This is somewhat counter-intuitive, as it is well known that the recognition performance obtained using mixtures of Gaussians is better than that achieved using single Gaussian densities. One explanation for the degradation in performance using mixtures of Gaussians lies in the mismatch in content between the training and testing data. As described in Section 3.5.1, the CMU-8 corpus consists primarily

strings of connected digits and letters along with some additional keywords. Unfortunately, no training corpus large enough data to train context-dependent continuous density HMMs was available for such a task. As a result, the HMMs were trained using the WSJ corpus, a large vocabulary task consisting of continuous read speech. Thus, there is somewhat of a mismatch in the tasks of the training and test sets, which inhibits the performance when mixtures of Gaussians are used for filter optimization.

4.6.3 Summary of Results Using Oracle LIMABEAM

In this section, we have shown that the proposed Likelihood Maximizing Beamforming (LIMABEAM) approach is capable of achieving significant improvements over a conventional delay-and-sum beamformer provided that the most likely state sequence for the correct transcription of the utterance is known *a priori*. Such improvements are possible even when the filter lengths are small, *e.g.* 20 taps. This compares favorably to the recognition performance of the Generalized Sidelobe Canceller, as was shown in Figure 3.5. Using the GSC, the WER with 50-tap filters was worse than that of delay-and-sum, and the WER with 200-tap filters was only marginally better. Using the ML array processing approach described here, 200-tap filters resulted in a 25% relative improvement over delay-and-sum.

We also saw that for filter optimization, modeling the HMM state output distributions as mixtures of Gaussians resulted in worse recognition accuracy on the CMU-8 corpus than single Gaussians. We believe this is due in large part to the mismatch in task between the training and testing corpora. Optimization with mixtures of Gaussians will be revisited in Chapters 5 and 6. However, for the remainder of the experiments in this chapter, we will use single Gaussian distributions for optimization.

Of course, all the improvements in recognition accuracy were achieved using oracle state sequences generated from the transcriptions of the utterances and the close-talking microphone signal, both assumed to be known *a priori*. Of course, in a realistic scenario, this information is not available. In the following sections, LIMABEAM-based algorithms that do not require oracle information will be presented.

4.7 The Calibrated LIMABEAM Algorithm

In Section 4.3, an approach to array processing was presented in which the array processor combined the received signals in such a manner so as to maximize the likelihood that the recognition system would estimate the correct hypothesis. This was achieved by choosing array parameters (in this case, a set of filter coefficients) which generate a sequence of

feature vectors for which the likelihood of the correct transcription is maximum. This approach resulted in significantly improved recognition performance over a conventional delay-and-sum beamformer. However, the proposed algorithm required *a priori* knowledge of the utterance transcription in order to generate the optimal state sequence. Clearly, we are faced with a paradox: prior knowledge of the correct transcription is required in order to maximize its likelihood. Yet, if we had such knowledge, there would be no need for recognition in the first place.

In this section, we present one solution to this paradox. The LIMABEAM algorithm is cast as a method of *microphone array calibration*. The array parameters are optimized using an utterance with a known transcription spoken by the user. After optimization, these parameters are fixed for future processing. Because the optimization is performed using a known transcription, we refer to this as *supervised* optimization. We now describe the calibration algorithm in more detail.

In the calibration scenario, the user is asked to speak an enrollment utterance with a *known* transcription. As before, an estimate of the most likely state sequence corresponding to the enrollment transcription is made using the Viterbi algorithm. However, because the close-talking microphone signal is no longer available, the features used to estimate the state sequence are derived directly from the array signals themselves. These features can be generated using an initial set of filters, *e.g.* from a previous calibration session or a simple delay-and-sum configuration.

Using this estimated state sequence, the filter parameters are optimized as before. This constitutes one iteration of calibration. Of course, this is not to be confused with the number of iterations of conjugate gradient descent in the filter optimization process, which is run to convergence unless otherwise noted. Using the optimized filter parameters, a second iteration of calibration can be performed. An improved set of features for the calibration utterance is generated and used to re-estimate the state sequence. The filter optimization process can then be repeated using the updated state sequence. The calibration process continues in an iterative manner until the overall likelihood converges. Once convergence occurs, the calibration process is complete. The resulting filters are now used to process future incoming speech to the array. Because we are calibrating the array parameters to maximize the likelihood of the enrollment utterance, we refer to this method as *Calibrated LIMABEAM*. A flowchart of the calibration algorithm is shown in Figure 4.4.

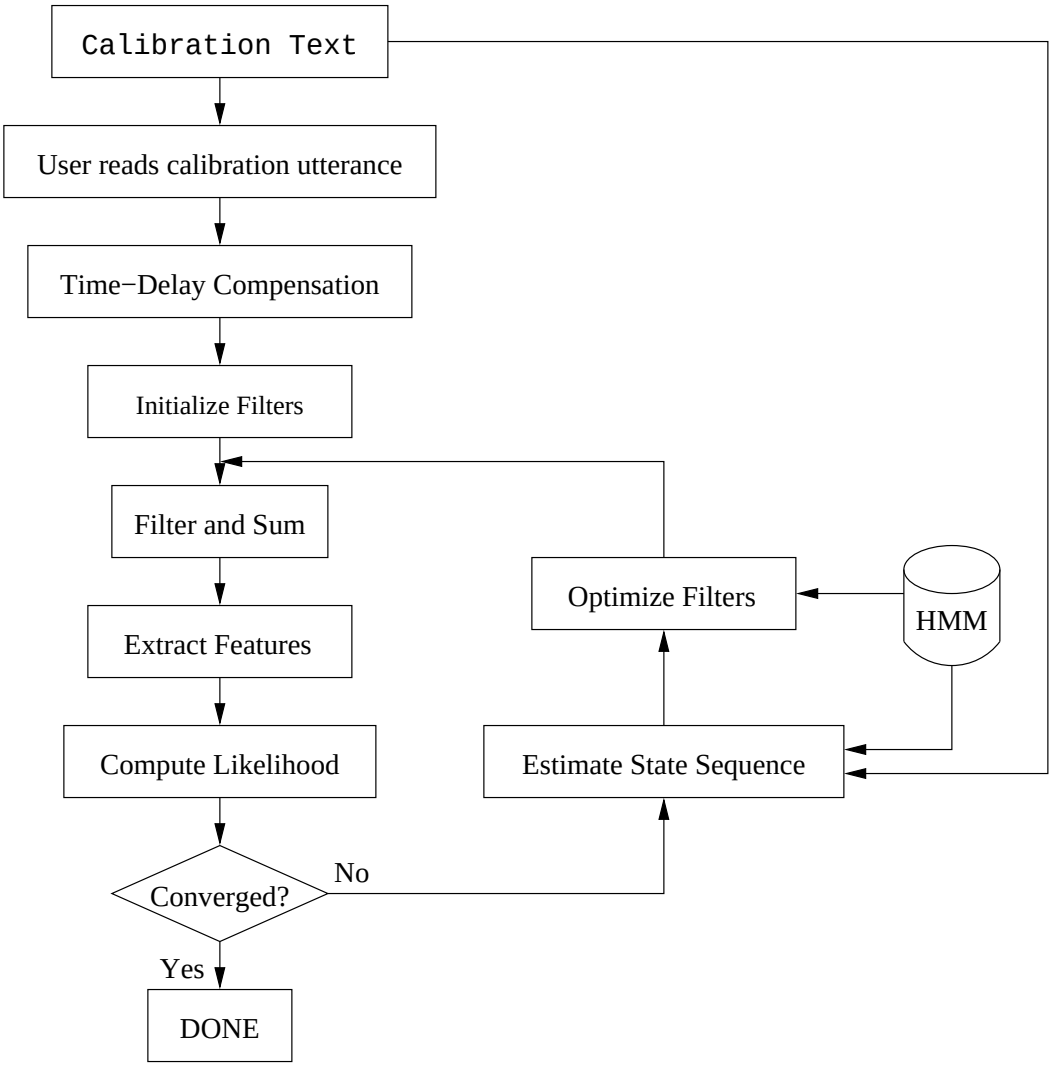

Figure 4.4: Flowchart of LIMABEAM Calibration

4.7.1 Experimental Results Using Calibrated LIMABEAM

Experiments were performed to test the proposed array calibration procedure. In the first series of experiments, a single utterance from each speaker was used for calibration. An utterance common to all speakers was chosen as the calibration utterance (`P-I-T-T-S-B-U-R-G-H`). For each speaker, the filters were initialized to the delay-and-sum configuration in Equation (4.24). The array signals of the calibration utterance were processed and recognition features generated from the delay-and-sum output signal. Using these features and the known utterance transcription, the most likely state sequence was estimated via forced alignment. The filter parameters were then optimized to maximize the likelihood of this state sequence. As before, the filter parameter optimization was performed in the log mel spectral domain and the likelihood expression for the calibration utterance was formed from single Gaussian HMM state distributions. In these experiments, calibration was terminated after one full iteration. After calibration was complete, the optimized filters were fixed and used to process the remaining utterances for that speaker.

Figure 4.5 shows the WER obtained using Calibrated LIMABEAM as a function of filter length. Also shown in the figure are the results from the oracle experiment performed in Section 4.6.1, in which the filter parameters were optimized for each utterance individually using *a priori* knowledge of the transcription and close-talking microphone signal. As the figure indicates, the calibration algorithm tracks the oracle experiment quite closely until filters with more than 20 taps are used. At that point, the performance becomes increasingly worse than the oracle case as the number of filter parameters increases. As the number of taps per filter approaches 200, the calibration algorithm performs worse than delay-and-sum beamforming.

The degradation in performance obtained when the filter length exceeds 20 taps is likely caused by overfitting of the filters to the calibration utterance. Because we are attempting to obtain filters that generalize to future utterances using a very small amount of data (only a single utterance), the chances of overfitting are quite high. As a result, the number of parameters to optimize needs to be limited in order to obtain performance that will generalize to unseen utterances.

We expect that as the amount of data used for calibration increases, the number of parameters that can be reliably estimated will also increase. To test this hypothesis, the calibration experiment previously described was repeated. However, in this case, calibration was performed using three utterances concatenated together, rather than just a single utterance. The results are shown in Table 4.1 for calibration of filters with 20 and 50 taps. Note that the word error rates obtained using conventional delay-and-sum processing and

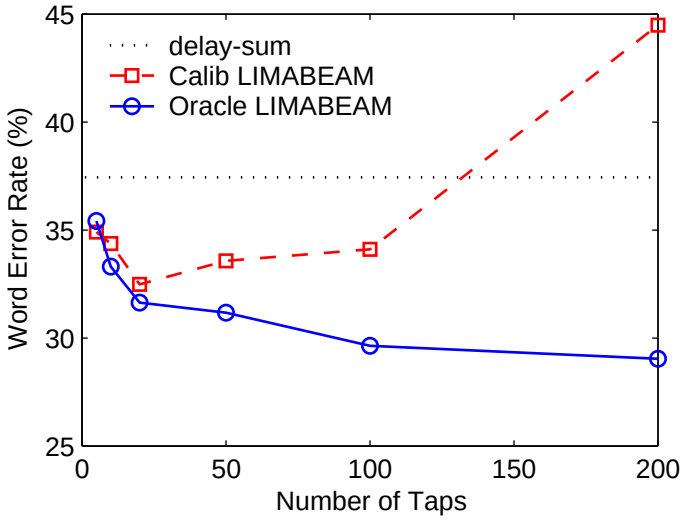

Figure 4.5: WER vs. filter length obtained using the Calibrated LIMABEAM algorithm. The solid line shows performance obtained when the array parameters are optimized using oracle state sequences while the dashed line shows performance for the array calibration approach when the filter parameters are optimized using only a single utterance with known transcription. The performance obtained using conventional delay-and-sum processing is shown for reference.

using array calibration based on a single utterance are slightly different from those obtained in the previous experiment. This change arises because we are performing recognition with fewer utterances, since two of the utterances for each speaker previously in the test set are now used for calibration, and hence not scored in decoding.

As the results in the table show, the calibration algorithm has approximately the same performance when 20-tap filters are calibrated using a single utterance or three concatenated utterances. However, the performance obtained when 50-tap filters are calibrated dramatically improves when more calibration data is used. As expected, we achieve better performance using more filter parameters, provided there is enough calibration data to reliably estimate filters that generalize well to unseen test data. Furthermore, with increased calibration data, the WER achieved by the calibration algorithm using 50 taps per filter is very close to that of the oracle case with the same number of parameters.

Finally, an experiment was performed to determine if additional improvement could be obtained from additional calibration iterations. The experiment was performed on the longer, concatenated calibration utterances described in the previous experiment, with 50-tap filters. After the initial pass of calibration was complete, a new set of features was derived from the calibration utterance by processing the array signals through the optimized

Array Processing Method	# of Taps per Filter	Duration of Calib Utt (sec)	WER (%)
delay-and-sum	–	–	39.1
Calibrated LIMABEAM	20	3.3s	35.0
Calibrated LIMABEAM	20	8.3s	34.7
Oracle LIMABEAM	20	–	32.6
Calibrated LIMABEAM	50	3.3s	36.2
Calibrated LIMABEAM	50	8.3s	32.9
Oracle LIMABEAM	50	–	32.3

Table 4.1: WER obtained using Calibrated LIMABEAM on the CMU-8 corpus for different calibration utterance durations.

	Iteration (Initialization Method)		
	1 (init D&S)	2 (init Calib)	2 (init D&S)
Calibrated LIMABEAM - 50 taps	32.9	33.2	33.1

Table 4.2: WER obtained using multiple iterations of LIMABEAM calibration on the CMU-8 corpus.

filters. These features and the known transcription were then used to re-estimate the most likely state sequence. Filter parameter optimization was repeated using the new state sequence. For the second iteration, two methods of filter initialization were tried. In the first experiment, the filters were initialized to the parameters obtained from the previous iteration of calibration. In the second experiment, they were initialized to the delay-and-sum configuration as before. The results of this experiment are shown in Table 4.2.

As the results in the table indicate, no significant differences were obtained using a second iteration of calibration. This is not too surprising, since the performance after a single iteration of calibration is already very close to the oracle case. Based on this result, additional iterations were not performed. Nevertheless, further iterations of calibration may improve performance on other tasks.

4.7.2 Summary of Results Using Calibrated LIMABEAM

Using the Calibrated LIMABEAM algorithm, a 13.2% improvement in WER was acheived using 20-tap filters. This result was obtained by calibrating to a single utterance with an average duration of 3.3s. When more calibration data are used, more parameters can be reliably estimated. Using 8.3s of calibration data, a relative improvement of 15.7%

was achieved using 50 taps per filter. Finally, it was experimentally determined that the calibration algorithm had converged after a single iteration. Performing a second iteration of calibration did not result in any additional improvement in recognition accuracy over the first iteration.

The use of any calibration algorithm such as this one carries with it the implicit assumption that the parameters learned during calibration will be valid for the future. This implies that the conditions of interest (user location, environmental conditions, etc.) do not change over time. While there are several environments where this is a valid assumption, there are certainly many examples of applications where it is not. In the next section, we describe an implementation of the LIMABEAM algorithm for use in situations where conditions are changing, *i.e.* for time-varying environments.

4.8 The Unsupervised LIMABEAM Algorithm

The calibration algorithm described in the previous section was effective at finding array parameters to improve recognition accuracy. However, for this algorithm to be useful, the filters learned during calibration must be valid for future incoming speech. This implies that the user will not significantly move and the environment will not significantly change, a reasonable assumption for several situations, such as operating a vehicle or sitting in front of a desktop terminal. However, there are several applications in which either the environment or the position of the user will vary over time. In these cases, filters obtained from calibration may no longer be valid. Furthermore, there may be situations in which requiring the user to speak a calibration utterance is undesirable. For example, at an information kiosk, where the interaction will be relatively brief, requiring the user to calibrate the system will significantly increase the time it takes for the user to complete a task.

In these situations, it is more appropriate to optimize the array parameters more frequently, *e.g.* on an utterance-by-utterance basis. However, we are again faced with the paradox discussed earlier. Because we attempt to maximize the likelihood of the correct transcription of the test utterances, we require *a priori* knowledge of the very transcriptions that we desire to recognize. In this case, where the use of a calibration utterance is no longer appropriate, we solve this dilemma by estimating the transcriptions and using them in an *unsupervised* manner to perform the array parameter optimization.

Whereas the filters were optimized on the basis of a known transcription in the calibration algorithm, we now optimize the filters on the basis of a hypothesized transcription, generated from an initial estimate of the filter parameters. Thus, this algorithm is a multi-pass algorithm. For each utterance or series of utterances, the current set of filter parameters

Filter Length	WER (%)	Relative Improvement (%)
20	35.6	8.0
50	37.9	2.1

Table 4.3: WER obtained using Unsupervised LIMABEAM on the CMU-8 corpus.

are used to generate a set of features for recognition which in turn, are used to generate a hypothesized transcription. Using the hypothesized transcription and the associated feature vectors, the most likely state sequence is estimated using Viterbi alignment as before. The filters are then optimized using the estimated state sequence, and a second pass of recognition is performed. This process can be iterated until the likelihood converges. We refer to this method as *Unsupervised LIMABEAM*. A flowchart of the algorithm is shown in Figure 4.6.

4.8.1 Experimental Results Using Unsupervised LIMABEAM

To evaluate the effectiveness of the Unsupervised LIMABEAM algorithm, experiments were performed using the CMU-8 corpus. In these experiments, only a single iteration of unsupervised processing was performed. For each utterance, the following procedure was followed. The filters were initialized to delay-and-sum. The array signals were processed and an initial hypothesized transcription was generated. Using this hypothesized transcription, the corresponding most likely state sequence was estimated and filter optimization was performed. The array signals were then processed using the optimized filters. Features were extracted from the output signal and passed to the recognizer for decoding. Table 4.3 shows the WER obtained when unsupervised optimization was performed on filters of length 20 and 50. For reference, the relative improvement over delay-and-sum processing is also shown.

As the table indicates, the improvement over conventional delay-and-sum processing achieved by the unsupervised optimization approach is marginal. However, in this particular corpus, many of the utterances are very short, consisting of only a few tokens. For unsupervised optimization to be successful, there has to be a sufficient number of correctly labeled frames in the utterance. Performing unsupervised optimization on an utterance with too few correctly hypothesized labels will only degrade performance, propagating the recognition errors further. To increase the amount of data in each utterance processed by the unsupervised optimization algorithm, utterances were concatenated together to form longer utterances, and the experiment described above was repeated on these longer utterances. In these experiments, 20-tap filters, initialized to delay-and-sum, were optimized using a single iteration of the algorithm.

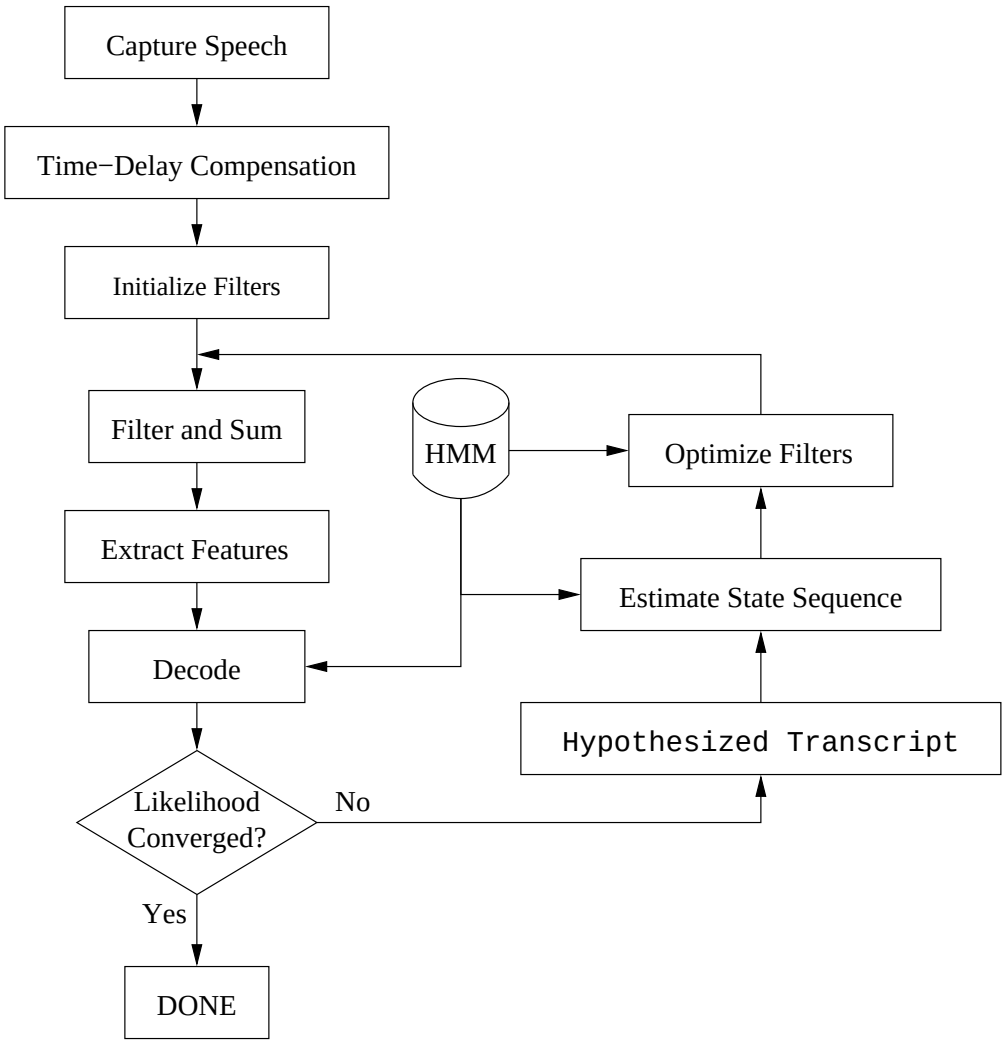

Figure 4.6: Flowchart of Unsupervised LIMABEAM

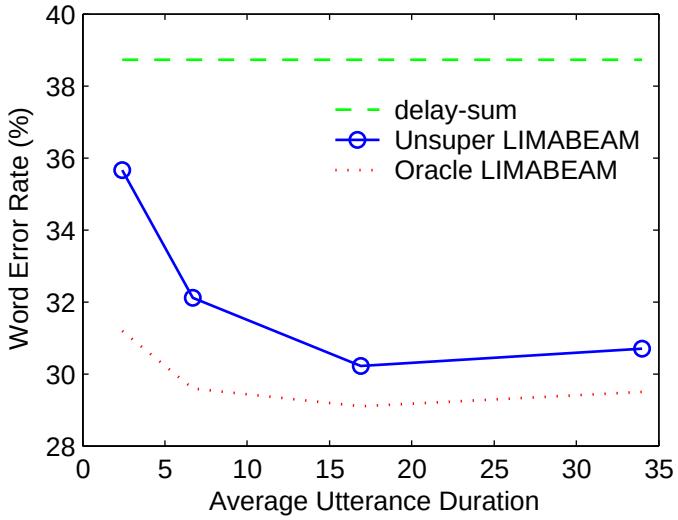

Figure 4.7: WER vs. the average utterance duration obtained using the Unsupervised LIMABEAM approach. To increase the amount of data used for parameter optimization, short utterances were concatenated to form longer ones. The performance obtained using delay-and-sum processing and using oracle state sequences is also shown.

Figure 4.7 shows the results of this experiment. The figure shows the WER achieved using unsupervised processing as a function of the average utterance duration. The WER achieved using oracle state segmentations on the concatenated utterances is also shown, as well as the performance of delay-and-sum processing. As the plot indicates, concatenating utterances together greatly improves the performance of the unsupervised approach. Clearly, using more data in the optimization enables the filter parameters to be optimized more reliably. However, it is interesting to note that the performance improves with increasing utterance duration until the duration reaches about 16 s. Increasing the utterance duration further results in slightly worse performance. This implies that for this particular corpus, on average, there are non-negligible variations in the environment or the user's position over periods of time longer than 16 s. Because the filters are optimized under the assumption that the conditions do not change over the course of the utterance, optimization performed on these very long utterances results in performance that is slightly degraded.

Finally, an experiment was performed to see if additional iterations of unsupervised processing would improve the performance of the algorithm. This experiment was performed on the concatenated utterances that had the best performance after the first iteration (an average duration of 16 s). For each utterance, the features generated by the first iteration of unsupervised processing and the resulting recognition hypothesis were used to estimate

	Iteration	
	1	2
Unsupervised LIMABEAM - 20 taps	30.2	30.3

Table 4.4: WER obtained using multiple iterations of Unsupervised LIMABEAM on the CMU-8 corpus.

the most likely state sequence of that hypothesis. This new state sequence was then used as the basis of the unsupervised filter parameter optimization. For the second iteration, the filters were re-initialized to the delay-and-sum configuration. The results of this experiment are shown in Table 4.4. As was the case using the calibration algorithm, no significant improvement is obtained from a second iteration of unsupervised processing. Here too, the results from the first iteration are very close to the oracle performance, so there is not much room for improvement. Again, on other corpora, additional iterations may further improve performance.

4.8.2 Summary of Results Using Unsupervised LIMABEAM

Overall, the Unsupervised LIMABEAM algorithm was shown to be very effective provided there is enough data to perform the filter optimization. Using utterances of 2-3 s in duration, unsupervised optimization of 20-tap filters resulted in a relative improvement of 8% in WER over delay-and-sum beamforming. When the average utterance duration was increased to 16 s, the relative improvement increased to 22%. Increasing the utterance duration beyond 16 s resulted in a slight degradation in performance, presumably because of changes in the environment or user's position. Furthermore, as in the calibration algorithm, the recognition performance converged after a single iteration of unsupervised processing.

The improvements achieved by unsupervised processing are very close to the performance obtained using oracle state segmentations. Thus, this maximum likelihood approach is quite effective even when the state sequences are estimated on the basis of erroneous transcriptions.

4.9 Analysis of Optimized Array Parameters and the Output Waveform

Throughout this work, we have maintained that for microphone-array-based speech recognition applications, the design of array processing algorithms should focus on the features

that are computed from the array output and the manner in which the recognition system processes these features. In this chapter, we have shown that performing array processing according to a maximum likelihood criterion directly related to the speech recognizer results in significant improvements in speech recognition accuracy over conventional array processing methods that operate according to signal processing criteria. Nevertheless, we can still examine the filters and output signals produced by the algorithms presented in this chapter from a more traditional array processing point of view.

4.9.1 The Optimized Filters of the Array

In this work, we are performing array processing for speech recognition applications. Speech recognition features are derived from the spectrum of the incoming speech signal. Therefore, it is worthwhile to examine the spectral response of the filters learned during the optimization process. Furthermore, because we are utilizing multiple spatially-separated microphones, the filters also produce a spatial response, also worth examining. Unfortunately, while we can look at the spectral and spatial responses in isolation, it is impossible to decouple the relative contributions of the two. That is, while an interesting question might be whether the likelihood was maximized as a result of the spatial response of the array, by the overall filter-and-sum frequency response, or some combination thereof, there is no way of truly knowing. However, by studying each in isolation, we can gain some insight into how the algorithm is improving recognition accuracy.

The overall frequency response of a filter-and-sum beamformer is given by the sum of the frequency responses of the individual filters. This frequency response for 50-tap filters generated by the Calibrated LIMABEAM algorithm is shown in Figure 4.8. The figure shows that the overall response is clearly highpass. This makes sense as the CMU-8 corpus was recorded in a room with predominantly low frequency noise. Furthermore, the filters have a peak-value nature similar to speech signals. This shows a possible attempt to preserve the features of the speech spectrum important for accurate feature extraction, *i.e.* the formant frequencies.

We can also examine the spatial response of the array filters. Figure 4.9 shows the directivity patterns of the 8-channel linear microphone array used in the CMU-8 corpus over a four octave frequency range. The array is located along the $0^\circ - 180^\circ$ axis, and the user is located at 90°. The solid lines show the beampatterns that result from Calibrated LIMABEAM of 50-tap filters. For reference, the dashed lines show the beampattern for a conventional delay-and-sum beamformer. To truly analyze these beampatterns, it is necessary to know the locations of any interfering noise sources. Unfortunately, this information

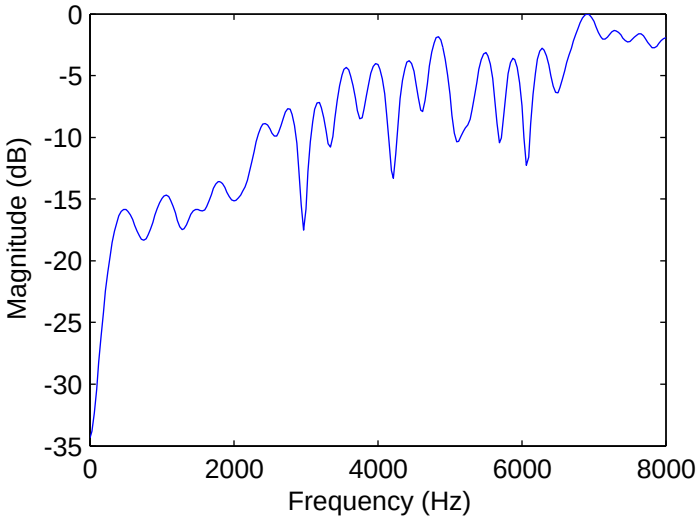

Figure 4.8: Overall look-direction frequency response of the filter-and-sum beamformer obtained by performing Calibrated LIMABEAM on an utterance from the CMU-8 corpus.

is unavailable. However, we can make some observations. At 800 Hz, the calibrated filters generate a narrower main lobe than the delay-and-sum beamformer, but also produce side lobes that are as large or larger than the main lobe. At 1600 Hz and 3200 Hz, the optimized filters generate a main lobe almost identical to that produced by the delay-and-sum beamformer, and yet they have significantly larger side lobes. However, the results of the experiments performed in this chapter indicate that this clearly does not have a negative impact on recognition accuracy. In fact, these plots further validate our belief that optimizing the array parameters according to a criteria that is disjoint from the speech recognition system (in this case, for example, the beampattern) will not necessarily improve recognition performance.

On the other hand, by not imposing any criteria on the beampattern, and letting the filters be learned in a data-driven manner, the algorithm can decide whether components at a particular frequency coming from a particular direction should be amplified, attenuated, or treated as a "don't care" by the array. By treating certain directions of the spatial response as "don't care" regions, the array is able to optimize the response (spatially and spectrally) in other directions/frequencies that are more critical for recognition. This is a key benefit of this data-driven approach. For a given utterance or configuration, it is difficult, if not impossible, to predict which components (in frequency and direction) of the array's response are most important for recognition accuracy. Only by incorporating the recognition system into the array processing and learning the filters in a data-driven way

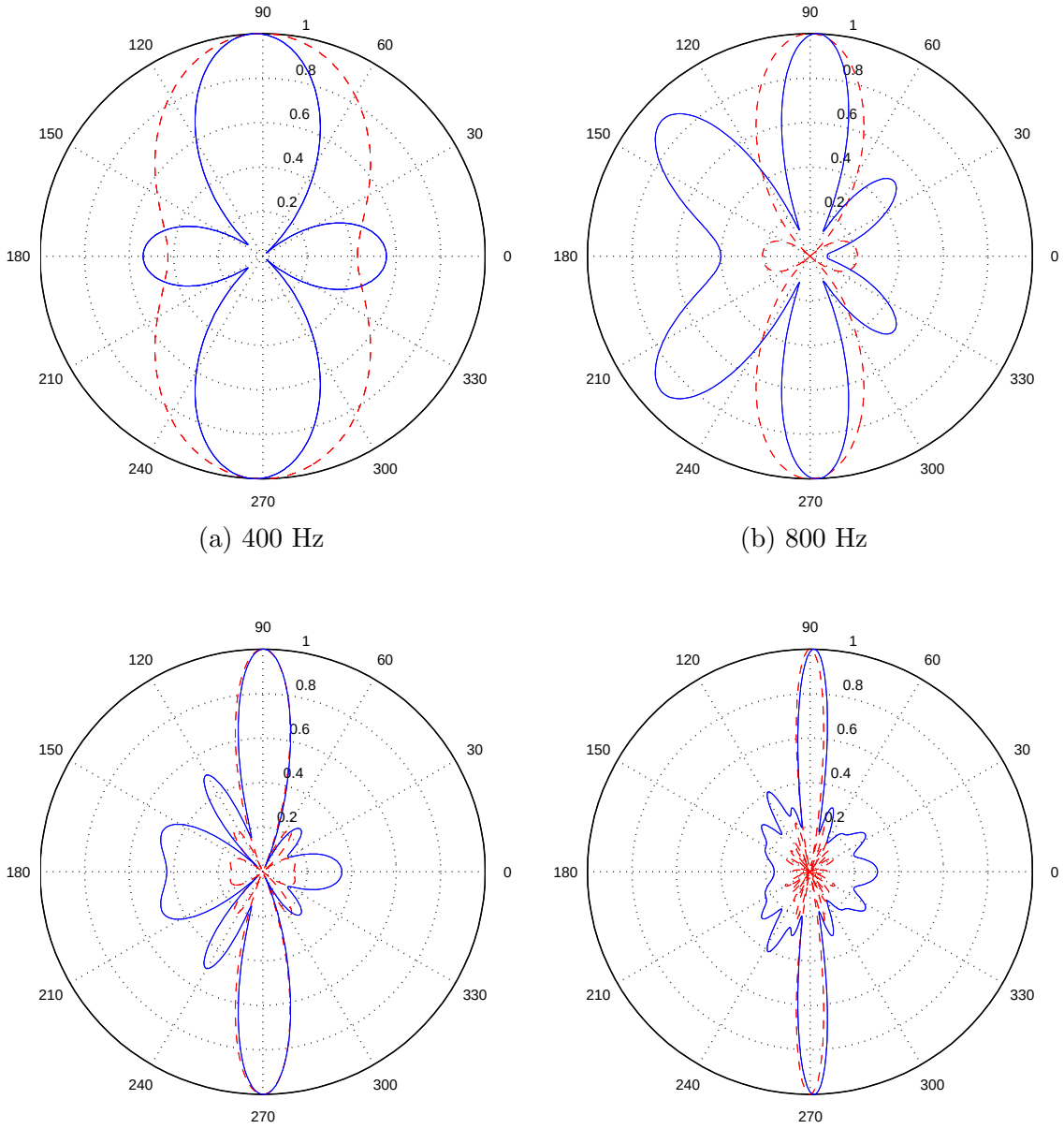

(a) 400 Hz

(b) 800 Hz

(c) 1600 Hz

(d) 3200 Hz

Figure 4.9: Beampatterns of the filter-and-sum beamformer obtained by performing Calibrated LIMABEAM on an utterance from the CMU-8 corpus.

are we able to do so.

4.9.2 The Array Output Waveform

Although we specifically did not optimize the array parameters according to any waveform-level criteria, we can examine the resulting output waveform nonetheless. Figure 4.10 shows four spectrograms of the utterance "A-L-E-X-E-I". The first panel shows the the spectrogram of the utterance captured by a single microphone of the array. The second panel shows the same utterance processing by delay-and-sum beamforming using all 8 microphones. The third panel is the same utterance processed using filter-and-sum with 50-tap filters optimized by the Calibrated LIMABEAM algorithm. Finally, the last panel shows the spectrogram of the utterance recorded by a close-talking microphone. The color scale in all four spectrograms is identical. Comparing the spectrograms of the delay-and-sum beamformer to the calibrated filter-and-sum configuration, we can see that the optimized filters significantly reduced the low frequency environmental noise. This is expected as it is well-known that delay-and-sum beamformers have poor low frequency response (as shown by the 400 Hz delay-and-sum beampattern in Figure 4.9). Perhaps more interesting is the fact that at the middle and high frequencies, delay-and-sum beamforming actually suppresses more background noise than the calibrated filter-and-sum array does. However, the calibrated filters do a far better job of enhancing the spectral features of the speech at these frequencies, for example, the voiced /el/ segment from $0.75 - 1$ s and the unvoiced /s/ at 1.75 s. This is further evidence that simply suppressing the environmental noise (as done by conventional noise-canceling schemes) is not necessarily optimal for speech recognition if it results in the loss of important spectral features of the speech signal.

4.10 Other Considerations

In this section, we discuss some final considerations regarding the LIMABEAM algorithms described in this chapter.

4.10.1 Incorporating Feature Mean Normalization

Speech recognition systems usually perform better when feature mean normalization (Liu et al., 1992) is performed on the features prior to being processed by the recognizer, both in training and decoding. In feature mean normalization, also called feature mean subtraction, the mean value of the feature vectors in an utterance is computed and then subtracted from each of the vectors. Because the features are generated from the logarithm of the spectrum,

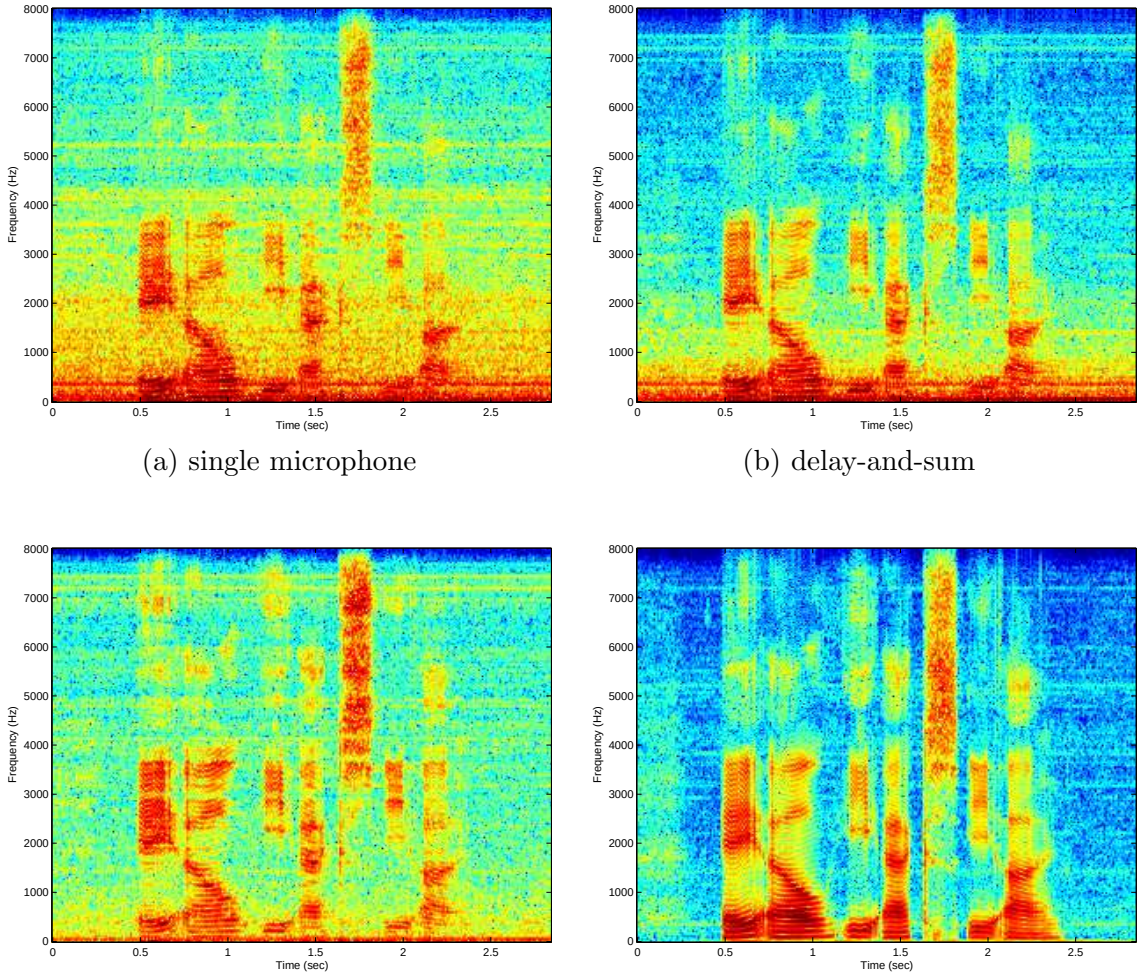

(a) single microphone

(b) delay-and-sum

(c) Calibrated LIMABEAM

(d) close-talking microphone

Figure 4.10: Spectrograms of an utterance from the CMU-8 corpus obtained using (a) single microphone only, (b) delay-and-sum beamforming (c) Calibrated LIMABEAM, and (d) the close-talking microphone.

this subtraction operation basically performs equalization in the feature domain. It removes constant short-term (less than a frame) channel effects from the features, *e.g.* the spectral tilt induced by the microphone response.

Feature mean normalization can easily be incorporated into the LIMABEAM algorithms presented in this chapter. To do so, the feature vector $\boldsymbol{z}_i(\boldsymbol{\xi})$ in Equations (4.14) and (4.17) is replaced by $(\boldsymbol{z}_i(\boldsymbol{\xi}) - \boldsymbol{\mu}_{\boldsymbol{z}}(\boldsymbol{\xi}))$ where $\boldsymbol{\mu}_{\boldsymbol{z}}(\boldsymbol{\xi})$ is the mean feature vector, computed over all frames in the utterance. Because $\boldsymbol{\mu}_{\boldsymbol{z}}(\boldsymbol{\xi})$ is a function of $\boldsymbol{\xi}$ as well, the gradient expressions also have to be modified. It can be shown that incorporating mean normalization into the gradient can be done simply by performing mean normalization on the Jacobian matrix.

However, we found no additional benefit to incorporating feature mean normalization into the array parameter optimization process. We believe this is because the array processing algorithm is already attempting to perform some degree of channel compensation for both the room response *and* the microphone channel, as it is impossible to separate the two. Therefore, the parallel log mel spectral HMMs used for filter optimization were trained without mean normalization, as stated in Section 4.6. For decoding, mean normalization was applied to the cepstral features derived from the output of the array.

4.10.2 Sum-and-Filter Processing

There is another class of methods for microphone array processing which can be referred to as *sum-and-filter* methods. In such methods, the array signals are processed using conventional delay-and-sum beamforming or another array processing algorithm and the single-channel output signal is then passed through an additional filter, called a *post-filter*, in order to provide additional spectral shaping and noise removal (Zelinkski, 1988; Marro et al., 1998). We wanted to compare the performance of the maximum likelihood filter-and-sum beamformer proposed in this chapter to that obtained by simply performing the same maximum likelihood optimization on a single filter applied to the output of a conventional delay-and-sum beamformer.

We performed an experiment using the unsupervised filter optimization algorithm described in Section 4.8, again using concatenated utterances from the CMU-8 corpus. In this case, the estimated state sequence was used to optimize the parameters of a single filter applied to the output of a delay-and-sum beamformer. The frequency response of an optimized post-filter with 50 taps is shown in Figure 4.11. Comparing Figures 4.8 and 4.11, the spectral responses of the optimized filter-and-sum beamformer and the optimized post-filter are clearly similar. The speech recognition results obtained using this maximum likelihood sum-and-filter approach are shown in Figure 4.12 as a function of the length of

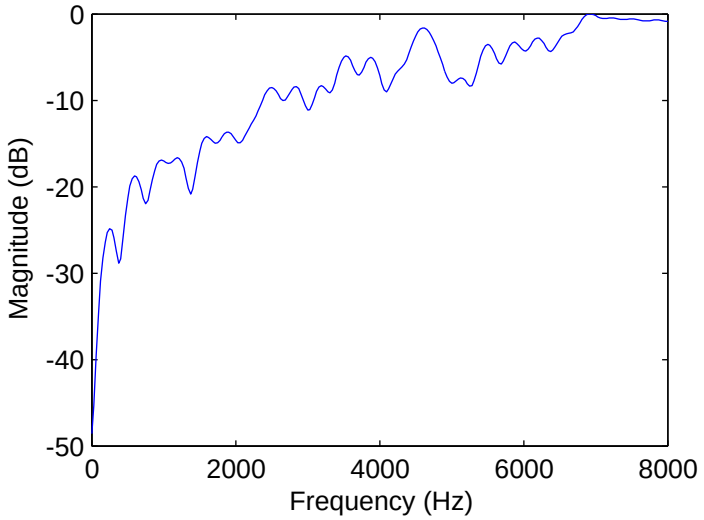

Figure 4.11: Frequency response of the post-filter optimized using unsupervised maximum likelihood filter optimization applied to the delay-and-sum output signal.

the post-filter. As the figure shows, the best performance, obtained using a post-filter with 300 taps, is substantially worse than that obtained by Unsupervised LIMABEAM with 20 taps per microphone, or 160 total parameters. Thus, jointly optimizing the parameters of a filter-and-sum beamformer provides significantly better speech recognition performance compared to optimizing the parameters of a single-channel post-filter.

4.10.3 Combining LIMABEAM with Other Compensation Techniques

There is a vast literature of single channel speech recognition compensation algorithms designed to improve recognition accuracy under adverse conditions, most notably, additive noise. Because the proposed algorithm generates a sequence of conventional speech recognition features, we can apply one of these methods to the array output as a post-processing step. We can think this as the equivalent of applying a feature-domain post-filter to the array. One such compensation technique is Codeword-Dependent Cepstral Normalization (CDCN), previously discussed in Section 3.4.1. We performed experiments applying CDCN to the features generated from the array output, prior to recognition. The results are shown in Table 4.5 for the calibration case and Table 4.6 for the unsupervised case.

As the tables show, there is a large improvement across all array processing methods when CDCN is applied to the features generated from the array output. When delay-and-sum combined with CDCN, the performance approaches that obtained by LIMABEAM alone. However, the performance of the proposed LIMABEAM methods improves further

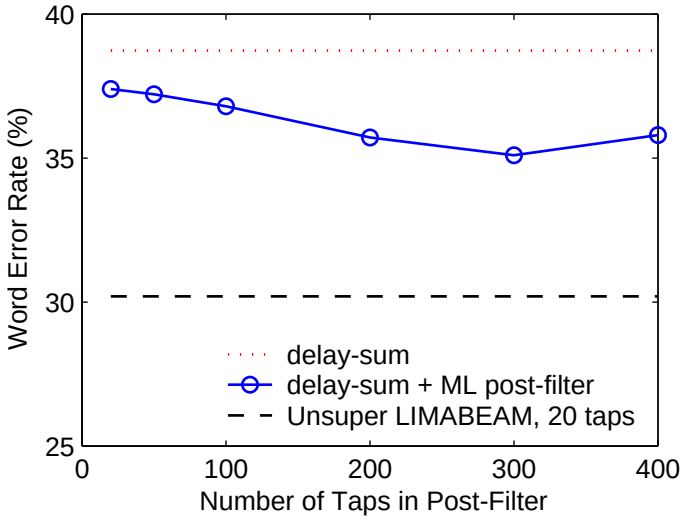

Figure 4.12: WER obtained by performing unsupervised maximum likelihood filter optimization on a post-filter applied to the output of a delay-and-sum beamformer, shown as a function of the length of the post-filter. The WERs obtained using delay-and-sum beamforming alone and using Unsupervised LIMABEAM with 20 taps per microphone are also shown.

still when combined with CDCN.

4.10.4 Computational Complexity

The algorithms presented in this chapter use gradient-descent-based optimization to obtain a locally optimal solution for the set of filter parameters that maximize the likelihood of the given HMM state sequence. As a result, the computational complexity of the algorithm cannot be determined in closed-form since it is highly dependent on many factors which vary from utterance-to-utterance, such as the number of iterations needed to reach a local maximum and the number of function evaluations used to determine the step size in each iteration of the conjugate gradient algorithm. At best, we can make some general observations, *e.g.* that the complexity of the gradient vector computation increases linearly with the number of array parameters.

We can obtain a sense of the complexity of the LIMABEAM algorithm by observing how long it takes to find a solution. We computed the average time taken to estimate 20-tap filters for both a single microphone and an array of 8 microphones. Figure 4.13 shows these values in terms of times-real-time. It should be noted that no effort was made to optimize the speed of the algorithm.

Array Processing Method	WER (%)
delay-and-sum	39.1
delay-and-sum + CDCN	33.3
Calibrated LIMABEAM	32.9
Calibrated LIMABEAM + CDCN	31.1

Table 4.5: WER obtained when delay-and-sum beamforming and Calibrated LIMABEAM are followed by CDCN on the CMU-8 corpus.

Array Processing Method	WER (%)
delay-and-sum	38.7
delay-and-sum + CDCN	31.7
Unsupervised LIMABEAM	30.2
Unsupervised LIMABEAM + CDCN	27.0

Table 4.6: WER obtained when delay-and-sum beamforming and Unsupervised LIMABEAM are followed by CDCN on the CMU-8 corpus.

4.11 Summary

In this chapter, we introduced Likelihood Maximizing Beamforming (LIMABEAM), a new approach to array processing designed specifically for improved speech recognition performance. This method differs from previous array processing algorithms in that no waveform-level criteria are used to optimize the array parameters. Instead, the array parameters are chosen to maximize the likelihood of the correct transcription of the utterance, as measured by the statistical models used by the recognizer itself. We showed that finding a solution to this problem involves the joint optimization of the array parameters and the most likely state sequence for the given transcription.

We evaluated this approach through a series of oracle experiments and showed that if the transcriptions are known *a priori*, this approach results in significant improvements in recognition accuracy. Two implementations of LIMABEAM that operate without *a priori* knowledge of the utterance transcripts were then presented, one that operates as an array calibration algorithm and one that performs parameter optimization in an unsupervised manner.

In Calibrated LIMABEAM, the filter parameters are optimized using a single enrollment utterance spoken by the user. These parameters are then fixed for future processing. This calibration algorithm resulted in significant improvement in recognition accuracy, provided there was ample calibration data to prevent overfitting. Significant improvements over

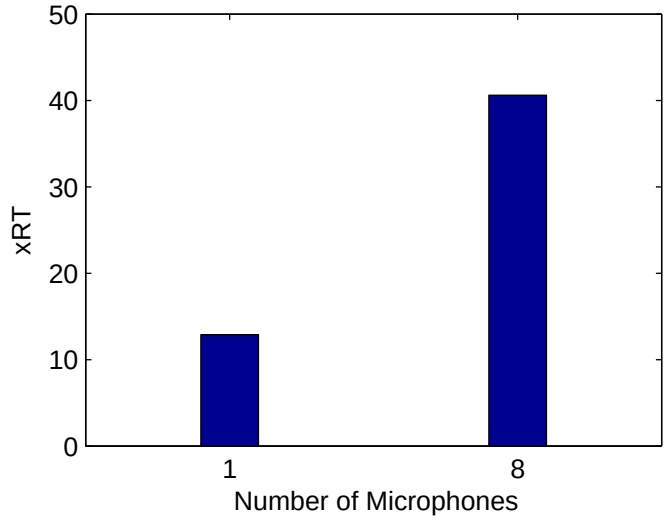

Figure 4.13: Average times-real-time to convergence of the LIMABEAM algorithm to optimize 20-tap filters for a single microphone and for an array of 8 microphones.

delay-and-sum beamforming were obtained with less than 10 s of calibration data.

In Unsupervised LIMABEAM, the filter parameters are optimized for each utterance individually, based on a hypothesized transcription. Because this data operates in an unsupervised manner, its performance is dependent on the presence of enough correctly labeled frames in the hypothesized transcription. In order to increase the number of such frames, short utterances were concatenated into longer utterances for processing. This dramatically improved the effectiveness of the algorithm.

Additionally, we analyzed the filters generated by the LIMABEAM algorithm and resulting waveforms they produced. Strictly from a signal processing point of view, the parameters could be viewed as sub-optimal compared to other methods. Yet, these parameters resulted in significantly better recognition accuracy than such methods. This further highlights the importance of acknowledging the differences between the objectives of signal processing algorithms and speech recognition systems. Finally, some additional issues pertinent to the proposed algorithms were discussed.

The algorithms presented in this chapter were all evaluated using the a microphone array corpus recorded in an environment with a low SNR (6.5 dB) and moderate reverberation (0.24 s). In the next chapter, we turn our attention to microphone-array-based speech recognition in highly reverberant environments.

Chapter 5

Subband-Likelihood Maximizing Beamforming

5.1 Introduction

In the previous chapter, a microphone array processing framework for speech recognition applications was presented in which the parameters of a filter-and-sum beamformer were optimized according to the same objective criterion used by the recognition system itself. In doing so, we were able to achieve significant improvements over conventional microphone array processing algorithms that operate according to traditional signal processing criteria. The experiments performed in the previous chapter showed that this approach is capable of good performance in noisy environments with moderate reverberation. The speech data used in the experiments were recorded in a room with a reverberation time of 0.24 s and had an average SNR of 6.5 dB.

Although the objective function is significantly different from those used by conventional adaptive filtering schemes, the LIMABEAM algorithm is nevertheless a gradient-descent-based LMS type of algorithm. Conventional LMS adaptive filtering algorithms are known to exhibit poor convergence behavior when the input signals are highly correlated and the filter length is long (Haykin, 2002). Unfortunately, both of these conditions are generally present in highly reverberant environments. Therefore, it is unclear whether the algorithms proposed in this thesis will be effective in such environments, or if the performance will be plagued by the same poor convergence issues that hinder more traditional adaptive filtering algorithms.

In the following section, the performance of the LIMABEAM approach is evaluated in an environment with significant reverberation. We will see that although small im-

provements are achieved, the existing adaptive filtering architecture is indeed inadequate to effectively improve speech recognition performance in such environments. We then examine the principles of subband filtering and explore its potential as a means of compensation for the distortions caused by long reverberation times. The remainder of the chapter is spent describing how subband filtering can be incorporated into the speech-recognizer-based maximum likelihood framework established in Chapter 4.

5.2 LIMABEAM in Highly Reverberant Environments

In this section we evaluate the Likelihood Maximizing Beamforming approach described in the previous chapter for use in highly reverberant operating environments. To do so, we will use the 7-microphone reverberant WSJ corpora described in Chapter 3. These corpora were created by convolving the WSJ test set with a series of room impulse responses recorded in rooms with reverberation times ranging from 0.3 s to 1.3 s.

In this section we limit our experiments to the data captured in a room with a reverberation time of 0.47 s, approximately twice as long as the reverberation time of the CMU-8 corpus used in the previous chapter. We refer to this corpus as $\text{WSJ}_{0.47}$.

The Calibrated LIMABEAM algorithm described in Section 4.7 was performed on the $\text{WSJ}_{0.47}$ corpus. For each speaker, a single utterance was chosen at random from the utterances that were at least 10 s in duration. As before, the known transcription and features derived from delay-and-sum processing were used to generate the target state sequence. A filter-and-sum beamformer was then optimized and used to process the remaining utterances of that speaker. The recognition system used for decoding was the same one used in the previous chapter. Figure 5.1 shows the WER obtained using this calibration approach for different filter lengths. The baseline WER obtained from delay-and-sum processing is also shown.

This figure looks similar to Figure 4.5, the results of the calibration experiment in the previous chapter. In that chapter, we attributed the poor performance to overfitting. When many parameters are learned from only a small amount of calibration data, filters are generated that do not generalize well to unseen test data. Recall that increasing the amount of calibration data from 3.3 s to 8.3 s significantly improved the performance of the calibration algorithm when longer filters were optimized.

We can try the same approach to improve the performance here as well. Table 5.1 shows the performance of the calibration algorithm when 100-tap FIR filters are optimized using additional calibration data.

In this case, increasing the amount of calibration data does not significantly improve

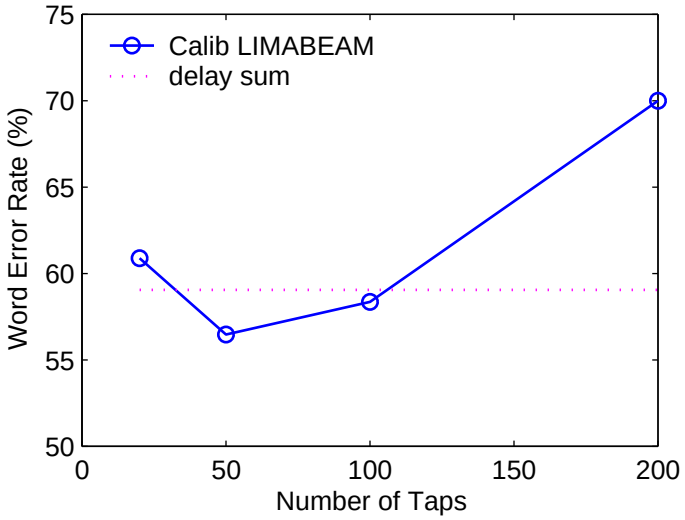

Figure 5.1: WER as a function of filter length for the $WSJ_{0.47}$ corpus when the filter parameters are optimized using Calibrated LIMABEAM. The performance using conventional delay-and-sum processing is also shown.

# of Calib Utterance	Duration of Calib Data	WER (%)
1	11.7 s	58.3
2	18.9 s	53.5
3	28.1 s	57.0

Table 5.1: WER obtained using the Calibrated LIMABEAM algorithm for the $WSJ_{0.47}$ corpus when 100-tap FIR filters are optimized using different amounts of calibration data.

the performance of the calibration algorithm, even though far more data are being used compared to the calibration experiments in the previous chapter. More troubling still, the optimization algorithm seems less well-behaved in a highly reverberant environment. One would not expect performance to degrade as the amount of calibration data is increased. In this case, using 28.1 s of data for calibration resulted in worse performance than using 18.9 s.

Based on these results, it is likely that the problems that plague conventional LMS adaptive filtering algorithms, *i.e.* poor performance when the input signals are highly correlated and the filter length is long, cause the performance of our algorithm to degrade as well. Furthermore, as the severity of the reverberation increases, we require an increasingly large number of parameters to effectively compensate for its effects. In order to estimate a large number of parameters effectively, we need ample adaptation data. We have seen that using almost 30 s of speech resulted in little improvement in optimizing filters with 100 taps, a relatively modest number of parameters. It is likely that an inordinate amount of data will be required to estimate even longer filters reliably. Even if there were enough data, the total number of parameters in the array could easily be in the hundreds or thousands, and the process of jointly optimizing this many parameters would be exceedingly slow.

Clearly we need an alternate solution. Ideally, this solution would both reduce the number of parameters that would have to be jointly optimized and improve the convergence performance of the algorithm. We must also be able to incorporate this solution into the recognizer-based maximum likelihood framework developed in Chapter 4. In this chapter, we present the use of subband filtering as a solution to this problem. We begin our discussion by reviewing the general concepts of subband filtering.

5.3 An Overview of Subband Adaptive Filtering

Subband filtering has been proposed as a means to improve the rate of convergence of adaptive filtering algorithms when the desired filter to be estimated is very long and the input signals are highly correlated. The subband filtering approach has received much interest from the acoustic echo cancellation (AEC) community, *e.g.* (Gilloire & Vetterli, 1992), where these characteristics embody the problems in AEC. Conventional subband adaptive filtering can be thought of as a combination of traditional adaptive filtering and multirate signal processing. In subband filtering, the input signal is first decomposed into a series of independent subbands using a bank of bandpass filters, called *analysis filters*. Because each subband signal has a narrower bandwidth that the original signal, the signals can be downsampled. Each subband signal is now processed independently using an adaptive fil-

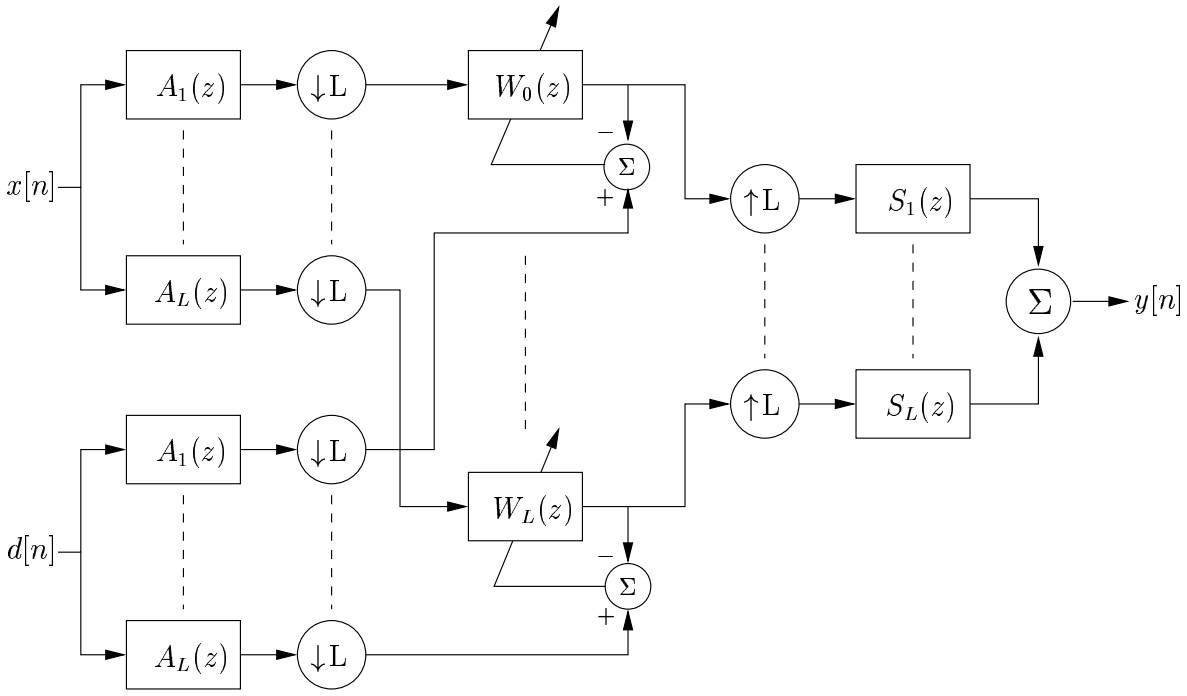

Figure 5.2: A block diagram of conventional subband adaptive filtering. In this figure, $x[n]$ represents the received signal and $d[n]$ represents the desired signal.

ter to minimizing the *subband error*. After processing, the fullband signal is reconstructed by upsampling the output signals of the subband filters, and then passing them through another set of filters called *synthesis filters*. The subband filtering approach is shown in Figure 5.2.

Subband filtering provides an improvement in convergence over conventional fullband filtering for two reasons. First, when the signal is divided into subbands, the *learning rate* or *step size* used for adaptation in each subband can be chosen independently of the other subbands. By using subband-specific step sizes rather than a single step size for the entire broadband signal, it is possible to compensate for variations in the signal power across subbands and as a result, obtain an improvement in convergence (Haykin, 2002) . Second, because processing takes place in subbands, the number of parameters that needs to be jointly estimated is reduced. Because each subband filter is operating on a narrowband, downsampled version of the input signal, processing requires fewer parameters. This improves the computational complexity of the adaptation process. While the total computation can be shown to be approximately the same (Pradhan & Reddy, 1999), the computation *per subband* is less. Because the subbands are independent, the adaptation of

the different subband filters can be performed in parallel.

Subband filtering has been applied to microphone array processing by other researchers. However, all proposed methods have generated subband versions of conventional microphone array algorithms. For example, several researchers have proposed subband versions of the Generalized Sidelobe Canceller, *e.g.* (Neo & Farhang-Boroujeny, 2001; Liu et al., 2001). However, subband filtering is simply a way improving the efficiency of the filter adaptation process. Its success or failure is still dependent on the objective criteria used for the adaptation. As we have seen, algorithms which rely on waveform-level criteria for filter adaptation do not to improve recognition accuracy significantly, and as such, we can expect the same performance from their subband counterparts.

5.4 Subband Filtering for Microphone-array-based Speech Recognition

The attributes that make subband processing useful for applications such as AEC make it similarly appealing for use in recognizing speech that has been distorted by significant amounts of reverberation. However, subband processing is a means of improving the efficiency of a given algorithm or approach, not an algorithm unto itself. Therefore, unless the original fullband algorithm improves recognition accuracy, we cannot expect the subband version of the algorithm to do so either. It will simply be a more efficient way to generate poor results! Thus, the goal of this chapter is to develop a microphone array processing algorithm which exploits the benefits of subband filtering while maintaining the recognizer-based maximum likelihood framework developed in the previous chapter.

In this section, we begin to address this goal, by demonstrating that subband filtering can be readily incorporated into the processing already performed by the recognizer for feature extraction.

5.4.1 Incorporating Subband Processing into the ASR Front-End

As described in Section 2.2.1, a Short-Time Fourier Transform (STFT) is used for spectral estimation in the feature extraction process of most recognition systems. The incoming waveform is segmented into a series of overlapping frames. In this work, a frame length of 25 ms is used and the starting sample of the frame is shifted 10 ms between consecutive frames. The samples in the frame are then windowed using a Hamming window and transformed to the frequency domain using a DFT. This process generates a series of short-time spectral vectors. Features are then extracted from these vectors through a series of additional

processing stages. The motivation for this style of processing is to be able to track changes in the speech spectrum over time, essentially creating a series of spectral snapshots.

This procedure has been described as the *Fourier transform view* of the STFT, for obvious reasons. However, the STFT can also be interpreted as a filtering operation, where the window function (in this case, a Hamming window) plays the role of filter impulse response. In this *filtering view* of the STFT, the window function combined with the DFT operation creates a bank of bandpass filters centered at the DFT bin frequencies and having the impulse response of the window function (Nawab & Quatieri, 1988). Furthermore, because of the 10-ms shift between successive frames, the front end is also performing downsampling of the input signal.

Thus, subband processing can be easily incorporated into the speech recognition front end because we get the required analysis processing, *i.e.* the bandpass filtering and downsampling, without any additional computation. In addition, because the STFT vectors are converted to feature vectors for decoding, there is no need to resynthesize the fullband signal after processing.

5.4.2 Subband Filter-and-Sum Array Processing

When subband processing is performed using a DFT filterbank, the subband signals are simply the DFT coefficients themselves. Consider a sequence of spectral vectors derived from several frames of speech waveform. The DFT coefficients at a particular frequency over all frames can be considered a time-series of (complex) samples that describes the variation over time in the signal at that particular frequency. In subband filtering, each subband signal is processed by a separate filter. In this work, each subband is assigned an FIR filter with complex tap values. Furthermore, because we are operating in a multichannel microphone array environment, we assign one such filter to each channel in the array. This leads to a *subband filter-and-sum* array processing architecture, which can be expressed as

$$Y_i[k] = \sum_{m=0}^{M-1} \sum_{p=0}^{P-1} H_p^{m*}[k] X_m^{i-p}[k] \tag{5.1}$$

where $X_m^i[k]$ is the value of the STFT in subband k captured by microphone m at frame i, $H_p^m[k]$ is the pth complex tap of the subband filter assigned to that microphone and subband and * denotes complex conjugation.

If we define N to be the frame size in samples used for feature extraction and R to be the frame shift in samples, it can be shown (see Appendix B) that a bank of P-point subband

filters in the DFT domain is equivalent to a single fullband filter spanning P frames or $N + (P-1) \cdot R$ taps in the sample domain. Furthermore, because typically $P << N$, the number of parameters that have to be jointly estimated in each subband is much smaller, as each subband can be optimized independently. As a result, the parameters can be estimated more reliably.

In the next section, these ideas are used as the basis of a new array processing algorithm which incorporates subband processing into the maximum likelihood array processing framework developed in Chapter 4.

5.5 Subband-Likelihood Maximizing Beamforming (S-LIMABEAM)

In the previous chapter, we saw that optimizing the array processing parameters according to the same maximum likelihood criterion used by the recognition system resulted in significant improvements in recognition accuracy. We noted in this chapter however, that this approach suffers from the same convergence and dimensionality issues that degrade the performance of traditional adaptive filtering algorithms in highly reverberant environments, and presented subband filtering as a means of alleviating these problems. We now turn to the question of how to incorporate subband filtering into our recognizer-based maximum likelihood array processing framework.

In general, developing a subband processing implementation of a fullband adaptive filtering algorithm is fairly straightforward. The signal is divided into subbands and the processing normally performed on the fullband signal is simply performed on each of the subbands independently. However, because the HMMs in the recognizer model distributions of *features*, there is no notion of a desired subband signal or subband signal error. Furthermore, we will demonstrate that processing all subbands independently is potentially sub-optimal for recognition-based applications. Because of these factors, it is decidedly non-trivial to incorporate subband processing into the LIMABEAM algorithms presented in Chapter 4.

In this section, we attempt to do so by developing a subband filtering architecture which explicitly considers how the recognition features are computed. We then present an algorithm for optimizing the subband filter parameters using the statistical models of the recognition system. We refer to this approach as *Subband-LIkelihood MAximizing BEAMforming* (S-LIMABEAM).

5.5.1 Feature-based Subband Filtering

In conventional subband adaptive filtering techniques, the filter coefficients $H_p^m[k]$ for particular subband k are adapted independently from the other subbands. However, closer examination of the feature extraction process used in speech recognition will reveal that for our purposes, this is sub-optimal.

The mel spectrum is derived from the STFT by computing the energy in a series of weighted overlapping frequency bands. Each component of the mel spectral vector is computed as a linear combination of energy in a particular subset of DFT subbands. If we define M_i^l as the lth component of the mel spectrum of frame i and $V^l[k]$ as the value of the lth mel triangle applied to subband k, this can be expressed as

$$M_i^l = \sum_{k=l_-}^{l_+} V^l[k] Y_i[k] Y_i^*[k] \tag{5.2}$$

where l_- and l_+ are the DFT bins corresponding to the left and right edges of the lth mel filter, respectively. Outside of this range, the value of $V^l[k]$ is 0.

Substituting Equation (5.1) into Equation (5.2) clearly reveals that a given mel spectral component M_i^l is a function of the subband filter parameters of all microphones and *all subbands in the frequency range spanned by its mel filter*. Processing the subbands independently ignores this relationship. A more optimal approach would consider this set of filter coefficients *jointly* for each mel spectral component, and in the following section, we describe a method that does so.

5.5.2 Maximum Likelihood Estimation of Subband Filter Parameters

As before, we will assume that maximizing the likelihood of a recognition hypothesis can be accomplished by maximizing the likelihood of the most likely HMM state sequence for that transcription. We further assume that the components of the feature vectors are independent. This is the same assumption used by the recognizer in modeling the HMM state output distributions as Gaussians with diagonal covariance matrices. Under this assumption, the likelihood of a given state sequence can be maximized by maximizing the likelihood of each component in the feature vector independently.

If we operate in the log mel spectral domain, each component of the feature vector is a function of only a subset of DFT subbands, as shown in Equation (5.2). Therefore, to maximize the likelihood of a given vector component, we only need to optimize the parameters of the subband filters that are used to compute that component. Note that

if we were to operate in the cepstral domain we could not do this because each cepstral coefficient is a linear combination of *all* log mel spectral components and therefore a function of *all* subbands.*

We can now define $\boldsymbol{\xi}_l$ to be the vector of subband filter parameters required to generate the lth log mel spectral component. $\boldsymbol{\xi}_l$ is a complex vector of length $M \cdot P \cdot (l_+ - l_- + 1)$ covering all filter taps of all microphones for the group of subbands from which the lth mel spectral component is computed. The length of $\boldsymbol{\xi}_l$ varies depending on the number of subbands used to compute a particular mel spectral component.

For each dimension of the feature vector $l = \{0, \ldots, L-1\}$, we want to maximize the log likelihood of the given HMM state sequence with respect to $\boldsymbol{\xi}_l$, the vector of subband array parameters for that dimension. Thus, we perform L maximum likelihood optimizations of the form

$$\hat{\boldsymbol{\xi}}_l = \underset{\boldsymbol{\xi}_l}{\operatorname{argmax}} \sum_i \log(P(z_i^l(\boldsymbol{\xi}_l)|s_i)) \qquad l = \{0, \ldots, L-1\} \tag{5.3}$$

where $z_i^l(\boldsymbol{\xi}_l)$ is lth component of log mel spectrum at frame i and s_i is the most likely HMM state at frame i.

Figure 5.3 shows an example of this maximum likelihood subband filter optimization for an array of two microphones, for the lth log mel spectral component which is composed of three DFT subbands.

5.6 Optimizing the Subband Filter Parameters

For the reasons originally discussed in Section 4.5, Equation (5.3) cannot be directly maximized with respect to $\boldsymbol{\xi}_l$, and therefore we do so using iterative non-linear optimization methods. We will again employ conjugate gradient descent as our optimization method. Therefore, we need to compute the gradient of Equation (5.3) with respect to the corresponding set of array parameters, $\boldsymbol{\xi}_l$.

*In most speech recognition systems, the mel triangles do not actually span the *entire* frequency range. The lowest frequency is typically between 100 and 150 Hz and the highest frequency depends on the sampling rate but is usually somewhat less than the Nyquist frequency.

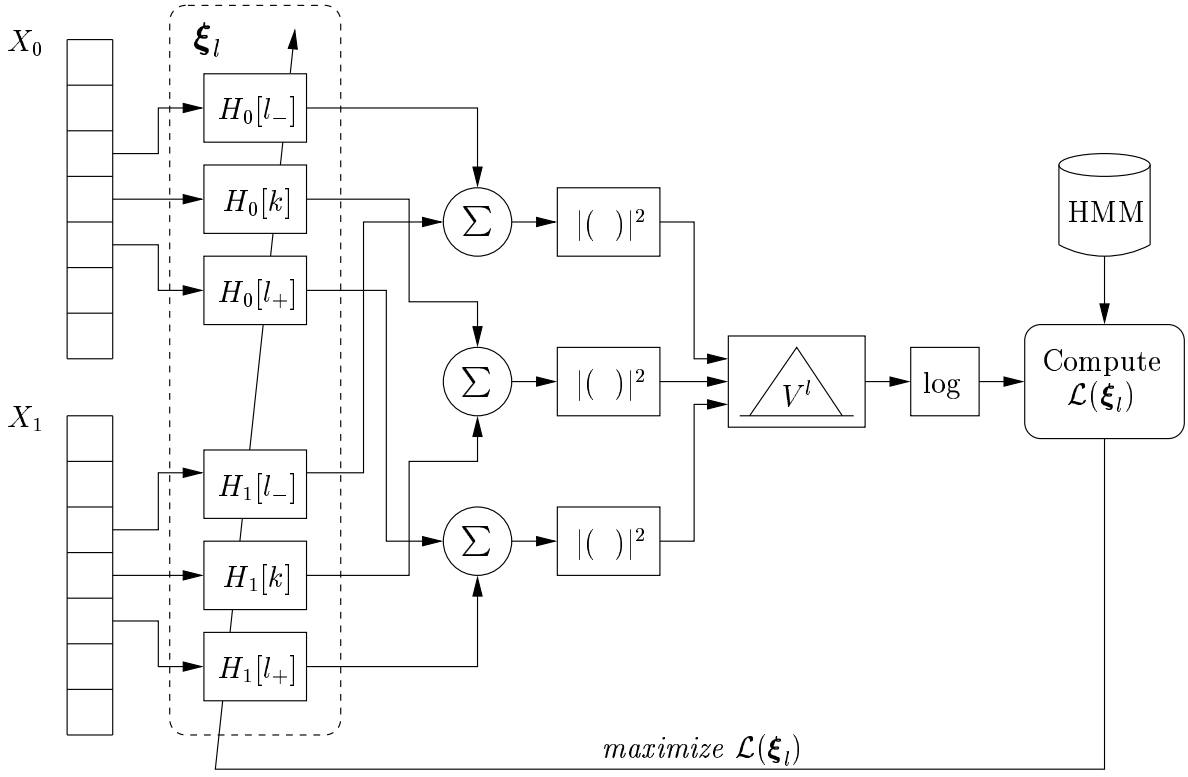

Figure 5.3: S-LIMABEAM for an array of two microphones for the lth log mel spectral component which is composed of three subbands. X_0 and X_1 are the STFT vectors for microphones 0 and 1, respectively, and V^l is the lth mel filter.

5.6.1 Gaussian State Output Distributions

If the HMM state output distributions are assumed to be Gaussian, then the log-likelihood expression in Equation (5.3) can be written as

$$\mathcal{L}(\boldsymbol{\xi}_l) = \sum_i -\frac{1}{2}\frac{\left(z_i^l(\boldsymbol{\xi}_l) - \mu_i^l\right)^2}{\sigma_i^{l\,2}} + \kappa_i^l \tag{5.4}$$

where μ_i^l and $\sigma_i^{l\,2}$ are the mean and variance of the lth dimension of the Gaussian of state s_i and κ_i^l is a normalizing constant. The gradient of Equation (5.4) can be expressed as

$$\nabla_{\boldsymbol{\xi}_l}\mathcal{L}(\boldsymbol{\xi}_l) = -\sum_{i=0} \frac{\left(z_i^l(\boldsymbol{\xi}_l) - \mu_i^l\right)}{\sigma_i^{l\,2}} \frac{\partial z_i^l(\boldsymbol{\xi}_l)}{\partial \boldsymbol{\xi}_l} \tag{5.5}$$

where $\partial z_i^l(\boldsymbol{\xi}_l)/\partial \boldsymbol{\xi}_l$ is the gradient vector. In the previous chapter, we were differentiating the full feature vector with respect to a vector of array parameters, which resulted in a Jacobian matrix. Here, we are differentiating only a single component of the feature vector, *i.e.* a scalar, with respect to the array parameters, which produces a gradient vector. The gradient vector is a complex vector with dimension that varies according to the log mel spectral component. For the lth component, the length of the gradient vector is $M \cdot P \cdot (l_+ - l_- + 1)$. The complete derivation of the gradient vector is given in Appendix C

5.6.2 Mixture of Gaussians State Output Distributions

In the case where the state densities are mixtures of Gaussians, the log-likelihood expression is expressed as

$$\mathcal{L}(\boldsymbol{\xi}_l) = \sum_{i=0}^{N-1} \log\left\{\sum_{k=1}^{K} \exp\left(-\frac{1}{2}\frac{\left(z_i^l(\boldsymbol{\xi}_l) - \mu_{ik}[l]\right)^2}{\sigma_{ik}^{l\,2}} + \log(\alpha_{ik}) + \kappa_{ik}^l\right)\right\} \tag{5.6}$$

In a similar manner as before, we will use $G_{ik}^l(\boldsymbol{\xi}_l)$ to represent the term inside the exp() operator, giving the following more compact representation of the log likelihood

$$\mathcal{L}(\boldsymbol{\xi}_l) = \sum_{i=0}^{N-1} \log\left\{\sum_{k=1}^{K} \exp\left(G_{ik}^l(\boldsymbol{\xi}_l)\right)\right\} \tag{5.7}$$

The derivation of the gradient is very similar to the derivation of the Jacobian matrix

in the fullband filter case in Chapter 4. The expression is

$$\nabla_{\boldsymbol{\xi}}\mathcal{L}(\boldsymbol{\xi}) = -\sum_{i}\sum_{k=1}^{K}\gamma_{ik}^{l}(\boldsymbol{\xi}_l)\frac{\left(z_i^l(\boldsymbol{\xi}_l)-\mu_{ik}^l\right)}{\sigma_{ik}^{l\,2}}\frac{\partial z_i^l(\boldsymbol{\xi}_l)}{\partial \boldsymbol{\xi}_l} \tag{5.8}$$

where $\gamma_{ik}^{l}(\boldsymbol{\xi}_l)$ is the *a posteriori* probability that the lth dimension of the kth Gaussian in the mixture modeling state s_i generated the observed log mel spectral component $z_i^l(\boldsymbol{\xi}_l)$.

Because we are doing component-wise optimization, there are L separate optimizations performed, one for each dimension of the log mel spectral vector. Again, because we are performing subband processing, there are far fewer parameters to optimize *per optimization* than in the fullband case. Because the mel triangles are spaced along the frequency axis so that adjacent triangles overlap each other by 50%, each DFT subband contributes to the value of two mel spectral components. By processing the DFT subbands jointly within each mel component, but independently across mel components, the optimization of the complete log mel spectral vector has twice as many degrees of freedom compared to conventional subband filtering schemes.

In the next section we analyze the number of parameters required in the subband filtering approach compared to the number of parameter required in a more conventional fullband filtering approach.

5.7 Analysis of the Dimensionality of Subband Filtering

As stated earlier, one of the major benefits of subband filtering schemes is a reduction in the number of parameters that have to be jointly estimated. Simply put, in the subband approach, a single filter whose parameters must be optimized *jointly* is replaced by multiple filters that can be optimized *independently*, each with fewer parameters. In this section we highlight the savings in parameters obtained for the specific case of subband filtering using the bandpass filtering and downsampling inherent in the feature extraction process.

In the S-LIMABEAM scheme described in Section 5.5, an independent optimization is performed for each dimension of the log mel spectral vector. The number of parameters to be learned in each optimization depends on the mel filter used to compute the particular vector component. The value can be computed as $M \cdot P \cdot (l_+ - l_- + 1)$ where M is the number of microphones, P is the number of taps per filter, and l_- and l_+ are the lowest and highest bins, respectively, in the lth mel filter. Because the filter taps are complex valued, the total number of parameters to be optimized is actually twice this number, as both the real and imaginary components of each tap must be estimated.

As shown in Appendix B, a bank of P-point subband filters is equivalent to a single fullband filter spanning P frames or $N + (P-1) \cdot R$ samples, where N is the frame size and R is the frame shift in samples. In this work, $N = 400$ and $R = 160$, corresponding to a 25-ms window and 10-ms shift for speech sampled at 16 kHz. A total of 256 subbands were computed from a 512-point DFT. The features were derived from 40 mel triangles covering a frequency range from 125 Hz to 6850 Hz, and the number of subbands in each triangle ranged from 2 to 23. These values are typical for state-of-the-art HMM speech recognition systems. Thus, the maximum number of free parameters that have to jointly optimized is $M \cdot P \cdot 23 \cdot 2$, or $46 \cdot P$ per microphone.

Figure 5.4 shows the number of parameters per microphone that need to be jointly optimized as a function of the effective filter length in frames. The dashed line shows the number of parameters required for a fullband time-domain FIR filter, as used in the previous chapter. The solid line shows the number of parameters required to optimize the vector component that corresponds to the widest mel filter. This represents the maximum number of parameters that need to be estimated jointly for the proposed feature-based subband filtering scheme. Finally, the dotted line shows the total number of parameters over *all* dimensions of the feature vector that need to be optimized using this method. Thus, the total number of parameters that need to be optimized is actually greater than in the fullband case. However, because the parameters for each dimension of the feature vector are optimized independently, the number of parameters that need to be *jointly* estimated is greatly reduced.

5.8 Applying S-LIMABEAM to Reverberant Speech

In this chapter a new method has been described in which filter parameters are optimized in subband domain to maximize the likelihood of a given transcription. This method can be readily incorporated into the two algorithms presented in Chapter 4. The only significant change to the algorithms is that the single optimization over all filter parameters for all microphones in the original algorithms is replaced by L independent optimizations, where L is the length of the log mel spectral feature vector.

In the following section, we evaluate the performance of the described subband filter architecture in a reverberant environment by optimizing the subband parameters using oracle state sequences. As before, this will define the upper bound on the performance of the subband approach. We then perform experiments to evaluate the performance of the subband filtering approach when it is incorporated into both the array calibration algorithm and the unsupervised array processing algorithm.

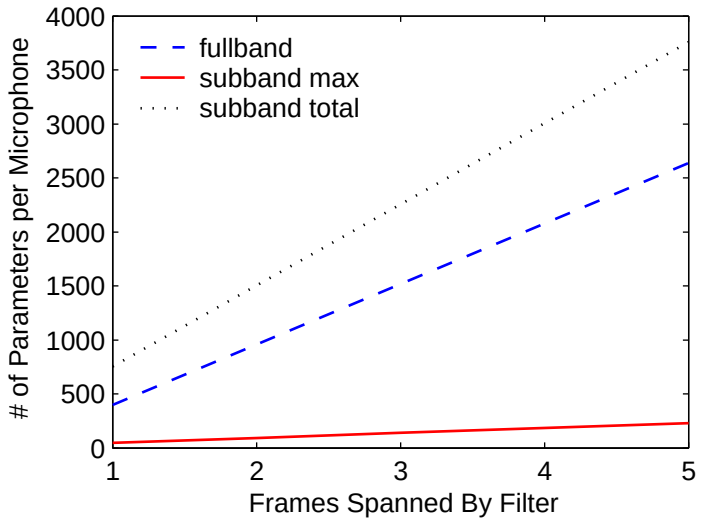

Figure 5.4: The maximum number of parameters per microphone that need to be jointly optimized as a function of the effective filter length in frames. In LIMABEAM, this value corresponds to all filter parameters, while in the S-LIMABEAM, because each log mel spectral component is optimized independently, this value is the number of parameters required to compute the widest mel filter. Also shown is the total number of parameters needed in the subband case, accumulated over all mel spectral components.

In all experiments, the forced alignment and decoding are performed using HMMs trained on cepstra. The parameter optimization is performed using a parallel set of HMMs trained on log mel spectra without feature mean normalization.

5.9 Evaluating S-LIMABEAM Using Oracle State Sequences

In the first series of experiments, we will experimentally determine the upper bound on the performance of the proposed algorithm by optimizing the subband filter parameters using oracle HMM state sequences. As before, these state sequences are obtained from forced alignment using *a priori* knowledge of the utterance transcriptions and feature vectors derived from the close-talking microphone recordings.

Subband filter optimization was performed on $\text{WSJ}_{0.47}$, the 7-microphone reverberant WSJ corpus with $T_{60} = 0.47$ s. The experimental procedure was the same as that used in the oracle experiments described in Section 4.6. First, Time-Delay Compensation was performed using the PHAT technique to align the array signals. These signals were then aligned to the close-talking microphone signal to ensure that the state sequence derived from the close-talking recording is valid for the array signals. The subband filter parameters

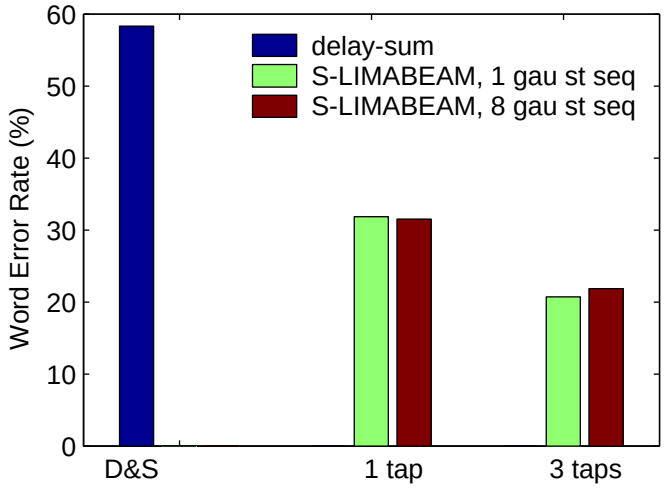

Figure 5.5: WER obtained using Oracle S-LIMABEAM for the $\text{WSJ}_{0.47}$ corpus. The figure shows the performance obtained when 1- or 3-tap subband filters are optimized using HMM distributions modeled by single Gaussians or mixtures of 8 Gaussians. The performance obtained using delay-and-sum beamforming is also shown.

were initialized to an unweighted delay-and-sum configuration and then optimized using conjugate gradient descent. Finally, the array signals were processed by the optimized subband filters and converted to cepstral features for recognition.

Because the subband filters operate on the DFT coefficients, the delay-and-sum configuration in Equation (4.24) used for initialization must be transformed into the spectral domain. Thus, after TDC has been performed, the initial values of the filter parameters are expressed as

$$H_p^m[k] = \begin{cases} 1/M & p = 0, \forall\ m, k \\ 0 & p \neq 0, \forall\ m, k \end{cases} \tag{5.9}$$

where m is the microphone index, p is the tap index, and k is the subband index. Alternatively, the delays required for TDC can be incorporated into Equation (5.9) by multiplying the subband tap values by the appropriate phase terms.

In these experiments, we evaluated the performance of the subband filter architecture when filters composed of 1 tap and 3 taps were optimized. For both of these filter lengths, the optimization was performed using both single Gaussians and mixtures of 8 Gaussians to model the state output distributions in the log-likelihood expression. The results of these experiments are shown in Figure 5.5.

There are several interesting points to note from these results. First, incorporating sub-

band filtering into the maximum likelihood parameter optimization framework developed in Chapter 4 has the potential to dramatically improve recognition performance in reverberant environments. The figure shows that relative improvements over delay-and-sum beamforming of more than 45% are possible with only a single tap per subband filter, and of more than 60% are possible with 3 taps per filter.

Second, significant improvements can be obtained with only a single tap in the subband domain. With only a single tap for each subband filter, no processing across frames is occurring as each subband component is simply multiplied by a weight. This shows that in a microphone array scenario, significant improvements can be achieved without inverse filtering. If inverse filtering *were* required, one would expect that filters spanning several frames would be necessary, and little improvement in recognition accuracy would be seen with only a single tap. The figure does show however, that when the 3 taps are used and processing does occur across time, substantial additional improvement is possible.

Finally, these plots show that, at least for the oracle case, there is not a significant advantage to using more complicated densities to model the state output distributions. However, unlike the experiments using mixtures of Gaussians in the previous chapter, the results between single Gaussians and mixtures are comparable. In the previous chapter, we claimed that the poor performance of the optimization using mixtures of Gaussians could be attributed to the mismatch in task between the WSJ training data and the CMU-8 test data. In these experiments, the test data is derived from the WSJ test set, and therefore is clearly well-matched in task to the training data. Thus, according to our claim, we should expect either similar or better performance using mixtures of Gaussians compared to single Gaussians. This experiment shows the former to be the case.

Of course, it remains to be seen if the conclusions drawn from these experiments continue to be valid in more realistic situations, where the state sequence is no longer known *a priori*. We now turn our attention to these scenarios.

5.10 The Calibrated S-LIMABEAM Algorithm

We now present Calibrated S-LIMABEAM algorithm, the subband filtering counterpart of the array parameter calibration algorithm presented in Section 4.7. In this algorithm, the subband filter parameters are optimized during a calibration phase. As before, calibration is performed using an enrollment utterance with a known transcription. The user speaks this utterance and the speech is captured by the array. The array signals are processed in some manner, *e.g.* delay-and-sum beamforming, and features are extracted. These features and the known utterance transcription are then used to estimate the most likely HMM state

sequence. Using this state sequence, the subband filter parameters are optimized.

The only difference between this algorithm and the original calibration described in Section 4.7 is that the single joint optimization over all parameters is now replaced with L independent optimizations, each operating on a subset of the total set of subband filter parameters. As before, this optimization process can be iterated. That is, once the filters have been optimized, they can be used to generate a new set of features which can then be used to obtain a better estimate of the target HMM state sequence. The subband filter parameters can then be re-optimized using this improved state sequence, and so on.

5.10.1 Experimental Results Using Calibrated S-LIMABEAM

To evaluate the performance of Calibrated S-LIMABEAM, experiments were performed on the $\text{WSJ}_{0.47}$ corpus. The first series of experiments compared the WER obtained using the calibration algorithm for different subband filter lengths. For each experiment, the filter length was constant over all subbands. For convenience, we restricted these initial experiments to a single speaker from the test set. The filter parameters were calibrated using a only single utterance from the test set, chosen at random from those utterances at least 10 s long. The same calibration utterance was used for all experiments.

For these experiments, a single iteration of calibration was performed as follows. Using the known transcription of the calibration utterance and features generated from the delay-and-sum output signal, the most likely state sequence was estimated. The filter parameters were then initialized to the delay-and-sum configuration and optimized. The state output distributions in the log-likelihood expression being maximized were represented by mixtures of 8 Gaussians. Once the subband filter parameters were calibrated, they were used to process the remaining test set utterances. The results of these experiments are shown in Figure 5.6.

As the figure shows, this calibration technique is able to dramatically improve the WER compared to delay-and-sum processing for this speaker. As expected in a calibration scenario, when too many parameters are learned from too little data, overfitting occurs and performance suffers. Comparing the relative improvements using 1 and 3 taps to those shown in Figure 5.5, we can see that quite a bit of performance is lost over the oracle case. This differs from the results in the previous chapter, where the calibration algorithm was able to come quite close to oracle performance. One possible explanation for this difference is that the "noise" in a highly reverberant environment is inherently non-stationary, as it is composed primarily of reflections of the target speech signal. Nevertheless, these results are quite convincing that incorporating subband processing into the LIMABEAM framework is

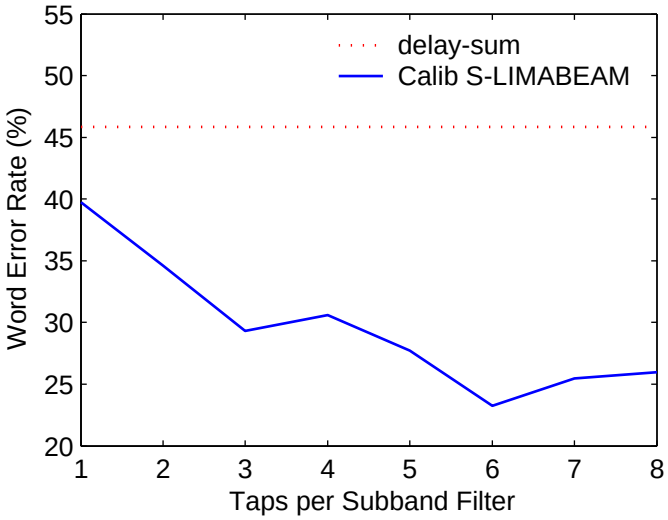

Figure 5.6: WER obtained using Calibrated S-LIMABEAM vs. the number of taps used in each subband filter, for single speaker from the $WSJ_{0.47}$ corpus. The performance of delay-and-sum beamforming is shown for comparison.

highly advantageous in reverberant environments. This is evident when we compare these results to those in Figure 5.1, obtained using the original fullband LIMABEAM algorithm.

Figure 5.7 shows four spectrographic displays of 40-dimensional log mel spectral feature vectors for a segment of one of the utterances in the test set. The figure compares the log mel spectra extracted from a single microphone from the array, the output of a delay-and-sum beamformer, the output of the Calibrated S-LIMABEAM algorithm with 5 taps per filter, and the close-talking recording. As the figure shows, delay-and-sum processing does little to reduce the temporal smearing caused by the reverberation, and in fact, the delay-and-sum spectrogram is virtually indistinguishable from that of the single microphone. Compared to the close-talking log mel spectra, all the distinction between high and low energy regions across time has been lost. On the other hand, the features generated by the calibrated subband filtering algorithm look significantly sharper and the low energy regions between speech segments have been restored.

In the next series of experiments, we evaluated the performance of the calibration algorithm in rooms with other reverberation times. The calibration experiment described above was repeated for speech captured in rooms with T_{60} ranging from 0.3 s up to 1.3 s. In these experiments, calibration was performed for all speakers in the test set, using a single calibration utterance per speaker chosen randomly in the manner described previously. The

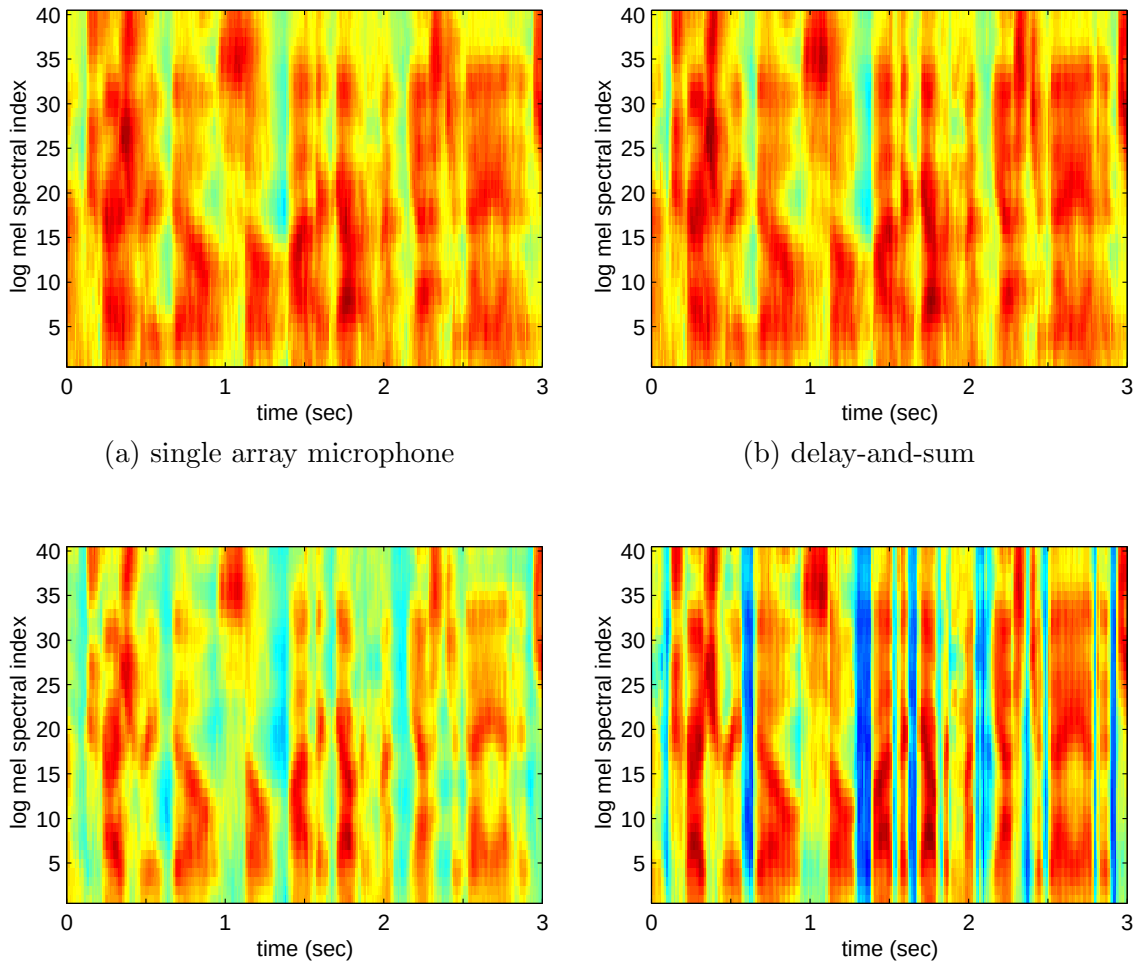

(a) single array microphone

(b) delay-and-sum

(c) Calibrated S-LIMABEAM

(d) close-talking microphone

Figure 5.7: Log mel spectrograms of a segment of an utterance from the $\text{WSJ}_{0.47}$ corpus obtained from (a) a single channel in the array, (b) delay-and-sum beamforming, (c) the Calibrated S-LIMABEAM algorithm with 5 taps per filter, and (d) the close-talking microphone signal.

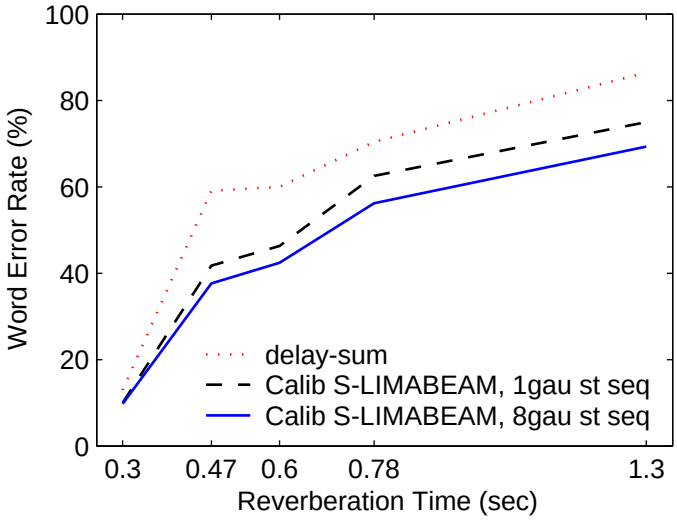

Figure 5.8: WER obtained using Calibrated S-LIMABEAM shown as a function of reverberation time for the reverberant WSJ corpora. The performance of a delay-and-sum beamforming is also shown.

same set of calibration utterances was used across all room conditions. Subband filters with a 1 tap were used for the 0.3 s case, while filters with 5 taps were used for the remaining reverberation conditions. The results of this experiment are shown in Figure 5.8.

As the figure indicates, Calibrated S-LIMABEAM produces significant improvements over conventional delay-and-sum processing at all reverberations times. Using this approach, the relative improvement over delay-and-sum beamforming, averaged over all reverberation times, is 26.0%, with a minimum improvement of 19.7% at 1.3 s and a maximum improvement of 36.2% at 0.47 s. Based on these results, it is likely that further improvements in WER, especially at the very high reverberation times, could be achieved if more data were used for calibration, enabling longer subband filters to be reliably estimated. Interestingly, there is a clear improvement in the performance of the calibration algorithm when the parameter optimization is performed using mixtures of Gaussians rather than single Gaussians. Although this makes intuitive sense, as we are performing the actual recognition using mixtures of Gaussians, it is unclear why similar results were not seen in the oracle experiments in Section 5.9.

Clearly, we are able to achieve significant improvements in WER over a wide range of reverberation times. However, to be fair, we must also acknowledge that the data used in these experiments are ideally suited for a calibration algorithm. Because the reverberant

speech corpora were created by convolving clean speech with recorded room impulse responses, the distortion caused by the reverberation was exactly the same for all utterances in the test set. This would occur if the user's position was fixed throughout. This is a bit unrealistic, as even a user trying to remain in place would not be perfectly still. Therefore, it is possible that the algorithm's performance would degrade a bit if it were applied to data recorded by actual users. Based on our results in Chapter 4 on the CMU-8 corpus, we expect the loss in performance to be minimal. This hypothesis, however, remains untested, as a suitable reverberant corpus was not available.

These experiments show that the filter parameter calibration algorithm can be successfully incorporated into the S-LIMABEAM framework. We now turn to the unsupervised processing case for use in situations in which the environmental conditions and/or the user's position may vary across utterances.

5.11 The Unsupervised S-LIMABEAM Algorithm

In Section 4.8, an algorithm was described for optimizing array processing parameters in situations in which significant variability is expected across utterances. Recall that in this approach, the array parameters were optimized for each utterance independently, using an HMM state sequence derived in an unsupervised manner from a hypothesized transcription.

As in the calibration algorithm described above, the proposed subband filtering architecture can be readily incorporated into the unsupervised array processing algorithm by simply replacing the one joint optimization over all parameters with several independent optimizations, one for each component of the log mel spectral feature vector.

5.11.1 Experimental Results Using Unsupervised S-LIMABEAM

Unsupervised S-LIMABEAM was performed on the reverberant $\text{WSJ}_{0.47}$ corpus. In all experiments, the initial transcript used to estimate the most likely HMM state sequence was generated using features derived from delay-and-sum processing. For optimization, the filters were initialized to the delay-and-sum configuration after TDC was performed, as given by Equation (5.9). Performance was evaluated using 1-, 3-, or 5-tap subband filters and either Gaussians or mixtures of Gaussians for optimization. The results are shown in Figure 5.9

As the figure shows, the improvement over delay-and-sum processing obtained using unsupervised processing is only about 7% relative. Using more parameters does not improve the performance greatly. The difference between using 1 tap and 3 taps is statistically

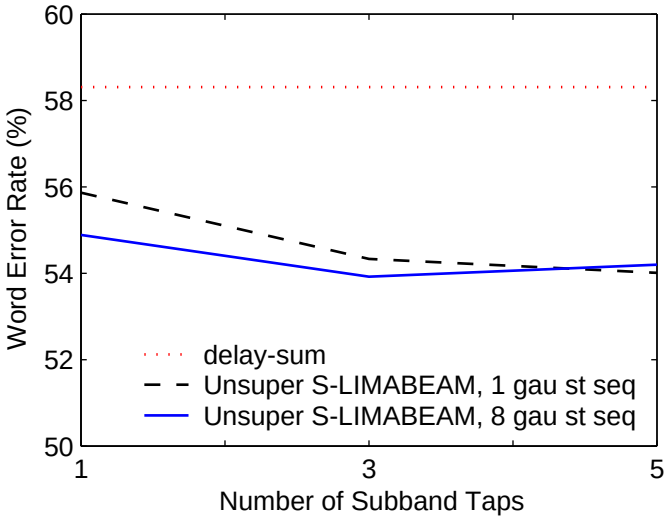

Figure 5.9: WER obtained using Unsupervised S-LIMABEAM vs. the number of taps used in each subband filter for the $\text{WSJ}_{0.47}$ corpus. The figure shows the performance when single Gaussians or mixtures of Gaussians are used in the likelihood expression being maximized. The performance of delay-and-sum beamforming is shown for comparison.

significant only with $p = 0.1$ and there is no significant difference between using 3 taps and 5 taps. These results highlight the difficulties of performing unsupervised adaptation in situations in which the initial error rate is very high. Because the error rate of the first-pass recognition is almost 60%, the state sequences used to optimize the filter parameters generally contain more incorrect state labels that correct ones. In this situation, it is very difficult to improve performance in an unsupervised manner.

To confirm that the high error rate is indeed is the source of the poor performance, we repeated the same experiment using the speech captured in a room with a 0.3 s reverberation time. These data had a much higher first-pass recognition accuracy. The experimental procedure was identical to the previous experiment, except that only subband filters with 1 tap were optimized. The results are shown in Table 5.2. As expected, the unsupervised parameter optimization algorithm is much more successful when the first-pass recognition accuracy is higher. In this case, we were able to obtain a 23.4% relative improvement over delay-and-sum beamforming.

Based on these experiments, it is apparent that one obvious way to improve the performance of the unsupervised parameter optimization algorithm is to somehow obtain a better first-pass transcription. This is equivalent to needing better initial filter parameters. While this is somewhat of a chicken-and-egg problem (*i.e.* if we had better parameters,

Array Processing Algorithm	WER (%)
delay-and-sum	12.8
Unsupervised S-LIMABEAM, 1 tap, 1 gau st seq	9.9
Unsupervised S-LIMABEAM, 1 tap, 8 gau st seq	9.8

Table 5.2: WER obtained using Unsupervised S-LIMABEAM on the $WSJ_{0.3}$ corpus

additional processing would be unnecessary), there are some feasible solutions. For example, if the environment is changing slowly, array parameters obtained from calibration could be used to generate an initial transcription. Also, in these unsupervised experiments, we have considered each utterance independently. However, one useful set of initial parameters would be the filter parameters obtained from unsupervised processing of the previous utterance. Because both the environment and user location are stationary in our test corpora, performing unsupervised adaptation in either of these two ways would generate unfairly optimistic results. Therefore, these experiments were not performed in this thesis. However, both approaches are viable methods of improving the performance of the Unsupervised S-LIMABEAM algorithm.

One additional method of improving the performance of the unsupervised algorithm when the initial transcriptions have a high WER is to simply perform additional iterations of unsupervised processing. We performed additional iterations of unsupervised processing on the $WSJ_{0.47}$ corpus. Because the results of the initial pass of unsupervised processing were comparable for different filter lengths and number of Gaussians, further iterations were restricted to using 3 taps in the subband filters and single Gaussians in the likelihood expression. Figure 5.10 shows the WER obtained after each iteration of unsupervised processing. The performance of delay-and-sum beamforming is shown as iteration 0.

As the figure shows, the WER begins to asymptote after two iterations of unsupervised processing. While the relative improvement over delay-and-sum beamforming increases to 10.6%, additional iterations are not expected to improve performance significantly.

As is the case with all unsupervised processing algorithms, if the initial hypotheses are poor, then additional unsupervised processing will likely degrade performance, as parameters are being optimized using incorrect target values. For this reason, these experiments were not repeated for environments with more severe reverberation. If any improvement was obtained from unsupervised processing in these cases, it would be slight, and obtaining significant improvement would require a prohibitively large number of iterations.

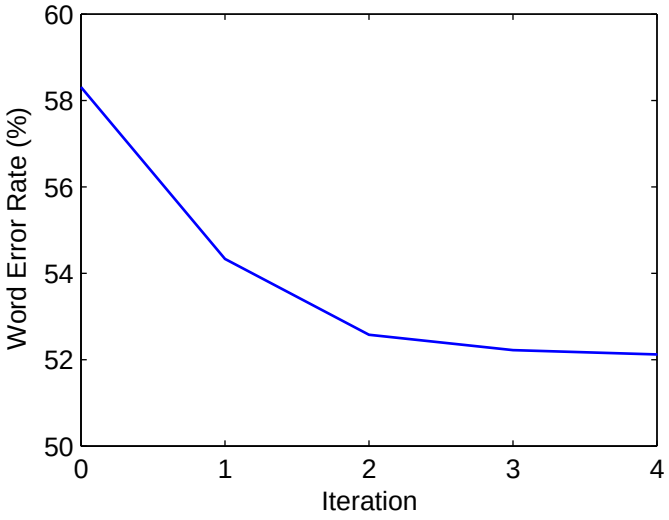

Figure 5.10: WER obtained using Unsupervised S-LIMABEAM on the $WSJ_{0.47}$ corpus as a function of the number of iterations of optimization performed.

5.12 Computational Complexity

As discussed in Section 4.10.4, it is difficult to determine the computational complexity of algorithms which employ gradient-descent-based optimization and obtain locally optimal solutions. As a result, we again use the average time required to process an utterance to get a sense of the complexity of the algorithm. Because an independent optimization is performed for each log mel spectral component, the optimizations can be done in parallel. Additionally, the number of taps used in each subband filter can vary from subband-to-subband. Because finding the optimal filter length for each subband would require an exhaustive search, all experiments performed in this thesis used a constant number of taps in all filters. To provide a sense of the computation required to perform S-LIMABEAM, we computed the average time required to optimize 1-tap and 5-tap subband filters for a single log mel spectral component using both single Gaussians and mixtures of 8 Gaussians in the likelihood function. This was performed on the 7-microphone $WSJ_{0.470}$ corpus. The results are shown in Figure 5.11, expressed as times-real-time.

If the subband parameters for each log mel spectral component are optimized in parallel, the values in the figure represent a reasonable measure of the required processing time. However, if the optimizations are performed sequentially, then the total processing time is approximately the values in the figure times the number of optimizations, *i.e.* the length of the log mel spectral vector. In this case, where 40 log mel spectral components are used,

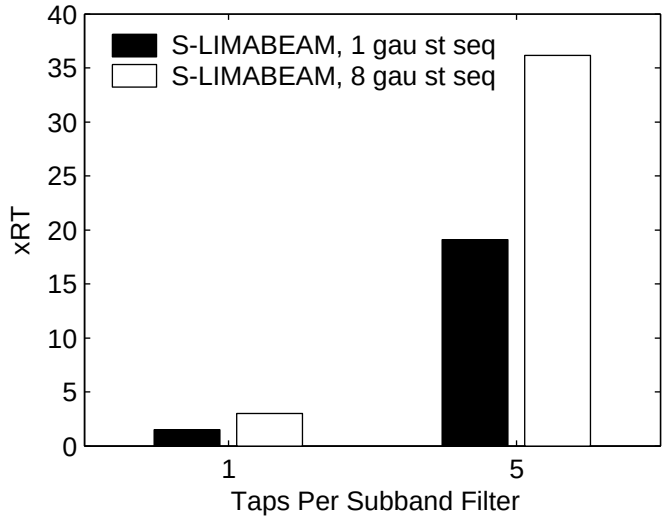

Figure 5.11: Average times-real-time to convergence of the subband filter parameter optimization for one log mel spectral component using subband filters with 1 tap and 5 taps and single Gaussians or mixtures of 8 Gaussians in the likelihood expression.

it is clear that the required computation is quite significant if subband filters with multiple taps are optimized.

In the next section we present some methods to reduce the number of subband filter parameters in an effort to improve the efficiency of the proposed algorithms.

5.13 Dimensionality Reduction via Parameter Sharing

Both the Calibrated and Unsupervised S-LIMABEAM algorithms have been shown to perform well in reverberant environments using the proposed subband filter architecture. Large improvements in recognition accuracy were obtained by applying subband filtering principles that enable a reduction in the number of parameters to be jointly optimized and an improvement in convergence. However, Section 5.12 showed that the computation required is still quite significant. By reducing the number of parameters to optimize, we can reduce the processing time and possibly improve the performance. We propose two parameter sharing approaches in order to reduce the number of subband filter parameters required. In the first approach, parameters are shared between subbands within same mel spectral component, and in the second approach, the parameters are shared across mel spectral components.

5.13.1 Sharing Parameters Within Mel Spectral Components

In this approach, subband filter parameters are shared across subbands within the same mel spectral component. Specifically, rather than estimating a separate filter for each subband and optimizing the parameters of all subband filters jointly, only a single set of filter parameters shared by all subbands is optimized.

By sharing parameters in this manner, the number of parameters is reduced from $M \cdot P \cdot (l_+ - l_- + 1)$ to simply $M \cdot P$. Clearly, the reduction in the number of parameters is proportional to the number of subbands in a particular mel filter. For the lowest frequency log mel spectral component, which is composed of only two subbands, the number of parameters is reduced by 50%. For the highest frequency log mel spectral component, composed of 23 subbands, the number of parameters required is reduced by 95.6%.

This configuration requires a small change to the formulation of the gradient for optimization. The details of the derivation are given in Appendix C.

5.13.2 Sharing Parameters Across Mel Spectral Components

In the algorithms presented in this chapter, the likelihood of each component of the log mel spectral feature vector is maximized by optimizing a set of filters applied to that component's constituent subbands. Because of mel filters overlap each other by 50%, this results in two distinct filters for each subband, one for each of the mel components to which it contributes.[†] This approach is well-suited to our assumption that the components of the log mel spectral vector are independent. Specifically, by using two different filters for the same subband, the likelihood of each of the log mel spectral components can be maximized independently, without affecting the likelihood of the other components.

However, adjacent mel components are actually highly correlated. The mel spectrum is derived from the energy in overlapping frequency bands such that subbands in the right half (higher frequencies) of one mel triangle are also in the left half (lower frequencies) of the next mel triangle. It is reasonable to expect, then, that for each subband, the two filters, optimized for adjacent mel components, will be similar. Therefore, we propose to reduce the number of total parameters estimated by optimizing a single filter for each subband, which will be used to generate both mel components.

The optimal way to estimate such a filter would be to jointly maximize the likelihood of both log mel spectral components. However, because of the overlap in subbands, jointly maximizing the likelihood of two components cannot be done without maximizing the likeli-

[†]In practice, because of the quantization in frequency caused by the DFT, the overlap between adjacent mel filters can vary and as a result, not all subbands are necessarily used by two mel filters.

hood jointly over all mel components. This requires a joint optimization over all subbands, which defeats the purpose of subband processing entirely.

Instead, we assume that for the subbands included in two mel components, the filter parameters that maximize the likelihood of one mel component also maximize the likelihood of the next component. In other words, the subband filter optimized when its corresponding subband is in the right half of one mel filter is also optimal for that same subband when it is in the left half of the next mel filter. Thus the components of the log mel spectral vector are optimized in succession. For each component, the filters used to optimize the previous component are copied and assumed fixed, and only the filters for new subbands (which will in turn be used for the next component) are optimized. The changes to the gradient derivation required to share parameters in this manner are described in Appendix C.

5.13.3 Experimental Results Using Parameter Sharing

Experiments were performed using these two methods of parameter reduction in order to compare their performance to the original subband filtering architecture. We will evaluate the methods both in terms of speech recognition accuracy and computational efficiency. In the first experiment, the Unsupervised S-LIMABEAM algorithm was applied to the $\text{WSJ}_{0.3}$ corpus using 1 tap per subband filter. In the second experiment, the array calibration algorithm was applied to the $\text{WSJ}_{0.47}$ corpus, using 5 taps per subband filter. In these experiments, we computed both the speech recognition accuracy and the average time to convergence of the two parameter sharing configurations, relative to the original subband architecture. These values were obtained as follows. Each experiment was run on the same computer and the average time to convergence was computed over all utterances for each configuration. The values were then normalized by the average time to convergence of the original subband algorithm. This measure provides some sense of the computational savings afforded by these parameter sharing methods and the potential performance versus time trade-offs. The results of these experiments are summarized in Table 5.3.

As the data in the table shows, these parameter sharing methods provide a significant reduction in computation for a small reduction in performance.

5.14 S-LIMABEAM in Environments with Low Reverberation

In this chapter we have proposed a subband filtering approach to the LIMABEAM framework presented in the previous chapter. The algorithms presented in this chapter were

T_{60} (sec)	Array Processing Algorithm	# of Taps	Subband Architecture	WER	Relative Time
0.30	delay-and-sum	-	-	12.8	-
0.30	unsupervised	1	original	9.8	1.0
0.30	unsupervised	1	share within	10.4	0.64
0.30	unsupervised	1	share across	10.5	0.58
0.47	delay-and-sum	-	-	59.0	-
0.47	calibrated	5	original	37.9	1.0
0.47	calibrated	5	share within	42.7	0.49
0.47	calibrated	5	share across	39.6	0.58

Table 5.3: Performance obtained using S-LIMABEAM using different methods of sharing subband filter parameters. In one case, filter parameters are shared across log mel spectral components and in the other case, they are shared within the same log mel spectral component. The table shows the resulting WER as well as the time to convergence relative to the original subband filtering architecture.

designed specifically to improve the performance of speech recognition in highly reverberant environments. However, these algorithms will be significantly more valuable if they are in fact general solutions for all environments, rather than limited solely to use in environments where the distortion is caused primarily by significant reverberation, rather than other sources, such as additive noise.

To evaluate the generality of the proposed subband algorithms, experiments were performed using the CMU-8 corpus. Recall that this database was recorded in a room with a 0.24 s reverberation time and the speech captured by the array had an SNR of about 6.5 dB. We repeated the unsupervised filter parameter optimization experiment previously performed in Chapter 4. In the original experiment, the parameters of a filter-and-sum beamformer composed of 20-tap FIR filters were optimized using Unsupervised LIMABEAM and a significant improvement in recognition accuracy was obtained over conventional delay-and-sum processing.

This experiment was repeated using the Unsupervised S-LIMABEAM approach presented in this chapter. As before, subband filters with a single tap were optimized using the hypothesized transcriptions from delay-and-sum processing to estimate the HMM state sequence. Experiments were performed using all three variants of subband filter optimization: the original method described in Section 5.11 and the two parameter sharing methods described in Section 5.13. The results of these experiments are shown in Table 5.4

There are no statistically significant differences between the fullband filter optimization method and the any of the subband methods. It is interesting to note that both

Unsupervised Parameter Optimization Method	WER (%)
Unsupervised LIMABEAM, 20 taps	30.2
Unsupervised S-LIMABEAM, 1 tap	30.3
Unsupervised S-LIMABEAM, 1 tap, share within	29.2
Unsupervised S-LIMABEAM, 1 tap, share across	31.4

Table 5.4: WER obtained on the CMU-8 corpus using unsupervised array parameter optimization for the fullband filter-and-sum architecture described in Chapter 4 and the three subband architectures described in this chapter.

shared-parameter architectures generated comparable performance to the original subband method with significantly fewer parameters. Thus, S-LIMABEAM is as effective as the original sample-domain LIMABEAM approach in environments where the distortion is largely caused by additive noise and the reverberation is less severe.

5.15 Summary

In this chapter we have presented an alternative approach to Likelihood Maximizing Beamforming (LIMABEAM) specifically designed for reverberant environments. We studied the performance of the LIMABEAM algorithm presented in the previous chapter in reverberant environments and found that its performance was hindered by the same problems seen in more conventional adaptive filtering schemes, *i.e.* poor convergence and high dimensionality when the input signal is highly correlated and the filter length is long.

We proposed subband filtering as a means of addressing these issues. Using subband filtering reduces the number of parameters that need to be jointly estimated which results in more robust parameter estimation. In addition, the ability to utilize a different step size in each subband improves convergence. We showed how subband filtering can be readily incorporated into the speech recognition front-end because the required bandpass filtering and downsampling are already accomplished by the STFT and the framing process.

We then presented a way of incorporating subband filtering into the speech-recognizer-based maximum likelihood framework developed in the previous chapter. Conventionally, subband processing is performed on each subband independently. However, we observed that doing so may be sub-optimal for speech recognition applications, as it ignores the manner in which the features are computed. Because each mel spectral component is derived from the energy in multiple subbands, we proposed to optimize the filters assigned to these subbands jointly for each mel spectral component. Thus, an independent likelihood maximization is performed for each log mel spectral component in order to optimize the subband

filter parameters required to compute that component. In short, a single joint optimization over all filter parameters for all microphones is replaced by multiple optimizations of select groups of subband filter parameters. We refer to this method as Subband-Likelihood Maximizing Beamforming (S-LIMABEAM).

This feature-based subband filter optimization scheme was then incorporated into the calibration and unsupervised array processing algorithms developed in the previous chapter. Using Calibrated S-LIMABEAM, we obtained significant improvements in recognition accuracy in environments with reverberation times up to 1.3 s. Predictably, the performance of Unsupervised S-LIMABEAM was dependent on the accuracy of the estimated transcriptions. At moderate reverberation levels, we were able to obtain substantial improvements in recognition accuracy. However, at higher levels of reverberation, the estimated transcriptions had error rates upwards of 60% and as a result, the improvements were smaller. We suggested some methods of obtaining better initial transcriptions in order to improve the performance in such situations.

We then examined the computational complexity of the algorithm and showed that although we are able to obtain substantial improvements in recognition accuracy, they come at a significant computational cost. However, we noted that there are several places where the efficiency of the algorithm could be improved. In an effort to reduce the computational complexity of the subband optimization scheme, we presented two methods of sharing filter parameters across subbands. In one method, filters are shared across mel spectral components and in the other, parameters are shared within mel spectral components. These methods reduced the time to convergence by $40-50\%$ with minimal degradation in performance.

Finally, we examined the performance of S-LIMABEAM on data with less reverberation and significant additive noise. We obtained the same performance as that achieved by the original fullband LIMABEAM algorithm, showing that the proposed method is not specific to reverberant environments and can be applied in all situations.

In the next chapter we apply both LIMABEAM and S-LIMABEAM to other multimicrophone applications in order to highlight additional benefits of using a purely data-driven approach to microphone array processing.

Chapter 6

LIMABEAM in Other Multi-Microphone Environments

6.1 Introduction

In Chapters 4 and 5, algorithms were presented for improving speech recognition performance in environments in which an array of microphones is used to capture the incoming speech signals. In these algorithms, the array processing parameters are manipulated in such a way so as to maximize the likelihood of the sequence of features generated from the array output signal for what is believed to be the correct recognizer hypothesis. This is done is a purely data-driven manner, using the statistical models of the recognition system to derive the target parameters of the likelihood function. As mentioned previously, these algorithms differ from previous methods in that the optimization is performed in the feature space used by the recognizer, rather that at the signal level using criteria such as SNR or the error compared to a desired waveform.

There is another key difference between the proposed method of processing and many other array processing algorithms. Many array processing methods require that the microphones to be configured according to some specific geometry, known *a priori*. For example, the harmonic-nested array uses a logarithmic spacing of the microphones to obtain a desired beampattern (Flanagan et al., 1991). Superdirective beamformers (Cox et al., 1987) require the microphones to be arranged in an endfire arrangement in order to obtain optimal gain in the look direction. Some algorithms actually optimize microphone placement or array geometry, *e.g.* (Rabinkin et al., 1997; Kajala & Hämäläinen, 1999). In contrast, the algorithms in this thesis place no such constraints on the array geometry. Because the processing is data-driven, no inherent assumption of array geometry is made. The algorithm merely

processes the input signals it receives. Because there are no assumptions about geometry, we can apply these algorithms to *any* multi-channel scenario, even if the arrangement of microphones varies widely or is sub-optimal from a traditional array processing point of view. Furthermore, regardless of the configuration of the microphones, no changes to the algorithms are necessary as all processing occurs in a data-driven manner.

In this chapter, two multi-microphone configurations are considered. First, the use of multiple microphones placed on a Personal Digital Assistant (PDA) is examined. In this case, the microphones are placed in a two-dimensional geometry at the four corners of the device. In the second case, a meeting room environment is studied in which four microphones are placed along the center of a long conference room table. From a traditional array processing point of view, the arrangement used is highly-suboptimal, but we can nevertheless attempt to process the signals with our algorithms. The experiments performed in this section show that the algorithms presented in this thesis are capable of good performance with only a small number of channels without any specific dependence on the geometric configuration of the microphones.

6.2 Multi-microphone Speech Recognition on a PDA

The use of PDAs has dramatically increased over the last several years. The interface of most PDAs is centered around the use of a pen-like device called a *stylus*. Clicking a mouse button is replaced by tapping the stylus on the screen. Text is entered by writing on the screen using the stylus, usually in some specific pre-defined fashion. This is suitable for short entries such as phone numbers but is inefficient for entering longer texts. Speech has been viewed as a viable modality for these interactions. While a good idea in principle, this is difficult in practice for several reasons. The memory size of a PDA is limited, so getting a recognizer to fit within the computational footprint of a PDA is a difficult task. Some researchers have avoided this problem by using an architecture in which the PDA is a client that communicates with a recognition server hosted on another larger machine, *e.g.* (Deng et al., 2002). Another significant hurdle is actually capturing the speech signal. Most PDAs have only a single low-cost microphone paired with a low-quality audio CODEC (COder/DECoder), which makes high quality sound capture difficult.

One potential method of improving the quality of the audio capture is to equip PDAs with multiple low-cost microphones and utilize array processing technology. To this end, we evaluated the performance of the algorithms in this thesis for PDA applications.

Figure 6.1: A 4-microphone PDA mockup used to record the CMU WSJ PDA corpus

6.3 The CMU WSJ PDA corpus

In order to evaluate the algorithms proposed in this thesis for speech recognition in a PDA environment, we employed the CMU WSJ PDA corpus. To record this corpus, a PDA mockup was created using a Compaq iPaq outfitted with 4 microphones using a custom-made frame attached to the PDA. The microphones were placed at the corners, forming a rectangle around the PDA, 5.5 cm across and 14.6 cm top-to-bottom. The four microphones plus a close-talking microphone worn by the user were connected to a digital audio multi-track recorder. The multi-channel PDA mockup is shown in Figure 6.1.

Recordings were made in a room approximately 6.0 m $\times$ 3.7 m $\times$ 2.8 m. The room contained several desks, three computers and a printer. Users read utterances from the WSJ test set which were displayed on the PDA screen. All users sat in a chair in the same location in the room and held the PDA in whichever hand was most comfortable. No instructions were given to the user about how to hold the PDA. Depending on the preference or habits of the user, the position of the PDA could vary from utterance-to-utterance or during a single utterance.

Two separate recordings of the WSJ test set were made with 8 different speakers in each set. In the first set, which we refer to as *PDA-A*, the average SNR is approximately 21 dB. In the second recording session, a humidifier was placed near the user, creating a noisier

Microphone Configuration	Set A WER (%)	Set B WER (%)
1 mic (top-left)	25.0	68.3
2 mics delay-and-sum (top)	22.2	63.5
4 mics delay-and-sum	20.3	58.9
close-talking mic	10.6	27.5

Table 6.1: WER obtained for the two WSJ PDA test sets using a 1 far-field microphone, delay-and-sum beamforming with 2 or 4 microphones or the close-talking reference microphone

recording environment. In the second set, referred to as *PDA-B*, the SNR is approximately 13 dB.

6.3.1 Experimental Results Using LIMABEAM

Experiments were performed to evaluate the LIMABEAM approach on the PDA corpus in both the calibration and unsupervised processing scenarios. The recognition system was the identical to that used in the previous experiments in this thesis.

The baseline speech recognition performance is shown in Table 6.1 for a single microphone and delay-and-sum processing using the top 2 microphones and all 4 microphones.

Experimental Results Using Calibrated LIMABEAM

In the first set of experiments, the Calibrated LIMABEAM algorithm described in Chapter 4 was performed. In this experiment, a single utterance from each speaker was used for calibration. For consistency, the utterances used for calibration were the same ones used in the calibration experiments performed in Chapter 5. The features derived from the output of delay-and-sum processing were used with the known transcription to estimate the most likely HMM state sequence. Using this state sequence, a set of 20-tap FIR filters was optimized and then used to process all remaining utterances for that speaker. In all cases, the filters were initialized to a delay-and-sum configuration for optimization.

In these experiments, we revisit the comments made in Section 4.6.2 with regard to optimization performed using state output distributions modeled as mixtures of Gaussians versus single Gaussians. Our conjecture in that section was that the poor performance using mixtures of Gaussians could be attributed to the mismatch between the domains of WSJ training data and CMU-8 test data. In the PDA experiments in this section, the test data and the training data are from the same domain, so we should expect better performance using mixtures of Gaussians in the optimization. The results of the PDA

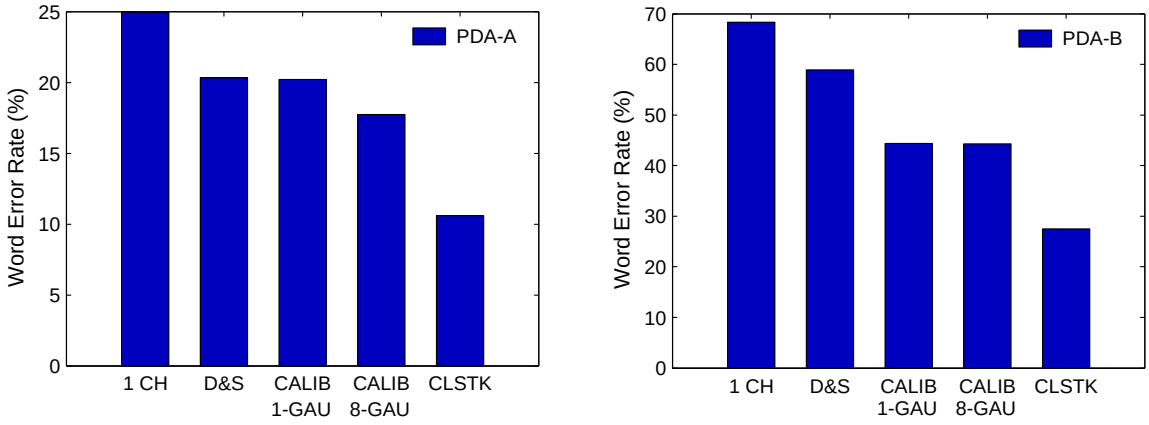

(a) (b)

Figure 6.2: WER obtained using the Calibrated LIMABEAM method on (a) the PDA-A corpus and (b) the PDA-B corpus

calibration experiment are shown in Figure 6.2 for both test sets, PDA-A and the noisier PDA-B.

As the figures show, the calibration approach is, in general, successful at improving the recognition accuracy over delay-and-sum beamforming. However, it is interesting to note that on the less noisy PDA-A test data, calibration using state output distributions modeled as mixtures of Gaussians resulted in significant improvement over conventional delay-and-sum processing, whereas the improvement using single Gaussian output distributions is negligible. On the other hand, the improvements obtained from using single Gaussians or mixtures in the noisier PDA-B set are substantial in both cases and the performance is basically the same. While it is difficult to compare results across the two test sets directly because the speakers are different in each set, these results do agree with intuition. When the test data are well matched to the training data, *i.e.* same domain and distortion, using more descriptive models is beneficial. As the mismatch in the training and test data increases, more general models give better performance. This agrees with the performance we saw in Chapter 4 where the CMU-8 array data was mismatched in both domain and distortion levels to the clean WSJ training data.

Also, it is interesting to note that the improvement in performance obtained using array calibration on the PDA-A test set is less than we have seen in other experiments in this thesis. As described above, the users were not given any instructions about keeping the PDA

in the same position from utterance to utterance. Therefore, we can expect some movement will naturally occur. Compared to the CMU-8 corpus, where users were seated in front of an array for a relatively brief amount of time (each speaker spoke only 14 utterances), the users in this corpus each read approximately 40 utterances while holding the PDA in their hand. Therefore, there is a higher probability that the PDA moved significantly with respect to the user's mouth over the course of the recording session. As a result, the filter parameters obtained from calibration using an utterance chosen at random may not be valid for many of the utterances from that user. We re-examine this hypothesis in the next section, where the parameters are adjusted for each utterance individually using the unsupervised approach.

Experimental Results Using Unsupervised LIMABEAM

Experiments were also performed using the Unsupervised LIMABEAM algorithm. In this case, the filter parameters were optimized for each utterance individually in the following manner. Delay-and-sum beamforming was used to initially process the microphone signals in order to generate a hypothesized transcription. Using this hypothesized transcription and the features derived from the delay-and-sum output, the state sequence was estimated. Using this state sequence, the filter parameters were optimized. As in the calibration case, 20 taps were estimated per filter and the filters were initialized to the delay-and-sum configuration. We compared the recognition accuracy obtained when optimization is performed using HMM state output distributions modeled as Gaussians or mixtures of Gaussians. The results shown in Figure 6.3 for both sets, PDA-A and PDA-B.

As the plots show, there is sizable improvement in recognition accuracy over conventional delay-and-sum beamforming in both test sets. It is interesting to note that by comparing Figure 6.2a and Figure 6.3a, we can see a dramatic improvement in performance using unsupervised performance, as compared to the performance of the calibration algorithm. This confirms our earlier conjecture that the data used for calibration was not representative of the data in the rest of the test set, possibly because the location and orientation of the PDA with respect to the user varied over the course of the test set.

Additionally, we see that the effect of using mixtures of Gaussians versus single Gaussian distributions for optimization in the unsupervised case is similar to that seen in the previous calibration experiments. When the test data is better matched to the clean training data, using more descriptive models is beneficial. However, as the mismatch between the training and test data increases, this benefit is reduced and in this case, simpler, more general models result in better performance.

A second experiment was performed to study the effect that the accuracy of the first

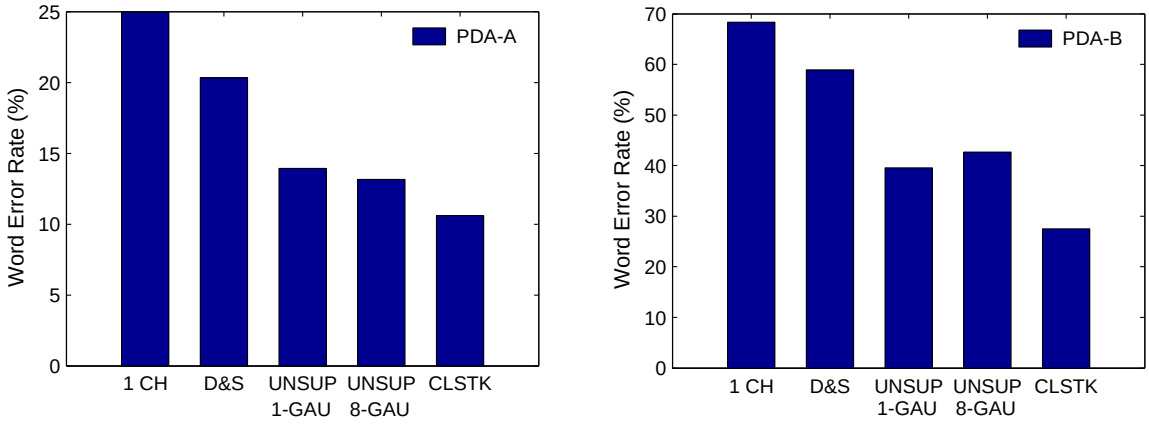

(a) (b)

Figure 6.3: WER obtained using the Unsupervised LIMABEAM on (a) the PDA-A corpus and (b) the PDA-B corpus

Hypotheses Used to Obtain State Sequences for Unsupervised LIMABEAM	Set A WER (%)	Set B WER (%)
Hypotheses from delay-and-sum output	13.1	42.8
Hypotheses from Calibrated LIMABEAM output	13.2	37.9

Table 6.2: WER obtained using Unsupervised LIMABEAM when the state sequences for optimization are derived using hypotheses obtained from delay-and-sum beamforming or from Calibrated LIMABEAM

pass of recognition used to estimate the state sequence has on the unsupervised filter optimization. In this experiment, we performed unsupervised array processing as previously described. This time however, the state sequences were derived from the hypotheses and feature vectors generated after calibration, rather than those generated by delay-and-sum processing. The experiment was performed using mixtures of 8 Gaussians for the filter parameter optimization. The results obtained using this approach are shown in Table 6.2.

Clearly and unsurprisingly, using the calibrated filters to generate the first-pass transcription results in the same or better performance than that obtained when conventional delay-and-sum beamforming is used for this purpose. As in any unsupervised processing algorithm, the more accurate the data used for adaptation, the better and more reliable the adaptation will be. In this case, we are able to use Calibrated LIMABEAM to obtain this more reliable adaptation data. Recalling Figure 6.2, calibration resulted in a modest

improvement over delay-and-sum processing for the PDA-A data set while the improvement for the PDA-B set was far greater. As a result, using the transcriptions from calibration for Unsupervised LIMABEAM resulted in the same performance on PDA-A (the difference between the two results is not statistically significant) and resulted in an additional 8.3% relative improvement over delay-and-sum processing on PDA-B.

6.3.2 Summary of Experimental Results

In this section, we examined the application of LIMABEAM to a PDA with 4-microphones for audio capture, rather than a single microphone. Experiments were performed in which 20-tap filters were optimized in the proposed LIMABEAM framework using both the calibration and the unsupervised approaches described in Chapter 4. Using Calibrated LIMABEAM, an average relative improvement of 18.8% over delay-and-sum beamforming over both PDA test sets was obtained. Using Unsupervised LIMABEAM, an average relative improvement of 31.4% over delay-and-sum beamforming was obtained. Finally, when these two methods were combined and the unsupervised adaptation was performed using transcriptions generated after calibration, the relative improvement increased to 35.3%. The Generalized Sidelobe Canceller (GSC) algorithm with parameter adaptation during the non-speech regions only was also attempted on the PDA data. The performance was significantly worse than simple delay-and-sum beamforming and therefore the results were not reported here.

6.4 Meeting Transcription with Multiple Tabletop Microphones

Recently, improvements in both speech recognition and audio indexing technologies have led to increased interest in the automatic transcription and indexing of meetings. In such a scenario, one or more microphones are used to capture the dialog during a meeting. This audio could then be processed and a transcription of the meeting obtained automatically via speech recognition. In addition, the transcriptions plus additional information extracted from the audio signal(s) could then be used to generate higher level descriptions of the meeting, such as the speaker turns, topic shift, etc. This is a very challenging problem receiving attention from several sites, *e.g.* (Morgan et al., 2003; Waibel et al., 2001; Cutler et al., 2002). In some meeting room environments, users wear either close-talking headset microphones or lapel microphones. The use of such microphones creates a cumbersome and unnatural experience for the participants. Ideally, the audio would be captured by one or

more farfield microphones.

Some sites have created rooms in which an extremely large number of microphones (> 100) are distributed around the room, *e.g.* (Silverman et al., 1996). While such approaches can produce significant speech enhancement, they are significantly more costly than microphone arrays with a smaller number of microphones and require much more hardware to process such a large number of data streams. In addition, these solutions are highly non-portable, a significant drawback when one considers the large number of conference rooms in a typical company or university. Installing such an array in each of these rooms would be prohibitively expensive.

A more conventional solution would utilize one or more arrays with a smaller number of microphones located on the table, walls or ceiling. A more appealing approach is to simply place a few microphones on the table either in a fixed geometry, or more interestingly, in some reasonable, though unspecified configuration, *e.g.* roughly equally distributed along the table. This latter scenario has the dual advantage of being an inexpensive and highly portable method of audio capture. One could imagine arriving to *any* room for a meeting, putting some number of microphones along the table, connecting them to a laptop computer, and recording the meeting directly to disk. In such a scenario, the array geometry is unknown *a priori* and as such, algorithms requiring a particular geometry will fail. Furthermore, the microphone configuration could be highly sub-optimal for conventional array processing approaches. In spite of these challenges, this is the scenario we explore in the next section.

6.5 The ICSI Meeting Recorder Corpus

Researchers at the International Computer Science Institute (ICSI) have collected a corpus of meeting data by recording their own meetings over the last three years. The audio in each meeting was captured by a close-talking microphone worn by each user, as well as four PZM microphones placed along the conference room table and two microphones embedded in a wooden PDA mockup. The meeting room environment is shown in Figure 6.4. The locations of the four PZM microphones are indicated by the black circles. The majority of the speech during these meetings was spontaneous, multi-party conversation typical of meetings. In addition, during each meeting, each participant read several strings of connected digits. The speech recorded during each meeting was transcribed by hand. More details about this corpus can be found in (Janin et al., 2003).

We are interested in determining if the methods presented in this thesis can be applied to this data in order to improve the speech recognition accuracy when only the four tabletop

Figure 6.4: The recording environment used in the ICSI Meeting Recorder corpus. The black circles identify the 4 PZM microphones used for farfield audio capture.

PZM microphones are used. Recordings from this corpus were obtained from researchers at ICSI. Because the work in this thesis is concerned with degradations in recognition accuracy caused by environmental conditions rather than speaking style, accent, or other factors, we chose to focus our experiments solely on the connected digits segments of the meetings. Furthermore, we restricted this data to only those meeting participants who were native speakers of English. The data set used for these experiments consisted of speech data from 16 different meetings, with an average of 4 people in each meeting. However, there were only 12 unique speakers in the data set, as many of the speakers participated in multiple meetings.

As shown in Figure 6.4, the four PZM microphones were spaced approximately one meter apart along the center of the table. This arrangement is highly sub-optimal from a traditional beamforming point-of-view, as it produces severe spatial-aliasing over the range of frequencies spanned by speech signals. Nevertheless, because the algorithms in this thesis are *data-driven* and do not rely on any particular geometry, it is worthwhile to see how they perform.

6.5.1 Experimental Results Using S-LIMABEAM

Experiments were performed to compare the accuracy obtained using the following four methods of processing

- Using one PZM microphone for all speakers
- Selecting the PZM microphone with the highest SNR for each utterance, *i.e.* the single best microphone
- Delay-and-sum processing
- Unsupervised S-LIMABEAM, as described in Chapter 5

In order to choose the microphone with the highest SNR for the second method, the SNR of each of the four microphones was estimated for every utterance using SNR estimation software from NIST (Pallett et al., 1996). For each utterance, the microphone with the highest SNR was used for recognition. For both delay-and-sum processing and the subband calibration method, Time-Delay Compensation was performed for using the PHAT algorithm, as in all previous experiments. The range of acceptable delay values was increased to account for the wide microphone spacing.

Unsupervised S-LIMABEAM was performed as follows. For all utterances, features derived from delay-and-sum processing were used to generate an initial transcription. Based on this transcription, the most likely HMM state sequence was estimated and used to optimize subband filters with a single tap.

The results of this experiment are shown in Figure 6.5. As the figure shows, simply selecting the one farfield microphone with the highest SNR (presumably the one closest to the user speaking) results in a relative improvement in WER of about 70% over the use of a single farfield microphone for all speakers. Although the microphone arrangement is highly sub-optimal, delay-and-sum processing is able to improve performance further still. Yet, even with this atypical multi-microphone configuration, the best results are obtained using Unsupervised S-LIMABEAM, which provides a 21.9% relative improvement over delay-and-sum processing.

6.6 Summary

In this chapter, we have examined the application of the array processing algorithms presented in this thesis to other multi-microphone applications. Specifically, we studied speech recognition on a PDA and automatic meeting transcription using multiple tabletop microphones. Because LIMABEAM is a purely data-driven approach, there are no constraints on the microphone array geometry and *a priori* knowledge is not required by the algorithms. Any signals received from multiple microphones can be processed without any modification to the algorithms.

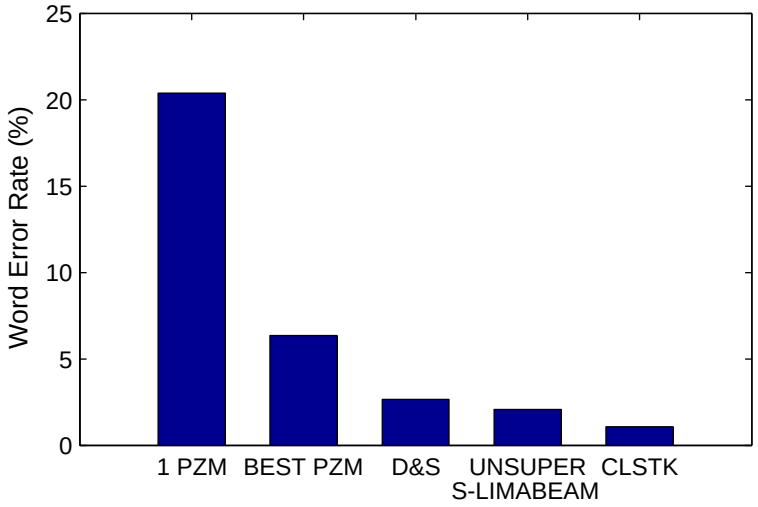

Figure 6.5: WER obtained on the connected digits portion of the ICSI meeting data, using only the PZM tabletop microphones. The WER obtained using a close-talking microphone is also shown for reference.

The LIMABEAM algorithm presented in Chapter 4 was applied to the PDA corpus and significant improvements were obtained in both the calibration and the unsupervised modes of operation. We saw that when the array test data are well matched to the training data, improved performance can be obtained by performing optimization using more descriptive HMM state distributions, *i.e.* mixtures of Gaussians. However, when there is significant mismatch between the test and training data, better performance is obtained using single Gaussians.

Unsupervised S-LIMABEAM was applied to speech from the ICSI meeting corpus, in an effort to improve the speech accuracy using four tabletop microphones. Although the microphones were arranged in a highly sub-optimal arrangement, we were able to obtain significant improvement in recognition accuracy over both the single best tabletop microphone as judged by SNR, and delay-and-sum processing.

In the next chapter, we summarize the work in this thesis, highlighting the major results and contributions.

Chapter 7

Summary and Conclusions

7.1 Introduction

In this thesis we have sought to improve speech recognition accuracy in environments where a close-talking microphone is not available and the speech is captured by an array of microphones located some distance from the user. As the distance between the user and the microphones increases, the speech signal is increasingly distorted by the effects of additive noise and reverberation, which in turn, degrade the performance of speech recognition systems.

Conventional microphone array processing algorithms manipulate the signals received by the array according to various waveform-level objective criteria in order to generate an enhanced output signal. In previous approaches to speech recognition with microphone arrays, one of these methods is used to pre-process the received signals in order to generate a higher quality single-channel output waveform for recognition. Such an approach to speech recognition incorrectly assumes that generating an enhanced waveform will necessarily result in improved recognition accuracy. By making this assumption, the manner in which a speech recognizer operates is ignored. As a result, sophisticated microphone array processing algorithms capable of generating high-quality output waveforms do not produce significant improvements in speech recognition accuracy over far simpler methods, such as delay-and-sum beamforming.

The work presented in this thesis takes a signficantly different approach by considering the microphone array processor and the speech recognition system as components of a single system. In this approach, the objective of the array processor is no longer to generate a higher-quality output waveform. Rather, the array processor and speech recognizer, operating in tandem, share the common objective of improved speech recognition accuracy. This

objective is met by incorporating into the array processing scheme both 1) how speech is processed by the recognizer, *i.e.* the feature extraction process, and 2) how these features are used to hypothesize the words spoken, *i.e.* according to a maximum likelihood criterion using statistical models of speech sound units. By creating such a framework, we are able to "close the loop" between the array processor and speech recognizer. This allows information from the recognition system to be used to optimize the array processing parameters specifically for improved recognition accuracy.

In the remainder of this chapter, we summarize the findings and contributions of this thesis, present some remaining open questions about the work described in this thesis, and suggest some directions for further research.

7.2 Summary of Findings and Contributions of This Thesis

In this thesis we have developed a filter-and-sum array processing algorithm called *Likelihood Maximizing Beamforming* (LIMABEAM) in which the filter parameters are optimized in a data-driven fashion using the statistical models of a speech recognition system. We formulate the optimization of the filters parameters as a maximum likelihood parameter estimation problem. We showed how the optimal values for the parameters are those which maximize the likelihood of the correct transcription of the given utterance. Via this likelihood function, we explicitly make the connection between the array processing parameters, the feature extraction process, and the statistical models of the recognizer. Optimizing the parameters in this manner ensures that signal components important for recognition are emphasized without undue emphasis on less important components.

Using this framework, we developed two algorithms to optimize the parameters of a filter-and-sum beamformer. In the first method, called *Calibrated LIMABEAM*, an enrollment utterance with a known transcription is spoken by the user and used to optimize the filter parameters (Seltzer & Raj, 2001). These filter parameters are then used to process future utterances. This algorithm is appropriate for situations in which the environment and the user's position do not vary significantly over time, such as in a car or in front of a desktop computer. For time-varying environments, we developed an algorithm for optimizing the filter parameters in an unsupervised manner. In *Unsupervised LIMABEAM*, the optimization is performed on each utterance independently using a hypothesized transcription obtained from an initial pass of recognition (Seltzer et al., 2002).

Both of these methods were able to obtain significant improvements in recognition accuracy in environments with moderate reverberation over a wide range of noise levels. However, we found that if too little speech data were used for the optimization, the im-

provements in recognition accuracy were small. In the calibration case, too little data resulted in overfitting and unreliable parameter estimation, while in the unsupervised case, very short utterances may not have enough correctly labeled tokens to produce significant improvements. However, with 10-15 s of speech data, both methods successfully optimized filters with up to 50 taps per microphone, which resulted in substantial improvements in speech recognition accuracy over delay-and-sum beamforming.

Additionally, we showed that further benefit can be obtained in noise-corrupted environments by combining the proposed array processing approach with a single-channel noise-compensation scheme. In this work, we obtained improved performance in both the calibration and unsupervised algorithms when these methods were followed by CDCN.

We analyzed both the output signals generated by the array and the optimized filters themselves and showed that they could be considered sub-optimal from a traditional signal processing point of view. The resulting beampatterns frequently had larger sidelobes compared to those of simple delay-and-sum beamforming. Furthermore, the output signals frequently sounded high-pass, reflecting the fact that recognition systems do not consider spectral information below about 100 Hz. In spite of these shortcomings or perhaps *because* of them, we were able to make gains in recognition accuracy unseen by other methods. Thus, we further confirmed our conjecture that objective functions based on waveform-level criteria are sub-optimal for speech recognition applications.

The proposed methods, which utilized an FIR filter-and-sum beamformer, provided only small improvements in environments with more severe reverberation. The long filter lengths required to compensate for long reverberation times and the increased correlation in the speech signal due to signal reflections combined to impede the performance of the algorithm. Joint estimation of such a large number of parameters would require a prohibitive amount of data and take too long to converge. To address these problems, we presented a subband filtering approach to LIMABEAM, called *Subband-Likelihood Maximizing Beamforming* (S-LIMABEAM) (Seltzer & Stern, 2003). In this algorithm, processing is performed in the DFT domain, treating each DFT coefficient over time as a time-series. We incorporated this subband filtering scheme into the recognizer-based array processing algorithm developed earlier. In this method, the likelihood of each component in the log mel spectral feature vector is maximized independently. This is done by optimizing the subband filter parameters of only those frequency bins needed to compute that particular mel component. This processing reduces the number of parameters that need to be jointly estimated, replacing a one joint optimization over many parameters by several optimizations, each of a much smaller number of parameters. In addition, the convegence of the algorithm is improved because a different step size can be used in each of the optimizations.

This subband processing approach was incorporated into both the calibration and the unsupervised processing methods. Experiments showed that *Calibrated S-LIMABEAM* was capable of significantly improving recognition accuracy in environments with a reverberation time exceeding one second. However, the performance of *Unsupervised S-LIMABEAM* was limited in environments with severe reverberation because of high error rates in the first-pass transcription. We also showed that the subband filtering approach can also generate good results in environments with less reverberation and significant additive noise. This showed that this approach is not specific to reverberant environments and is an effective general solution. The subband processing approach also has the additional benefit that because the likelihood of each component of the feature vector is maximized independently, the optimization of the different components can be performed in parallel.

The algorithms presented in this thesis are purely data-driven. As a result, no *a priori* knowledge of the room impulse response or the user location is required, nor is any particular number of microphones or microphone configuration required. We were able to obtain signficant improvements in recognition accuracy using both one-dimensional linear arrays and two-dimensional rectangular arrays. Even in highly sub-optimal microphone configurations, *e.g.* a few microphones casually placed on a table, improvements in accuracy were achieved.

7.3 Some Remaining Questions

In this section, we present some questions that have been raised over the course of this thesis.

In this work, we have assumed in all cases that the likelihood of a given transcription can be represented by the single most likely HMM state sequence. This assumption greatly simplifies the likelihood expression that is maximized during the filter optimization process. However, because the features used to derive the state sequence are distorted by noise and reverberation, the forced alignment algorithm may assign incorrect states to some frames, even if the transcription is known *a priori* as in the calibration case. This can be especially true in the regions where rapid changes occur, such as speech/non-speech boundaries. The performance of the algorithm may benefit, albeit at increased computational cost, by considering a number of possible states, rather than just the single most likely state, at each time instant. Deriving the likelihood function in this manner would be a better approximation to the actual likelihood expression for a given transcription, and therefore may improve the performance of the array parameter optimization.

In addition, the algorithms in this thesis used one recognizer trained on cepstra for

decoding and forced alignment, and a parallel recognizer trained on log mel spectra for the optimization. However, it is not clear whether the recognition system used for optimization needs to be of the same complexity as the one used for decoding. In the experiments in this thesis, both systems had a total of 4000 total senones. It is conceivable that for array parameter optimization, a far simpler recognizer, *i.e.* one with far fewer senones, could be used without a significant loss in performance. This would significantly reduce the memory required to store the HMMs used for optimization, potentially enabling the array processing to be performed on a device with limited memory, such as a PDA.

Finally, while we have shown that the algorithms presented in this thesis are capable of good performance in environments that contain significant levels of additive noise and reverberation, the performance in a competing talker scenario has yet to be fully explored. In this scenario, two or more users are speaking at the same time. We have performed some informal experiments in which a user was in front of an array while a talk-radio station, simulating a second user, was placed off-axis to the array. In these experiments, the algorithm performed well, virtually eliminating the radio source from the output signal. However, the user's location was assumed to be roughly in front of the array and the localization algorithm was only used to fine-tune the steering-delay estimates. Therefore, we hypothesize that the algorithms in this thesis will have good performance in multiple-talker environments *provided the location of the desired user can be reliably estimated.* However, this hypothesis remains to be tested.

7.4 Directions for Further Research

While the algorithms developed in this thesis have been quite successful at improving speech recognition performance using microphone arrays, the solutions presented still have ample room for improvement. Additional research in the following areas has the potential to provide significant additional improvement.

One of the more signficant drawbacks of the algorithms in this thesis is the inability adapt to a user who is moving while speaking. Currently, the algorithm can perform utterance-level adaptation, but cannot cope with the scenario of a user moving during an utterance. Doing so would require that both the state sequence estimation and the filter parameter optimization be performed in an online manner. The algorithm does not require the state sequence to be estimated per se. Ideally, an online solution would obtain these target parameters without having to perform the forced alignment step. Solutions for doing so using Gaussian mixture models have been proposed for other single-channel compensation algorithms *e.g.* (Acero, 1993; Moreno, 1996), and could possibly be adapted for use here.

However, the means of doing so here is not obvious as many of the assumptions made in those algorithms do not apply in reverberant environments or multi-channel situations. Given a method of acquiring target Gaussian parameters on an online fashion, online updating of the filter parameters is perhaps an easier problem to tackle. Several methods exist for online adaptation and could be employed here.

In the S-LIMABEAM algorithms, the subband decomposition is accomplished using a DFT filterbank and the downsampling is accomplished by the framing process in the front end. This particular method of subband processing is appealing for speech recognition applications, as it utilizes processing already being performed in the feature extraction process. However, it is possible that further parameter reduction and improved performance could be obtained from alternative methods of subband decomposition. For example, by using an analysis filterbank that approximates the mel filterbank, feature vectors could potentially be derived *directly* from the subband signals themselves. Currently, several DFT subbands must be combined in order to derive each component of the feature vector.

In speech enhancement or coding applications, it is desirable for the analysis and synthesis filterbanks to be capable of *perfect reconstruction*. This implies that in the absence of intermediate processing, the output signal equals the input signal to within a gain factor and a linear phase term. The DFT filterbank employed in this work is not capable of perfect reconstruction. Because a Hamming window is used for the analysis filter prototype, there is overlap between adjacent subbands which causes aliasing in the reconstructed signal. This was not considered a critical issue in this thesis because features are derived from the subband signals and the waveform is not resynthesized. However, if the array processing output is intended for human listeners as well as speech recognition systems, then it may be advantageous to use a filterbank capable of waveform resynthesis with minimal distortion, *e.g.* (de Haan et al., 2002).

We saw considerable benefit in noisy environments from performing CDCN on the output feature vectors produced by the array processing algorithm. This operation can be interpreted as applying a post-filter in the feature domain to the single-channel output of an array processing algorithm for additional noise reduction. In noisy environments, the array optimization algorithm can be improved by including this feature compensation step into the algorithm. This can be accomplished by explicitly incorporating a statistical noise model into the algorithm. Such a technique for single channel applications has been proposed by Attias et al. (2001). Furthermore, the noise model can be robustly updated online by steering the array toward the noise sources.

In the algorithms presented in this thesis, the selection of the optimal array parameters is performed according to a maximum likelihood (ML) criteria. However, such an approach

makes no use of any prior information about the filter parameters. Because a microphone array is generally placed in a fixed location, such prior information should be both available and useful. Specifically, reformulating the algorithms presented in this thesis using a maximum *a posteriori* (MAP) framework would allow *a priori* information about the filter parameters to be incorporated into the optimization scheme.

Appendix A

Derivation of the Jacobian Matrix for LIMABEAM

A.1 Introduction

In this appendix, we derive the Jacobian matrix required for the LIMABEAM algorithms. The Jacobian matrix is composed of the partial derivatives of the feature vector $\boldsymbol{z}$, with respect to the array processing parameter vector, $\boldsymbol{\xi}$. We assume that the array parameters are the taps of an FIR filter-and-sum beamformer and the features used for recognition are mel frequency cepstra or log mel spectra.

Let M be the number of microphones in the array and let P be the length of the FIR filters used to process the array signals. We define $\boldsymbol{\xi}$ to be the vector of length $M \cdot P$ composed of all filter parameters for all microphones, expressed as

$$\boldsymbol{\xi} = [h_0[0], h_0[1], \ldots, h_{M-1}[P-2], h_{M-1}[P-1]]^T \tag{A.1}$$

where $h_m[p]$ represents the pth tap of the FIR filter associated with microphone m.

Let C be the length of the cepstral vector $\boldsymbol{z}$. We define $\mathbf{J}_i$ to be the $MP \times C$ Jacobian matrix composed of the partial derivatives of each element of the feature vector $\boldsymbol{z}$ in frame

i with respect to each of the array parameters $h_m[p]$, as

$$\mathbf{J}_i = \frac{\partial \boldsymbol{z}_i}{\partial \boldsymbol{\xi}} = \begin{bmatrix} \frac{\partial z_i^0}{\partial h_0[0]} & \frac{\partial z_i^1}{\partial h_0[0]} & \cdots & \frac{\partial z_i^{C-1}}{\partial h_0[0]} \\ \frac{\partial z_i^0}{\partial h_0[1]} & \frac{\partial z_i^1}{\partial h_0[1]} & \cdots & \frac{\partial z_i^{C-1}}{\partial h_0[1]} \\ \vdots & \vdots & \ddots & \vdots \\ \frac{\partial z_i^0}{\partial h_{M-1}[P-2]} & \frac{\partial z_i^1}{\partial h_{M-1}[P-2]} & \cdots & \frac{\partial z_i^{C-1}}{\partial h_{M-1}[P-2]} \\ \frac{\partial z_i^0}{\partial h_{M-1}[P-1]} & \frac{\partial z_i^1}{\partial h_{M-1}[P-1]} & \cdots & \frac{\partial z_i^{C-1}}{\partial h_{M-1}[P-1]} \end{bmatrix} \tag{A.2}$$

To derive the expression for the Jacobian matrix, we first describe the feature extraction process, detailing how a speech waveform is converted into a sequence of mel frequency cepstral vectors. We then use this formulation to derive the expression for each term $\partial z_i^c / \partial h_m[p]$ in the Jacobian matrix.

A.2 Computing Mel Frequency Cepstral Coefficients

We begin by first describing how a sequence of mel frequency ceptral coefficients are computed from the output of a filter-and-sum beamformer. We assume that Time-Delay Compensation (TDC) has already been performed. If we define $x_m[n]$ as the signal captured by the mth microphone in the array, then the output signal $y[n]$ can be expressed as

$$y[n] = \sum_{m=0}^{M-1} \sum_{p=0}^{P-1} h_m[p] x_m[n-p] \tag{A.3}$$

This output signal is then segmented into a series of overlapping frames. If we define N as the length of a frame in samples and R the number of samples between starting points of consecutive frames, we can represent the Short-Time Fourier Transform (STFT) of frame i of the output signal as

$$Y_i[k] = \sum_{n=0}^{N-1} w[n] y[iR+n] e^{-j2\pi kn/N} \qquad 0 \le k \le N/2 \tag{A.4}$$

where $w[n]$ is a Hamming window applied to the signal at frame i. Note that we have only computed the non-negative frequencies of the DFT in this case. Because the input signal is real, the STFT has conjugate symmetry and the the features are only extracted from non-negative half of the STFT.

The squared magnitude of the STFT is computed and used to derive the mel spectrum,

a vector of length L that represents the energy in a series of overlapping frequency bands defined by a set of L triangular weighting functions called mel filters. We can define the lth component of the mel spectral vector as

$$M_i^l = \sum_{k=0}^{N/2} V^l[k] Y_i[k] Y_i^*[k] \qquad 0 \le l \le L-1 \tag{A.5}$$

where $Y_i^*[k]$ is the complex conjugate of $Y_i[k]$.

Finally, the mel frequency cepstral vector is derived from the mel spectral vector by first taking the logarithm of each component of the mel spectral vector, producing the log mel spectrum, and then performing a truncated DCT operation. The DCT operation is performed in order to reduce the dimensionality of the feature vector and decorrelate its components for better classification performance in the recognizer. Thus, for a cepstral vector of length C, we define $\mathbf{\Phi}$ as the $C \times L$ DCT matrix ($C \le L$), and express the cth cepstral coefficient as

$$z_i^c = \sum_{l=0}^{L-1} \Phi_{cl} \log(M_i^l) \qquad 0 \le c \le C-1 \tag{A.6}$$

A.3 Computing the Elements of the Jacobian Matrix

Having defined the computation of the feature vector, we are now ready to compute the elements of the Jacobian matrix defined in Equation (A.2). Clearly, each element of the feature vector is a function of each of the filter parameters through the relationship defined by Equations A.3 through A.6. Thus, the partial derivative of z_i^c with respect to the filter coefficient $h_n[q]$ can be expressed as

$$\frac{\partial z_i^c}{\partial h_n[q]} = \sum_{l=0}^{L-1} \frac{\Phi_{cl}}{M_i^l} \frac{\partial M_i^l}{\partial h_n[q]} \tag{A.7}$$

The partial derivative term $\partial M_i^l / \partial h_n[q]$, computed from Equation (A.5) using the product rule, can be expressed as

$$\frac{\partial M_i^l}{\partial h_n[q]} = \sum_{k=0}^{N/2} V^l[k] \left(Y_i[k] \frac{\partial Y_i^*[k]}{\partial h_n[q]} + \frac{\partial Y_i[k]}{\partial h_n[q]} Y_i^*[k] \right) \tag{A.8}$$

To compute $\partial Y_i[k] / \partial h_n[q]$, we first express $Y_i[k]$ as a function of the filter parameters

by substituting Equation (A.3) into Equation (A.4), producing

$$Y_i[k] = \sum_{n=0}^{N-1} w[n] \left(\sum_{m=0}^{M-1} \sum_{p=0}^{P-1} h_m[p] x_m[iR + n - p] \right) e^{-j2\pi kn/N} \tag{A.9}$$

Rearranging the order of summation to

$$Y_i[k] = \sum_{m=0}^{M-1} \sum_{p=0}^{P-1} h_m[p] \sum_{n=0}^{N-1} w[n] x_m[iR + n - p] e^{-j2\pi kn/N} \tag{A.10}$$

reveals that $Y_i[k]$ is a weighted sum of the STFTs of $x_m[n-p]$ over all channels and tap delays. If we define the STFT of $x_m[n-p]$ as

$$X_i^{mp}[k] = \sum_{n=0}^{N-1} w[n] x_m[iR + n - p] e^{-j2\pi kn/N} \tag{A.11}$$

then $Y_i[k]$ can be expressed as

$$Y_i[k] = \sum_{m=0}^{M-1} \sum_{p=0}^{P-1} h_m[p] X_i^{mp}[k] \tag{A.12}$$

where $X_i^{mp}[k]$ is the DFT of a frame of speech beginning p samples prior to the starting sample of the ith frame.

Using Equation (A.12), the partial derivatives in Equation (A.8) can be easily expressed as

$$\frac{\partial Y_i[k]}{\partial h_n[q]} = X_i^{nq}[k] \tag{A.13}$$

$$\frac{\partial Y_i^*[k]}{\partial h_n[q]} = X_i^{nq*}[k] \tag{A.14}$$

Substituting Equations (A.13) and (A.14) into Equation (A.8), we obtain the following

expression for $\partial M_l^i / \partial h_n[q]$:

$$\frac{\partial M_i^l}{\partial h_n[q]} = \sum_{k=0}^{N/2} V^l[k] \left(Y_i[k] X_i^{nq*}[k] + X_i^{nq}[k] Y_i^*[k] \right) \tag{A.15}$$

$$= 2 \sum_{k=0}^{N/2} V^l[k] \Re \left(X_i^{nq}[k] Y_i^*[k] \right) \tag{A.16}$$

Finally, by substituting Equation (A.16) into Equation (A.7), we obtain the complete expression for $\partial z_i^c / \partial h_n[q]$ as

$$\frac{\partial z_i^c}{\partial h_n[q]} = 2 \sum_{l=0}^{L-1} \frac{\Phi_{cl}}{M_i^l} \sum_{k=0}^{N/2} V^l[k] \Re \left(X_i^{nq}[k] Y_i^*[k] \right) \tag{A.17}$$

The Jacobian matrix $\mathbf{J}_i$ is formed by subsituting Equation (A.17) into Equation (A.2) for $c = \{0 \dots C-1\}$, $n = \{0 \dots M-1\}$, and $q = \{0 \dots P-1\}$.

In this thesis, optimization of the filter parameters was performed using log mel spectra rather than cepstra. In this case, the feature vector is of length L with elements $z_i^l = \log(M_i^l)$, and as a result, the Jacobian matrix is now $MP \times L$. The only difference in the expression in Equation (A.17) is the absence of the outermost summation representing the DCT operation. Thus, for log mel spectral features, the terms in the Jacobian are computed as

$$\frac{\partial z_i^l}{\partial h_n[q]} = 2 \frac{1}{M_i^l} \sum_{k=0}^{N/2} V^l[k] \Re \left(X_i^{nq}[k] Y_i^*[k] \right) \tag{A.18}$$

Appendix B

Parameter Reduction using ASR-based Subband Filtering

Subband processing has several advantages over the conventional fullband processing. Because the signal is divided into narrow independent subbands, the signals in each subband can be processed independently. The subband signals have less bandwidth than the corresponding fullband signal and as a result, they can be downsampled prior to processing. The combination of the independent subbands and the downsampling results in a reduction of the number of parameters that have to be jointly estimated in a subband processing scheme. Furthermore, a different step size can be used in each subband during adaptation, which improves the convergence of subband adaptive filtering schemes compared to their fullband counterparts.

In this appendix, we demonstrate the benefit of using subband filtering in speech recognition applications. Specifically, we derive the reduction in parameters obtained when the STFT is used as the analysis filterbank and the downsampling rate is governed by the frame shift defined by the feature extraction process of the recognizer. Here, we only consider a single channel of input. However, the results are easily generalized to the multi-microphone case.

We define N to be length of the frame in samples and R to be the frame shift in samples, *i.e.* the number of samples between starting points of consecutive frames. Given a waveform $x[n]$, let us define $x_i[n]$ as the ith frame of $x[n]$. That is,

$$x_i[n] = x[iR + n] \tag{B.1}$$

The previous frame $x_{i-1}[n]$ can be similarly represented as

$$x_{i-1}[n] = x[(i-1)R + n] \tag{B.2}$$
$$= x[iR + n - R] \tag{B.3}$$
$$= x_i[n - R] \tag{B.4}$$

We can generalize Equation (B.4), and define the pth frame before the current frame i as

$$x_{i-p}[n] = x_i[n - pR] \tag{B.5}$$

For notational convenience, we define the N-point discrete Fourier transform of $x_i[n]$ as

$$\boldsymbol{X}_i = \boldsymbol{\mathcal{F}}\{x_i[n]\} \tag{B.6}$$

and the corresponding inverse discrete Fourier transform as

$$x_i[n] = \boldsymbol{\mathcal{F}}^{-1}\{\boldsymbol{X}_i\} \tag{B.7}$$

where $\boldsymbol{X}_i$ is a vector of length N. We refer to the kth component or frequency bin of $\boldsymbol{X}_i$ as $X_i[k]$.

We express the subband filtering operation in the kth frequency bin as

$$Y_i[k] = \sum_{p=0}^{P-1} H_p[k] X_{i-p}[k] \tag{B.8}$$

where $H_p[k]$ is the pth complex filter tap of the subband filter applied to subband k. The complete spectral output vector is formed by stacking the individual subband output signals in Equation (B.8) for all subbands. If we define the vector operator $\circ$ to be the product of the corresponding elements of two vectors, we can express this output vector, $\boldsymbol{Y}_i$, as

$$\boldsymbol{Y}_i = \sum_{p=0}^{P-1} \boldsymbol{H}_p \circ \boldsymbol{X}_{i-p} \tag{B.9}$$

By taking the inverse Fourier transform of Equation (B.9), we can determine the equivalent time-domain representation of this subband processing operation. Thus, we have

$$y_i[n] = \boldsymbol{\mathcal{F}}^{-1}\{\boldsymbol{Y}_i\} \tag{B.10}$$

$$= \boldsymbol{\mathcal{F}}^{-1}\left\{\sum_{p=0}^{P-1} \boldsymbol{H}_p \circ \boldsymbol{X}_{i-p}\right\} \tag{B.11}$$

Substituting Equation (B.6) into Equation (B.11) gives

$$= \boldsymbol{\mathcal{F}}^{-1}\left\{\sum_{p=0}^{P-1} \boldsymbol{H}_p \circ \boldsymbol{\mathcal{F}}\{x_{i-p}[n]\}\right\} \tag{B.12}$$

and using Equation (B.5) gives

$$= \boldsymbol{\mathcal{F}}^{-1}\left\{\sum_{p=0}^{P-1} \boldsymbol{H}_p \circ \boldsymbol{\mathcal{F}}\{x_i[n-pR]\}\right\} \tag{B.13}$$

$$= \boldsymbol{\mathcal{F}}^{-1}\left\{\sum_{p=0}^{P-1} \boldsymbol{H}_p \circ \boldsymbol{\mathcal{F}}\{x_i[n]\} \circ e^{-\jmath 2\pi pR/N}\right\} \tag{B.14}$$

where $e^{-\jmath 2\pi pR/N}$ is a vector of the corresponding phase shift terms. Since $x_i[n]$ does not depend on p, and the $\circ$ operation is commutative, we can write

$$= \boldsymbol{\mathcal{F}}^{-1}\left\{\boldsymbol{\mathcal{F}}\{x_i[n]\} \circ \sum_{p=0}^{P-1} \boldsymbol{H}_p \circ e^{-\jmath 2\pi pR/N}\right\} \tag{B.15}$$

Finally, if we let $\otimes$ represent the convolution operator, then we can write Equation (B.15) as

$$= x_i[n] \otimes \boldsymbol{\mathcal{F}}^{-1}\left\{\sum_{p=0}^{P-1} \boldsymbol{H}_p \circ e^{-\jmath 2\pi pR/N}\right\} \tag{B.16}$$

$$= x_i[n] \otimes \sum_{p=0}^{P-1} \boldsymbol{\mathcal{F}}^{-1}\left\{\boldsymbol{H}_p \circ e^{-\jmath 2\pi pR/N}\right\} \tag{B.17}$$

$$y_i[n] = x_i[n] \otimes \left(\sum_{p=0}^{P-1} h_p[n-pR]\right) \tag{B.18}$$

The expression inside the parentheses in Equation (B.18) represents a conventional time-domain filter equivalent to the aggegrate of all subband filters. It is the summation of P filters, each of length N and delayed R samples, or *one frame*, from the previous one. Thus, this equivalent filter spans P frames and therefore has an effective total length of $N + (P - 1) \cdot R$ samples.

In typical speech recognition applications, for speech sampled at 16 kHz, $N = 400$ and $R = 160$, corresponding to a 25-ms frame size with a 10-ms frame shift. Using these values, a series of 2-tap subband filters is equivalent to a fullband filter of length $400 + 160 = 560$, a series of 3-tap subband filters is equivalent to a filter of length 720, and so on. Because each of these subband filters can be optimized independently, the number of parameters that need to be optimized jointly is significantly reduced. This enables the parameters to be estimated more reliably.

Appendix C

Derivation of the Gradient Vector for S-LIMABEAM

C.1 Introduction

In this appendix, we derive the expression for the gradient vector required for S-LIMABEAM. In this algorithm, subband filters operating on the output of a DFT filterbank are optimized to maximize the likelihood of the resulting log mel spectra. As described in Chapter 5, the likelihood of each component log mel spectral components is maximized independently. Therefore, for each log mel spectral component, we require the gradient vector composed of the partial derivatives of a particular log mel spectral coefficient with respect the each of the filter parameters of its constituent subbands.

C.2 Defining the Gradient Vector

We define $\boldsymbol{z}_i$ to be the log mel spectral feature vector of length L for frame i. Recall that each mel spectral component is the energy in a particular frequency band defined by an associated mel filter. Thus, the lth log mel spectral component can be expressed as

$$z_i^l = \log(M_i^l) \tag{C.1}$$

$$= \log\left(\sum_{k=l_-}^{l_+} V^l[k] S_i^Y[k]\right) \tag{C.2}$$

$$= \log\left(\sum_{k=l_-}^{l_+} V^l[k] Y_i[k] Y_i^*[k]\right) \tag{C.3}$$

where $Y_i[k]$ is the DFT of waveform $y[n]$ at frame i, $S_i^Y[k]$ is the magnitude squared of $Y_i[k]$, and $V^l[k]$ is the coefficient of the lth mel filter in frequency bin k. Complex conjugation is denoted by *. The limits of summation l_- and l_+ represent the lowest and highest bins, respectively, in the frequency band defined by the lth mel filter.

In the subband array processing algorithm, $Y_i[k]$ generated as the output of a subband filter-and-sum operation, expressed as

$$Y_i[k] = \sum_{m=0}^{M-1} \sum_{p=0}^{P-1} H_p^{m*}[k] X_{i-p}^m[k] \tag{C.4}$$

where $X_i^m[k]$ is the value of the STFT in subband k from microphone m at frame i and $H_p^m[k]$ is the pth complex tap of the subband filter assigned to that microphone and subband.

We define $\boldsymbol{\xi}_l$ to be the vector of array parameters needed to compute the lth log mel spectral component. By substituting Equation (C.4) into Equation (C.3) it is apparent that $\boldsymbol{\xi}_l$ is is a complex vector of length $M{\cdot}P{\cdot}(l_+ - l_- + 1)$ composed of the subband filter parameters $\{H_p^m[k]\}$ for $m = \{0, \ldots, M-1\}$, $p = \{0, \ldots, P-1\}$ and $k = \{l_-, \ldots, l_+\}$.

We can now define the gradient as the vector composed of the partial derivatives of z_i^l with respect to each of the elements of $\boldsymbol{\xi}_l$. We express this as

$$\frac{\partial z_i^l}{\partial \boldsymbol{\xi}_l} = \left[\frac{\partial z_i^l}{\partial H_0^0[l_-]}, \frac{\partial z_i^l}{\partial H_0^1[l_-]}, \ldots, \frac{\partial z_i^l}{\partial H_{P-1}^{M-1}[l_+]} \right]^T \tag{C.5}$$

C.3 Computing the Elements of the Gradient Vector

We can now derive the expression for each element of the gradient vector. We define one such element, corresponding to microphone n, tap q, and subband r, as $H_q^n[r]$. From Equations (C.1) – (C.2), we can express $\partial z_i^l / \partial H_q^n[r]$ as

$$\frac{\partial z_i^l}{\partial H_q^n[r]} = \frac{1}{M_i^l} \frac{\partial M_i^l}{\partial H_q^n[r]} \tag{C.6}$$

$$= \frac{1}{M_i^l} \frac{\partial M_i^l}{\partial S_i^Y[r]} \frac{\partial S_i^Y[r]}{\partial H_q^n[r]} \tag{C.7}$$

$$= \frac{V^l[r]}{M_i^l} \frac{\partial S_i^Y[r]}{\partial H_q^n[r]} \tag{C.8}$$

To compute $\partial S_i^Y[r]/\partial H_q^n[r]$, we first define the filter parameter $H_q^n[r]$ simply as

$$H_q^n[r] = a + \jmath b \tag{C.9}$$

We can now define $\partial S_i^Y[r]/\partial H_q^n[r]$ as

$$\frac{\partial S_i^Y[r]}{\partial H_q^n[r]} = \frac{\partial S_i^Y[r]}{\partial a} + \jmath \frac{\partial S_i^Y[r]}{\partial b} \tag{C.10}$$

Using Equations (C.3), (C.4), and (C.9), the partial derivative of $S_i^Y[r]$ with respect to a can be computed as

$$\begin{aligned}
\frac{\partial S_i^Y[r]}{\partial a} &= \frac{\partial}{\partial a}\left(Y_i[r]Y_i^*[r]\right) \\
&= Y_i[r]\frac{\partial Y_i^*[r]}{\partial a} + \frac{\partial Y_i[r]}{\partial a}Y_i^*[r] \\
&= Y_i[r]X_{i-q}^{n*}[r] + X_{i-q}^n[r]Y_i^*[r] \\
&= 2\Re\left\{X_{i-q}^n[r]Y_i^*[r]\right\}
\end{aligned} \tag{C.11}$$

We similarly derive the partial derivative of $S_i^Y[r]$ with respect to b as

$$\begin{aligned}
\frac{\partial S_i^Y[r]}{\partial b} &= Y_i[r]\frac{\partial Y_i^*[r]}{\partial b} + \frac{\partial Y_i[r]}{\partial b}Y_i^*[r] \\
&= Y_i[r]\jmath X_{i-q}^{n*}[r] - \jmath X_{i-q}^n[r]Y_i^*[r] \\
&= \jmath\left(X_{i-q}^{n*}[r]Y_i[r] - X_{i-q}^n[r]Y_i^*[r]\right) \\
&= \jmath\left(2\jmath\left\{\Im X_{i-q}^{n*}[r]Y_i[r]\right\}\right) \\
&= -2\Im\left\{X_{i-q}^{n*}[r]Y_i[r]\right\}
\end{aligned} \tag{C.12}$$

Substituting Equations (C.11) and (C.12) into Equation (C.10), we obtain the final expression for $\partial S_i^Y[r]/\partial H_q^n[r]$

$$\begin{aligned}
\frac{\partial S_i^Y[r]}{\partial H_q^n[r]} &= 2\Re\left\{X_{i-q}^n[r]Y_i^*[r]\right\} - 2\jmath\Im\left\{X_{i-q}^{n*}[r]Y_i[r]\right\} \\
&= 2\left(\Re\left\{X_{i-q}^n[r]Y_i^*[r]\right\} - \jmath\Im\left\{X_{i-q}^{n*}[r]Y_i[r]\right\}\right) \\
&= 2X_{i-q}^n[r]Y_i^*[r]
\end{aligned} \tag{C.13}$$

Finally, by substituting Equation (C.13) into Equation (C.8), we can express the element

of the gradient vector corresponding to microphone n, tap q, and subband r, as

$$\frac{\partial z_i^l}{\partial H_q^n[r]} = 2\frac{V^l[r]}{M_i^l} X_{i-q}^n[r] Y_i^*[r] \tag{C.14}$$

The full gradient vector $\partial z_i^l / \partial \boldsymbol{\xi}_l$ defined in Equation (C.5) can now be computed by evaluating Equation (C.14) over all microphones $n = \{0, \ldots, M-1\}$, taps $q = \{0, \ldots, P-1\}$, and subbands $r = \{l_-, \ldots, l_+\}$.

C.4 Computing the Gradient Vector When Filter Parameters Are Shared Within Mel Spectral Components

As described in Section 5.13.1, one method of reducing the number of subband filter parameters is to share filters across the subbands within the same mel spectral component. Thus, only a single set of filter parameters is optimized and shared by all subbands within a given mel filter.

In this configuration, the filter parameters are no longer depedent on subband, only on the microphone and tap index. Therefore, Equation (C.4) can be rewritten as

$$Y_i[k] = \sum_{m=0}^{M-1} \sum_{p=0}^{P-1} H_p^{m*} X_{i-p}^m[k] \tag{C.15}$$

As a result of the parameter sharing, there are now only $M \cdot P$ elements in the gradient vector, rather than $M \cdot P \cdot (l_+ - l_- + 1)$ as before. We will now derive the expression for the elements of the gradient vector to reflect the parameter sharing shown in Equation (C.15).

Starting from Equation (C.6), we now express $\partial M_i^l / \partial H_q^n$ as

$$\begin{aligned}
\frac{\partial z_i^l}{\partial H_q^n} &= \frac{1}{M_i^l} \frac{\partial M_i^l}{\partial H_q^n} \\
&= \frac{1}{M_i^l} \sum_{k=l_-}^{l_+} \frac{\partial M_i^l}{\partial S_i^Y[k]} \frac{\partial S_i^Y[k]}{\partial H_q^n} \\
&= \frac{1}{M_i^l} \sum_{k=l_-}^{l_+} V^l[k] \frac{\partial S_i^Y[k]}{\partial H_q^n}
\end{aligned} \tag{C.16}$$

Substituting Equation (C.13) into Equation (C.16) results in the final expression for

$\partial M_i^l / \partial H_q^n$.

$$\frac{\partial z_i^l}{\partial H_q^n} = 2\frac{1}{M_i^l}\sum_{k=l_-}^{l_+} V^l[k] X_{i-q}^n[k] Y_i^*[k] \tag{C.17}$$

The full gradient vector is now formed by evaluating Equation (C.17) over all microphones $n = \{0, \ldots, M-1\}$ and all taps $q = \{0, \ldots, P-1\}$.

C.5 Computing the Gradient Vector When Filter Parameters Are Shared Across Mel Spectral Components

Another method of reducing the total number of parameters needed for S-LIMABEAM is to exploit the overlap of adjacent mel filters and share subband filters *across* mel spectral components, as described in Section 5.13.2. In this approach, the filter optimization is not performed for subbands that overlap the previous mel filter. Rather, the filters resulting from the optimization of the previous log mel spectral component are copied and used for the current log mel component. Only the filter parameters of subbands not included in the previous mel filter are optimized.

In this case, the gradient formulation is identical to the original unshared parameter case. However, because the filters obtained from the previous log mel spectral component are fixed, the gradient vector is only computed for "new" subbands that do not overlap the previous mel filter. Therefore, the gradient vector is computed by evaluating Equation (C.14) over all microphones $n = \{0, \ldots, M-1\}$, taps $q = \{0, \ldots, P-1\}$, and subbands $r = \{l'_-, \ldots, l_+\}$, where $l'_- = (l-1)_+ + 1$, the first subband after the highest subband of the previous mel filter.

References

Acero, A. (1993). *Acoustical and environmental robustness in automatic speech recognition*. Boston, MA: Kluwer Academic Publishers.

Acero, A. (2002). personal communication.

Acero, A., Altschuler, S., & Wu, L. (2000). Speech/noise separation using two microphones and a vq model of speech signals. *Proceedings of the International Conference on Spoken Language Processing* (pp. 532–535). Beijing, China.

Allen, J. B., & Berkley, D. A. (1979). Image method for efficiently simulating small-room acoustics. *Journal of the Acoustical Society of America*, *65*, 943–950.

Araki, S., Mukai, R., Makino, S., Nishikawa, T., & Saruwatari, H. (2003). The fundamental limitation of frequency domain blind source separation for convolutive mixtures of speech. *IEEE Transactions on Speech and Audio Processing*, *11*, 109–116.

Attias, H., Deng, L., Acero, A., & Platt, J. C. (2001). A new method for speech denoising and robust speech recognition using probabilistic models for clean speech and for noise. *Proceedings of Eurospeech* (pp. 1903–1907). Aalborg, Denmark.

Bell, A. J., & Sejnowski, T. J. (1995). An information-maximization approach to blind separation and blind deconvolution. *Neural Computation*, *7*, 1129–1159.

Beranek, L. L. (1954). *Acoustics*. New York: American Institute of Physics.

Brandstein, M., & Ward, D. (Eds.). (2001). *Microphone arrays - signal processing techniques and applications*. New York: Springer-Verlag.

Cox, H., Zeskind, R. M., & Owen, M. M. (1987). Robust adaptive beamforming. *IEEE Transactions on Acoustics, Speech, and Signal Processing*, *ASSP-35*, 1365–1376.

Cutler, R., Rui, Y., Gupta, A., Cadiz, J. J., Tashev, I., wei He, L., Colburn, A., Zhang, Z., Liu, Z., & Silverberg, S. (2002). Distributed meetings: A meeting capture and broadcasting system. *Proceedings of ACM Multimedia*. Juan Les Pins, France.

Davis, S., & Mermelstein, P. (1980). Comparison of parametric representation for monosyllablic word recognition in continuously spoken sentences. *IEEE Transactions on Acoustics, Speech, and Signal Processing*, *28*, 357–366.

de Haan, J. M., Grbic, N., Claesson, I., & Nordholm, S. (2002). Design and evaluation of nonuniform DFT filter banks in subband microphone arrays. *Proceedings of the IEEE International Conference on Acoustics, Speech, and Signal Processing* (pp. 1173–1176). Orlando, FL.

Deng, L., Wang, K., Acero, A., Hon, H., Droppo, J., Boulis, C., Wang, Y., Jacoby, D., Mahajan, M., Chelba, C., & Huang, X. D. (2002). Distributed speech processing in miPad's multimodal user interface. *IEEE Transactions on Speech and Audio Processing*, *10*, 605–619.

Flanagan, J. L., Berkely, D. A., Elko, G. W., West, J. E., & Sondhi, M. M. (1991). Autodirective microphone arrays. *Acustica*, *73*, 58–71.

Flanagan, J. L., Johnston, J. D., Zahn, R., & Elko, G. W. (1985). Computer-steered microphone arrays for sound transduction in large rooms. *Journal of the Acoustical Society of America*, *78*, 1508–1518.

Flanagan, J. L., Surendran, A. C., & Jan, E. E. (1993). Spatially selective sound capture for speech and audio processing. *Speech Communication*, *13*, 207–222.

Frost, O. L. (1972). An algorithm for linearly constrained adaptive array processing. *Proceedings of the IEEE*, *60*, 926–935.

Gillespie, B., & Atlas, L. E. (2002). Acoustic diversity for improved speech recognition in reverberant environments. *Proceedings of the IEEE International Conference on Acoustics, Speech, and Signal Processing* (pp. 557–560). Orlando, FL.

Gillespie, B., Malvar, H., & Florncio, D. (2001). Speech dereverberation via maximum kurtosis subband adaptive filtering. *Proceedings of the IEEE International Conference on Acoustics, Speech, and Signal Processing* (pp. 3701 –3704). Salt Lake City, UT.

Gillick, L., & Cox, S. J. (1989). Some statistical issues in the comparison of speech recognition algorithms. *Proceedings of the IEEE International Conference on Acoustics, Speech, and Signal Processing* (pp. 532–535). Glasgow, UK.

Gilloire, A., & Vetterli, M. (1992). Adaptive filtering in subbands with critical sampling: analysis, experiments and application to acoustic echo cancellation. *IEEE Transactions on Signal Processing*, *40*, 1862–1875.

Giuliani, D., Matassoni, M., Omologo, M., & Svaizer, P. (1998). Experiments of HMM adaptation for hands-free connected digit recognition. *Proceedings of the IEEE International Conference on Acoustics, Speech, and Signal Processing* (pp. 473–476). Seattle, WA.

Griffiths, L. J., & Jim, C. W. (1982). An alternative approach to linearly constrained adaptive beamforming. *IEEE Transactions on Antennas and Propagation*, *AP-30*, 27–34.

Haykin, S. (2002). *Adaptive filter theory.* New Jersey: Prentice Hall.

Hazen, T. J., Seneff, S., & Polifroni, J. (2002). Recognition confidence scoring and its use in speech understanding systems. *Computer Speech & Language*, *16*, 49–67.

Hoshuyama, O., Sugiyama, A., & Hirano, A. (1999). A robust adaptive beamformer for microphone arrays with a blocking matrix using constrained adaptive filters. *IEEE Transactions on Signal Processing*, *47*, 2677 –2684.

Hughes, T. B., Kim, H. S., DiBiase, J. H., & Silverman, H. F. (1999). Performance of an HMM speech recognizer using a real-time tracking microphone array as input. *IEEE Transactions on Speech and Audio Processing*, *7*, 346–349.

Hwang, M.-Y. (1993). *Subphonetic acoustic modeling for speaker-independent conitnuous speech recognition.* Doctoral dissertation, Carnegie Mellon University, Pittsburgh, PA.

Hwang, M.-Y., & Huang, X. (1993). Shared-distribution hidden Markov models for speech recognition. *IEEE Transactions on Speech and Audio Processing*, *1*, 414–420.

Janin, A., Baron, D., Edwards, J., Ellis, D., Gelbart, D., Morgan, N., Peskin, B., Pfau, T., Shriberg, E., Stolcke, A., & Wooters, C. (2003). The ICSI meeting corpus. *Proceedings of the IEEE International Conference on Acoustics, Speech, and Signal Processing* (pp. 364–367). Hong Kong.

Jelinek, F. (1997). *Statistical methods for speech recognition.* Cambridge, MA: MIT Press.

Johnson, D. H., & Dudgeon, D. E. (1993). *Array signal processing.* New Jersey: Prentice Hall.

Kajala, M., & Hämäläinen, M. (1999). Broadband beamforming optimization for speech enhancement in noisy environments. *Proceedings of the IEEE Workshop in the Applications of Signal Processing to Audio and Acoustics* (pp. 19–22). New Paltz, NY.

Knapp, C. H., & Carter, C. (1976). The generalized correlation method for estimation of time delay. *IEEE Transactions on Acoustics, Speech, and Signal Processing*, *ASSP-24*, 320–327.

Kurita, S., Sauwatari, H., Kajita, S., Takeda, K., & Itakura, F. (2000). Evaluation of blind signal separation method using directivity pattern under reverberant conditions. *Proceedings of the IEEE International Conference on Acoustics, Speech, and Signal Processing* (pp. 3140–3143). Istanbul, Turkey.

Leggetter, C. J., & Woodland, P. C. (1994). *Speaker adaptation of HMMs using linear regression* (Technical Report CUED/F-INFENG/ TR. 181). Cambridge University, Cambridge, UK.

Liu, F.-H., Acero, A., & Stern, R. M. (1992). Efficient joint compensation of speech for the effects of additive noise and linear filtering. *Proceedings of the IEEE International Conference on Acoustics, Speech, and Signal Processing* (pp. 257–260). San Francisco, CA.

Liu, Q.-G., Champagne, B., & Kabal, P. (1996). A microphone array processing technique for speech enhancement in a reverberant space. *Speech Communication*, *18*, 317–334.

Liu, W., Weiss, S., & Hanzo, L. (2001). Subband adaptive generalized sidelobe canceller for broadband beamforming. *Proceedings of the IEEE Workshop on Statistical Signal Processing* (pp. 591–594). Singapore.

Malvar, H. A. (2002). personal communication.

Marro, C., Mahieux, Y., & Simmer, K. U. (1998). Analysis of noise reduction and dereverberation techniques based on microphone arrays with postfiltering. *IEEE Transactions on Speech and Audio Processing*, *6*, 240–259.

Miyoshi, M., & Kaneda, Y. (1988). Inverse filtering of room acoustics. *IEEE Transactions on Speech and Audio Processing*, *36*, 145–152.

Moreno, P. (1996). *Speech recognition in noisy environments.* Doctoral dissertation, Carnegie Mellon University, Pittsburgh, PA.

Moreno, P., Raj, B., & Stern, R. M. (1995). A unified approach for robust speech recognition. *Proceedings of Eurospeech* (pp. 481–485). Madrid, Spain.

Morgan, N., Baron, D., Bhagatl, S., Carvey, H., Dhillon, R., Edwards, J., Gelbart, D., Janin, A., Krupskil, A., Peskin, B., Pfau, T., Shriberg, E., Stolcke, A., & Wooters, C. (2003). Meetings about meetings: research at ICSI on speech in multiparty conversations. *Proceedings of the IEEE International Conference on Acoustics, Speech, and Signal Processing* (pp. 740–743). Hong Kong.

Nakamura, S., Hiyane, K., Asano, F., Nishiura, T., & Yamada, T. (2000). Acoustical sound scene database in real environments for sound scene understanding and hands-free speech recognition. *International Conference on Language Resources and Evaluation.* Athens, Greece.

Nawab, S. H., & Quatieri, T. F. (1988). *Advanced topics in signal processing*, chapter Short-Time Fourier Transform, 289–337. New Jersey: Prentice Hall.

Neely, S., & Allen, J. (1979). Invertibility of a room impulse response. *Journal of the Acoustical Society of America*, *66*, 165–169.

Neo, W. H., & Farhang-Boroujeny, B. (2001). Robust microphone arrays using subband adaptive filters. *Proceedings of the IEEE International Conference on Acoustics, Speech, and Signal Processing* (pp. 3721–3724). Salt Lake City, UT.

Nocedal, J., & Wright, S. (1999). *Numerical optimization.* New York: Springer.

Nordholm, S., Claesson, I., & Dahl, M. (1999). Adaptive microphone array employing calibration signals. *IEEE Transactions on Speech and Audio Processing*, *7*, 241–252.

Omologo, M., Matassoni, M., Svaizer, P., & Giuliani, D. (1997). Experiments of hands-free connected digit recognition using a microphone array. *Proceedings of the IEEE Workshop on Automatic Speech Recognition and Understanding* (pp. 490–497). Santa Barbara, CA.

Pallett, D. S., Fiscus, J. G., Fisher, W. M., Garofolo, J. S., Martin, A. F., & Przybocki, M. A. (1996). 1995 HUB-3 NIST multiple microphone corpus benchmark tests. *Proceedings of the ARPA Speech Recognition Workshop* (pp. 27–46). Harriman, NY.

Paul, D. B., & Baker, J. M. (1992). The design of the Wall Street Journal-based CSR corpus. *Proceedings of the ARPA Speech and Natural Language Workshop* (pp. 357–362). Harriman, NY.

Placeway, P., Chen, S., Eskenazi, M., Jain, U., Parikh, V., Raj, B., Ravishankar, M., Rosenfeld, R., Seymore, K., Siegler, M., Stern, R., & Thayer, E. (1997). The 1996 hub-4 sphinx-3 system. *Proceedings of the DARPA Speech Recognition workshop*.

Pradhan, S. S., & Reddy, V. U. (1999). A new approach to subband adaptive filtering. *IEEE Transactions on Signal Processing*, *47*, 655–664.

Putnam, W., Rocchesso, D., & Smith, J. (1995). A numerical investigation of the invertibility of room transfer functions. *Proceedings of the IEEE ASSP Workshop on Applications of Signal Processing to Audio and Acoustics* (pp. 249–252). Mohonk, NY.

Rabiner, L., & Juang, B.-H. (1993). *Fundamentals of speech recognition*. New Jersey: Prentice Hall.

Rabinkin, D., Renomeron, R., & Flanagan, J. (1997). Microphone array sensor placement optimization in reverberant environments. *Journal of the Acoustical Society of America*, *102*, 3207.

Rudnicky, A., Thayer, E., Constantinides, P., Tchou, C., Shern, R., Lenzo, K., Xu, W., & Oh, A. (1999). Creating natural dialogs in the Carnegie Mellon Communicator system. *Proceedings of Eurospeech* (pp. 1531–1534). Budapest, Hungary.

Sanders, G. A., Le, A. N., & Garofolo, J. S. (2002). Effects of word error rate in the DARPA Communicator data during 2000 and 2001. *Proceedings of the International Conference on Spoken Language Processing* (pp. 277–280). Denver, Colorado.

Seltzer, M., & Raj, B. (2001). Calibration of microphone arrays for improved speech recognition. *Proceedings of Eurospeech* (pp. 1005–1008). Aalborg, Denmark.

Seltzer, M. L., Raj, B., & Stern, R. M. (2002). Speech recognizer-based microphone array processing for robust hands-free speech recognition. *Proceedings of the IEEE International Conference on Acoustics, Speech, and Signal Processing* (pp. 897–900). Orlando, FL.

Seltzer, M. L., & Stern, R. M. (2003). Subband parameter optimization of microphone arrays for speech recognition in reverberant environments. *Proceedings of the IEEE International Conference on Acoustics, Speech, and Signal Processing* (pp. 408–411). Hong Kong.

Silverman, H. F., Patterson, W. R., & Flanagan, J. L. (1996). *The huge microphone array (HMA)* (Technical Report). Brown University, Providence, RI.

Sullivan, T. M. (1996). *Multi-microphone correlation-based processing for robust speech recognition.* Doctoral dissertation, Carnegie Mellon University, Pittsburgh, PA.

Sullivan, T. M., & Stern, R. M. (1993). Multi-microphone correlation-based processing for robust speech recognition. *Proceedings of the IEEE International Conference on Acoustics, Speech, and Signal Processing* (pp. 27–30). Minneapolis, MN.

Suzuki, Y., Asano, F., Kim, H.-Y., & Sone, T. (1995). An optimum computer-generated pulse signal suitable for the measurement of very long impulse responses. *Journal of the Acoustical Society of America*, *97*, 1119–1123.

Van Compernolle, D. (1990). Switching adaptive filters for enhancing noisy and reverberant speech from microphone array recordings. *Proceedings of the IEEE International Conference on Acoustics, Speech, and Signal Processing* (pp. 833–836). Albequerque, NM.

Viterbi, A. J. (1967). Error bounds for convolutional codes and an asymptotically optimum decoding algorithm. *IEEE Transactions on Information Theory*, *13*, 260–269.

Waibel, A., Bett, M., Metze, F., Ries, K., Schaaf, T., Schultz, T., Soltau, H., Yu, H., & Zechner, K. (2001). Advances in automatic meeting record creation and access. *Proceedings of the IEEE International Conference on Acoustics, Speech, and Signal Processing* (pp. 597–600). Salt Lake City, UT.

Walker, M. A., Rudnicky, A., Prasad, R., Aberdeen, J., Bratt, E. O., Garofolo, J., Hastie, H., Le, A., Pellom, B., Potamianos, A., Passonneau, R., Roukos, S., Sanders, G., Seneff, S., & Stallard, D. (2002). DARPA Communicator: cross-system results for the 2001 evaluation. *Proceedings of the International Conference on Spoken Language Processing* (pp. 269–272). Denver, Colorado.

Woodland, P. C., Gales, M. J. F., & Pye, D. (1996). Improving environmental robustness in large vocabulary speech recognition. *Proceedings of the IEEE International Conference on Acoustics, Speech, and Signal Processing* (pp. 65–69). Atlanta, GA.

Zelinkski, R. (1988). A microphone array with adaptive post-filtering for noise reduction in reverberant rooms. *Proceedings of the IEEE International Conference on Acoustics, Speech, and Signal Processing* (pp. 2578–2581). New York, NY.